The Open
University

Open Research Online

The Open University's repository of research publications
and other research outputs

A deep survey of heavy element lines in planetary nebulae - I. Observations and forbidden-line densities, temperatures and abundances

Journal Item

For guidance on citations see FAQs.

Version: Version of Record

Link(s) to article on publisher's website:
http://dx.doi.org/doi:10.1046/j.1365-8711.2003.06972.x

oro.open.ac.uk

A deep survey of heavy element lines in planetary nebulae – I. Observations and forbidden-line densities, temperatures and abundances

Y. G. Tsamis,[1,2]★ M. J. Barlow,[1]† X.-W. Liu,[1]‡ I. J. Danziger[3] and P. J. Storey[1]

[1]*Department of Physics and Astronomy, University College London, Gower Street, London WC1E 6BT*
[2]*The Met. Office, London Road, Bracknell RG12 2SZ*
[3]*Osservatorio Astronomico di Trieste, Via G. B. Tiepolo 11, I-34131 Trieste, Italy*

ABSTRACT

We present deep optical spectrophotometry of 12 Galactic planetary nebulae (PNe) and three Magellanic Cloud PNe. Nine of the Galactic PNe were observed by scanning the slit of the spectrograph across the nebula, yielding relative line intensities for the entire nebula that are suitable for comparison with integrated nebular fluxes measured in other wavelength regions. In this paper we use the fluxes of collisionally excited lines (CELs) from the nebulae to derive electron densities and temperatures, and ionic abundances. We find that the nebular electron densities derived from optical CEL ratios are systematically higher than those derived from the ratios of the infrared (IR) fine-structure (FS) lines of [O III]. The latter have lower critical densities than the typical nebular electron densities derived from optical CELs, indicating the presence of significant density variations within the nebulae, with the IR CELs being biased towards lower density regions.

We find that for several nebulae the electron temperatures obtained from [O II] and [N II] optical CELs are significantly affected by recombination excitation of one or more of the CELs. When allowance is made for recombination excitation, much better agreement is obtained with the electron temperatures obtained from optical [O III] lines. We also compare electron temperatures obtained from the ratio of optical nebular to auroral [O III] lines with temperatures obtained from the ratio of [O III] optical lines to [O III] IR FS lines. We find that when the latter are derived using electron densities based on the [O III] 52 μm/88 μm line ratio, they yield values that are significantly higher than the optical [O III] electron temperatures. In contrast to this, [O III] optical/IR temperatures derived using the higher electron densities obtained from optical [Cl III] λ5517/λ5537 ratios show much closer agreement with optical [O III] electron temperatures, implying that the observed [O III] optical/IR ratios are significantly weighted by densities in excess of the critical densities of both [O III] FS lines. Consistent with this, ionic abundances derived from [O III] and [N III] FS lines using electron densities from optical CELs show much better agreement with abundances derived for the same ions from optical and ultraviolet CELs than do abundances derived from the FS lines using the lower electron densities obtained from the observed [O III] 52 μm/88 μm ratios. The behaviour of these electron temperatures, obtained making use of the temperature-insensitive [O III] IR FS lines, provides no support for significant temperature fluctuations within the nebulae being responsible for derived Balmer jump electron temperatures that are lower than temperatures obtained from the much more temperature sensitive [O III] optical lines.

Key words: ISM: abundances – planetary nebulae: general.

★Present address: LAEC, Observatoire de Paris-Meudon, 92195 Meudon, France.
†E-mail: mjb@star.ucl.ac.uk
‡Present address: Department of Astronomy, Peking University, Beijing 100871, China.

1 INTRODUCTION

This is the first of two papers devoted to the study of elemental abundances in a sample of Galactic and Magellanic Cloud planetary nebulae which, together with a companion paper by Tsamis et al. (2003a) on H II regions, focus on the problem of the optical recombination-line emission from heavy element ions (e.g. C^{2+}, N^{2+}, O^{2+}) in planetary nebulae (PNe) and H II regions. The main manifestation of this intriguing question is the observed discrepancy between nebular elemental abundances derived from weak, optical recombination lines (ORLs; such as C II λ4267, N II λ4041, O II λλ4089, 4650) on the one hand, and the much brighter collisionally excited lines (CELs; often collectively referred to as forbidden lines) on the other (Liu et al. 1995, 2000, 2001b; Tsamis 2002; Tsamis et al. 2003a), with ORLs typically being found to yield ionic abundances that are factors of two or more larger than those obtained from CELs emitted by the same ions. A closely linked problem involves the observed disparity between the nebular electron temperatures derived from the traditional [O III] (λ4959 + λ5007)/λ4363 ratio and the H I Balmer discontinuity diagnostic: the latter yields temperatures that are in most cases lower than those derived from the [O III] ratio (Peimbert 1971; Liu & Danziger 1993; Liu et al. 2001b; Tsamis 2002).

Tsamis et al. (2003a) have presented new spectroscopic observations and an abundance analysis of the Galactic H II regions M17 and NGC 3576 and the Magellanic Cloud H II regions 30 Doradus, LMC N11B and SMC N66, involving both CELs and ORLs. We reported surprisingly large ORL versus CEL abundance discrepancies in these objects: the O^{2+}/H^+ abundance ratios derived from multiple O II ORLs were found to be higher than the corresponding values derived from [O III] CELs, typically by a factor of ∼2, though for one nebula, LMC N11B, a discrepancy of a factor of 5 was found.

In the present paper, we present deep, long-slit, optical spectrophotometry of 12 Galactic and three Magellanic Cloud PNe. We present an extensive list of all the detected emission lines, including the numerous C II, N II, O II and Ne II ORLs, along with their fluxes and dereddened intensities. We undertake a *forbidden-line* abundance study deriving C, N, O, Ne, S, Cl and Ar abundances from CELs, as well as He abundances from He I and He II ORLs. Along with the optical data, we analyze *International Ultraviolet Explorer* NEWSIPS spectra of 10 PNe, which yield fluxes of important C, N, O and Ne CELs. We further derive abundances for a number of PNe from the far-infrared (far-IR) [O III] 52- and 88-μm and [N III] 57-μm fine-structure lines using the *Infrared Space Observatory* LWS line fluxes by Liu et al. (2001a), as well as from the *IRAS* [Ne III] 15.5-μm line fluxes by Pottasch et al. (1984). In an accompanying paper (Tsamis et al. 2003b, hereafter Paper II), heavy-element ionic abundances are derived from the observed C II, C III, C IV, N II, N III, O II and Ne II ORLs and an extensive comparison between ORL and CEL elemental abundance ratios is made.

In Section 2 we describe our optical spectroscopic observations obtained with the European Southern Observatory (ESO) 1.52-m and New Technology Telescope (NTT) 3.5-m telescopes, as well as the data reduction process, and present emission line fluxes for all the PNe; we also present *IUE* ultraviolet (UV) observations and our data analysis methods. In Section 3 we describe the corrections for interstellar extinction to the UV and optical data. In Section 4 we present derived nebular electron temperatures and densities. In Section 5 we present our derived He/H ratios and the heavy element abundances derived from UV, optical and IR collisionally excited lines.

2 OBSERVATIONS

2.1 Optical spectroscopy

2.1.1 Description and data reduction

The planetary nebulae studied in this work were observed at ESO, using the 1.52-m telescope for the Galactic objects and the 3.5-m NTT for the Magellanic Cloud objects. The long-slit observations were taken during 1995 July and December, 1996 July and 1997 February. An observational journal is presented in Table 1.

The Boller & Chivens (B&C) spectrograph was used on the 1.52-m telescope in 1995 July, equipped with a Ford 2048 × 2048 pixel CCD detector, with each pixel 15 × 15 μm^2 in size. This detector was superseded in 1996 and 1997 by a UV-enhanced Loral 2048 × 2048, 15 × 15 μm^2 CCD of improved quantum efficiency. A 2-arcsec wide, 3.5-arcmin long slit was employed. During all runs the CCDs were binned by a factor of 2 along the slit direction, in order to reduce the read-out noise, yielding a spatial sampling of 1.63 arcsec per pixel projected on the sky. A 2400 line mm^{-1} grating was used in first order, along with an order-sorting WG360 filter, to cover the 3995–4978 Å wavelength range at a spectral resolution of 1.5 Å full width at half-maximum (FWHM). A second grating in first order, along with a WG345 filter, was used to cover the 3535–7400 Å range at a resolution of 4.5 Å (excluding NGC 2440 for which 4.5-Å resolution spectra were not obtained). For three objects (NGC 5882, 6302 and 6818) an extra wavelength range (3040–4040 Å) was covered with the holographic 2400 line mm^{-1} grating at a resolution of 1.5 Å so that the high-order H I Balmer lines – transitions $n \rightarrow 2$, from upper levels of principal quantum number up to $n = 24$ – were accurately recorded. The low-resolution (4.5 Å), wider spectral coverage spectra yielded fluxes of forbidden lines of N^+, O^+, O^{2+}, Ne^{2+}, S^+, S^{2+}, Cl^{2+}, Ar^{2+} and Ar^{3+}, etc., ions, as well as H^0, He^0 and He^+ lines, and covered the Balmer discontinuity (or Balmer jump; hereafter BJ). The higher resolution (1.5 Å), deep spectra recorded the optical recombination lines of C II, C III, C IV, N II, N III, O II and Ne II, the majority of which lay between 4000–5000 Å.

Typical exposure times for these Galactic PNe ranged between 20 s and 35 min. The short exposures were carefully chosen so that strong nebular lines, such as Hα, Hβ or the [O III] λλ4959, 5007 and [N II] λλ6548, 6584 lines, would not be saturated. On the other hand, the deep exposures were aimed at capturing the faint ORLs, whose typical intensities can be as low as 10^{-4} that of Hβ, at an appropriate resolving power.

For nine out of 12 observed Galactic nebulae (NGC entries 2022, 2440, 3132, 3242, 3918, 5315, 5882, and IC 4191 and 4406), mean spectra were obtained by uniformly scanning the long-slit of the B&C spectrograph across the nebular surfaces (IC 4406 was scanned only at a lower resolution of 4.5 Å). For these nebulae total fluxes of all detected lines can be derived, when total nebular Hβ line fluxes are adopted from the compilation of Cahn, Kaler & Stanghellini (1992, hereafter CKS92), as listed in column 2 of Table 1. Furthermore, these mean spectra are directly comparable with UV and IR spectra obtained from space-borne facilities (such as the *IUE*, *IRAS* and *ISO* satellites), whose large apertures usually capture most or all of the nebular emission, depending on the angular size of the observed nebulae and the pointing coordinates of such observations. In this way, several ionization stages of the same element can be traced, allowing a more complete picture to be drawn for properties such as reddening, excitation class and elemental abundances.

Table 1. Journal of ESO optical observations.

PN	log$F$(Hβ) (erg cm^{-2} s^{-1})	c(Hβ)$^{\text{radio}}$	Date (UT)	λ-range (Å)	FWHM (Å)	Mode	Exp. Time (s)
				ESO 1.52-m			
NGC 2022	−11.13	0.42	7 Feb 1997	3530–7428	4.5	scanning	40, 1155
			8, 10 Feb 1997	3994–4978	1.5	”	3 × 1500, 1800, 2100
NGC 2440	−10.50	0.47	9 Feb 1997	3994–4978	1.5	scanning	1800
NGC 3132	−10.45	0.30	7 Feb 1997	3530–7428	4.5	scanning	70, 1147
			8, 10 Feb 1997	3994–4978	1.5	”	2 × 1620, 2 × 1800
NGC 3242	−9.79	0.17	7 Feb 1997	3530–7428	4.5	scanning	25, 480
			8, 10 Feb 1997	3994–4978	1.5	”	1614, 2 × 1800, 2100
NGC 3918	−10.04	0.40	7 Feb 1997	3530–7428	4.5	scanning	20, 22, 40, 200
			8, 10 Feb 1997	3994–4978	1.5	”	1020, 1200, 2 × 1620
NGC 5315	−10.42	0.55	7 Feb 1997	3530–7428	4.5	scanning	30, 240
			9, 10 Feb 1997	3994–4978	1.5	”	1080, 1350, 2 × 1500
NGC 5882	−10.38	0.42	12 Jul 1996	3040–4050	1.5	fixed slit	2 × 1800
			7 Feb 1997	3530–7428	4.5	scanning	20, 220
			9, 10 Feb 1997	3994–4978	1.5	”	3 × 1500, 1800
NGC 6302	−10.55	1.39	11 Jul 1996	3040–4050	1.5	fixed slit	2 × 1800
			29 Jul 1995	3530–7428	4.5	”	30, 60, 300
			23 Jul 1995	3994–4978	1.5	”	3 × 1800
NGC 6818	−10.48	0.37	11 Jul 1996	3040–4050	1.5	fixed slit	2 × 1800
			29 Jul 1995	3530–7428	4.5	”	60, 300
			23 Jul 1995	3994–4978	1.5	”	3 × 1800
IC 4191	−10.99	0.70	7 Feb 1997	3530–7428	4.5	scanning	2 × 30, 500
			8 Feb 1997	3994–4978	1.5	”	900, 1200
			29 Jul 1995	3530–7428	4.5	fixed slit	5, 10, 300, 600
			22 Jul 1995	3994–4978	1.5	”	3 × 1800
IC 4406	−10.75	0.27	7 Feb 1997	3530–7428	4.5	scanning	50, 1080
			29 Jul 1995	3530–7428	4.5	fixed slit	2 × 300
			22 Jul 1995	3994–4978	1.5	”	5 × 1800
My Cn 18	−11.21	0.74	29 Jul 1995	3530–7428	4.5	fixed slit	2 × 120, 600
			23 Jul 1995	3994–4978	1.5	”	4 × 1800
				NTT 3.5-m			
SMC N87	−12.48		17 Dec 1995	6507–7828	3.8	fixed slit	1200
(SMP 27)			”	3635–4145	2	”	1200
			”	4060–4520	2	”	2 × 1800
			“	4515–4975	2	”	900, 3 × 1800
LMC N66	−12.68		17 Dec 1995	3800–8400	11	fixed slit	2 × 300
(SMP 83)			“	6507–7828	3.8	”	300
			“	3635–4145	2	”	300
			“	4060–4520	2	”	360
			“	4515–4975	2	”	600
LMC N141	−12.48		17 Dec 1995	6507–7828	3.8	fixed slit	1200
(SMP 63)			“	3635–4145	2	”	1800
			“	4060–4520	2	”	2 × 1800
			“	4515–4975	2	”	180, 4 × 1800

For the remaining three Galactic PNe, plus IC 4406 in the 3995–4978 Å range only, fixed-slit spectra were obtained (Table 1). In those cases, the slit was positioned through the nebular center – using the central star of the PN as a guide, if visible – and passing through the visually brightest parts of the nebula.

The Magellanic Cloud planetary nebulae LMC N66, LMC N141 and SMC N87 were observed at ESO with the 3.5-m NTT, in 1995 December (Table 1). The ESO Multi-Mode Instrument (EMMI) was used in the following modes: red imaging and low dispersion grism spectroscopy (RILD), blue medium dispersion spectroscopy (BLMD) and dichroic medium dispersion spectroscopy (DIMD). The detector was a TEK 1024 × 1024, 24 × 24 μm^2 CCD (no. 31; on the blue arm), used while in BLMD observing mode and a TEK 2048 × 2048, 24 × 24 μm^2 CCD (no. 36; on the red arm), while in RILD mode. Both cameras were in use when observing in

DIMD mode. In those cases, a dichroic prism is inserted into the beam path so that light is directed to the blue and red grating units in synchronization, allowing simultaneous exposures to be obtained in the blue and red parts of the optical spectrum. For all exposures, both CCDs were binned by a factor of 2 in both directions, in order to reduce the read-out noise. The spatial sampling was thus 0.74 and 0.54 arcsec pixel^{-1} projected on the sky, for CCDs no. 31 and no. 36, respectively.

Four wavelength regions were observed with two different gratings (#3, #7) at spectral resolutions of approximately 2 Å FWHM (3635–4145, 4060–4520, 4515–4975 Å), and 3.8 Å (6507–7828 Å), respectively. An extra wavelength range, 3800–8400 Å, was covered only for LMC N66 at a resolution of 11 Å, using a grism (#3). An OG530 filter was used when observing in DIMD mode. The slits used were 5.6-arcmin long and 1- and 1.5-arcsec wide,

but wide-slit 5-arcsec grism observations were also taken for LMC N66. Exposure times for the Magellanic Cloud PNe ranged from 3 to 30 min.

The two-dimensional Galactic PN spectra were reduced with the LONG92 package within MIDAS. They were bias-subtracted, flat-fielded via division by a normalized flat field, cleaned of cosmic-rays, and then wavelength-calibrated using exposures of a HeAr calibration lamp. The effect of atmospheric extinction was removed by correcting the spectra using extinction coefficients for the La Silla site. During the 1997 run, twilight sky flat-fields were also obtained with the purpose of correcting the small variations in illumination along the slit, which were ∼1–3 per cent. For the 1995 and 1996 runs, the spectra were flux-calibrated using wide-slit (8 arcsec) observations of the *HST* standard stars Feige 110 and the nucleus of the PN NGC 7293 (Walsh 1993). The flux distributions of the standards were modelled with high-order spline fits. In 1997, the CTIO standard stars LTT 4363, LTT 6248 (Hamuy et al. 1994) and the *HST* standard HD 49798 (Walsh 1993) were used.

The 3040–4040 Å spectra of NGC 5882, 6302 and 6818 are affected by ozone absorption bands, shortwards of 3400 Å (Schachter 1991). The bands have a typical width of ∼15 Å, i.e. much wider than the nebular emission lines (∼1.5 Å). In order to remove the ozone absorption we used the ozone-opacity template derived by Liu et al. (2000) for the study of NGC 6153 from the same site (ESO, La Silla) as the observations presented herein. The standard stars Feige 110 and the nucleus of NGC 7293 were observed with a narrow 2-arcsec slit, i.e. the same as the one used for nebular observations. These narrow-slit spectra were used to derive the ozone opacity per unit airmass as a function of wavelength, relative to the mean atmospheric extinction curve at La Silla. The opacity curve, scaled by the airmasses of the nebular exposures, was then used to divide out the ozone absorption bands.

The Cloud PN two-dimensional spectra were reduced with similar procedures as above; the wavelength calibration was done with respect to ThAr and HeAr calibration lamps within MIDAS, while flux calibration was performed with respect to wide-slit (8 arcsec) observations of the standard Feige 110, within the IRAF package.

For all flux-calibrated spectra, suitable sky windows were selected on each side of the nebular emission, their increments were summed-up, scaled to the total number of CCD pixels along the slit direction and subtracted. In this way we were able to subtract the sky emission for all PNe, since their angular diameters were always effectively contained within our long-slit. The resulting spectra were subsequently averaged along the spatial nebular emission – defined by the extent of the Hβ line – to yield the one-dimensional spectra on which our nebular analysis was performed. In a couple of cases, such as NGC 6302 and 6818 for which only fixed-slit spectra were obtained, the ORLs detected were rather weak and the spectra slightly noisier than the norm, so we decided to integrate the spectra along the spatial extent of the C II $\lambda4267$ line which is one of the strongest heavy element recombination lines in nebulae (the Hβ line was of course sampled over the same pixel numbers). This resulted in better signal-to-noise (S/N) ratios for the O II and N II recombination lines too, which are expected to originate from similar nebular volumes as the C II $\lambda4267$ line.

In other objects it was found that light from the central star of the nebula affects considerably the nebular line fluxes or the shape of the observed continuum spectrum. For instance, NGC 3132 harbours a binary nucleus whose primary component is the A-type star HD 87892 (Kohoutek & Laustsen 1977; Sahu & Desai 1986). The absorption line spectrum of this star severely affects the nebular Balmer lines by diminishing their intensities, so a few central

CCD pixels had to be excluded from the integration in order to prevent such contamination and to restore the nebular line profiles. Another example is NGC 5882, which possesses a weak emission line ('wel'), hydrogen-deficient nucleus, whose continuum energy distribution evidently affects the shape of the nebular continuum in the region of the Balmer discontinuity (∼3646 Å). Thus in order to get an accurate measurement of the Balmer jump intensity and the high-order Balmer lines from the deep 3040–4040 Å spectra of this object, we again excluded several central pixels when averaging the two-dimensional CCD frames. This restored the nebular continuum to its expected shape at those wavelengths.

In Fig. 1 we show a representative high resolution optical spectrum of NGC 3242 taken in scanning mode. It is a time-weighted average of four deep exposures which captured a particularly rich set of recombination lines from heavy element ions. Indicative line identifications are shown.

2.2 The *IUE* observations

We complemented our optical data set with *IUE* UV observations of 10 of the Galactic PNe, together with *IUE* observations of the three Magellanic Cloud nebulae; the remaining two Galactic PNe, IC 4191 and My Cn 18, were never observed by the *IUE*. Low-resolution, large-aperture spectra obtained with the SWP and LWP cameras were accessed via the Space Telescope Science Institute's web site.[1] The wavelength coverage of the two cameras is 1150–1975 and 1910–3300 Å respectively. All observations were obtained with the *IUE* large-aperture, a 10.3×23 arcsec^2 oval. The data were retrieved in final (NEWSIPS) calibrated form. When several spectra for one object were available, they were co-added and weighted by the integration time. The employed *IUE* exposures are listed in Table 2. For NGC 3918 the line fluxes reported by Clegg et al. (1987) were used, combined with those retrieved from a more recent exposure (SWP 47514). Similarly, in the analysis of NGC 5315 and 6818 we used the line fluxes recently listed by Feibelman (1998, see his table 3) and by Hyung, Aller & Feibelman (1999, see their tables 4 and 5), respectively. Regarding LMC N66, we used the observed *IUE* line fluxes listed by Peña & Ruiz (1988; from spectrum SWP 19905).

The apparent angular sizes of all nebulae in our sample, apart from NGC 5315 and the Magellanic Cloud nebulae, are larger than the *IUE* large aperture. Thus, in most cases only a certain fraction of the UV nebular emission was captured by the satellite. This delicate aspect of the observations is discussed in the following section.

2.3 Data analysis

With respect to the optical data we proceeded by normalizing the individual one-dimensional spectra to a flux scale such that $F(H\beta) = 100$, in order to merge them afterwards. When Hβ was found to be saturated in one spectrum, the scaling was achieved using a suitable unsaturated H I Balmer line from a shorter duration exposure. The 3040–4040 Å Galactic PN spectra were brought to scale with the rest, using emission lines detected in common with the 3535–7400 Å spectra, such as H 9 $\lambda3835$, [Ne III] $\lambda3868$, H 8 + He I $\lambda3889$, and [Ne III] $\lambda3967$ + Hϵ $\lambda3970$. In a similar fashion, the Magellanic Cloud PN spectra from different grating settings were brought to scale via their overlapping portions. For two of them, SMC N87 and LMC N141, their 6507–7828 Å spectra had no overlap in wavelength with other grating settings. In this case we normalized the spectra to $F(H\beta) = 100$, using the theoretical

---

[1] http://archive.stsci.edu.iue
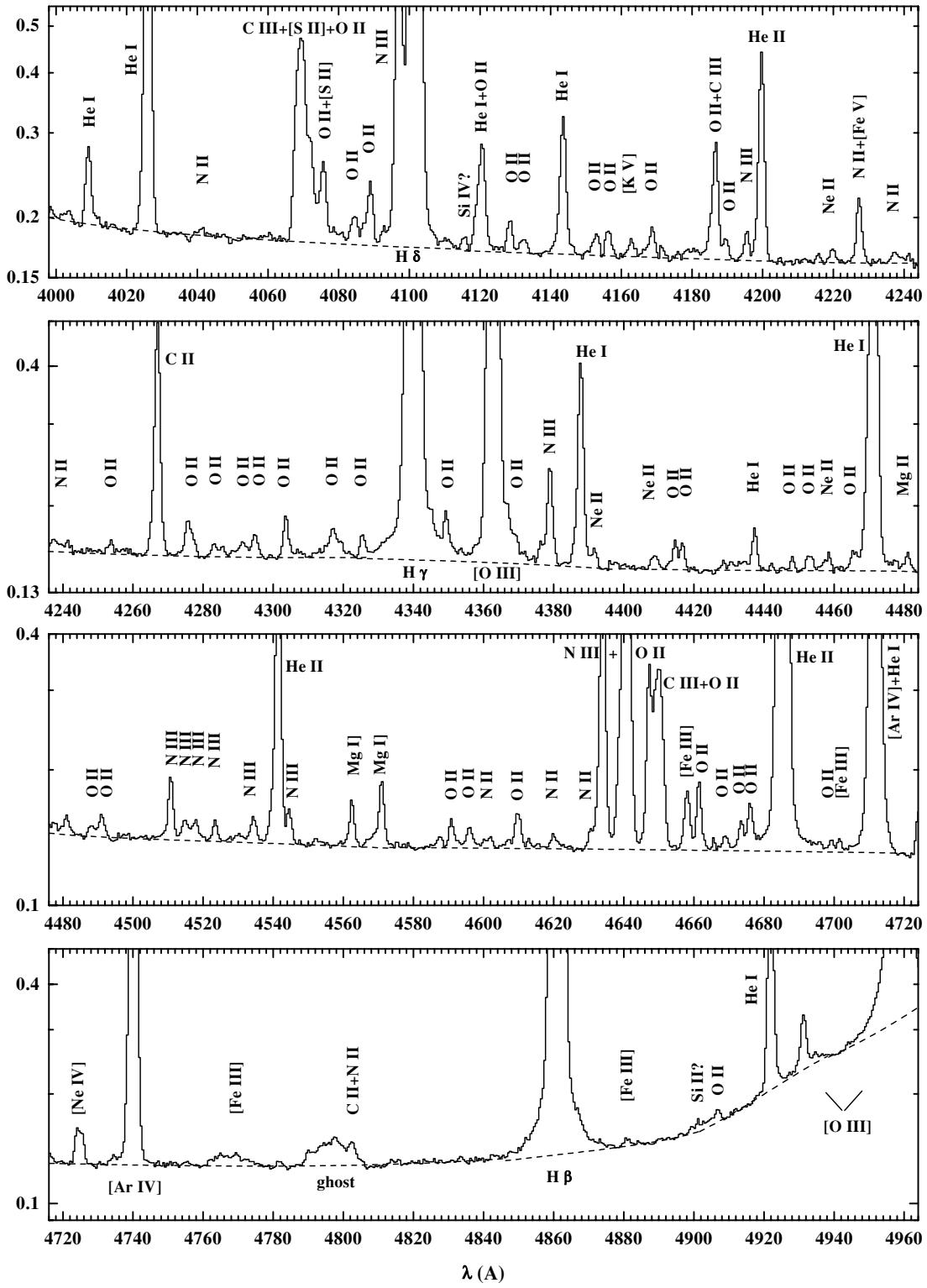
Figure 1. The spectrum of NGC 3242 from 4000 to 4960 Å featuring the prominent recombination lines from C, N, O and Ne ions; it was obtained by uniformly scanning the entire nebular surface using a narrow long-slit. The dashed lines show the adopted continuum level. The steep rise of the continuum after 4880 Å is an instrumental artifact. The intensity is in units such that $F(H\beta) = 100$; the spectrum is not corrected for interstellar extinction.

intensity ratio $I(H\alpha)/I(H\beta) = 2.85$, a value predicted for representative nebular conditions of $T_e = 10\,000$ K and $N_e = 5000$ cm^{-3} (Storey & Hummer 1995); we also took into account the amount of reddening estimated towards these objects (Section 5). Finally, the normalized spectra taken at each grating setting were co-added,

weighted by the exposure time, in order to achieve an optimum S/N ratio.

Regarding the UV data, a way had to be found to scale them to the normalized optical spectra. For all Galactic nebulae (except NGC 5315, NGC 6818 and IC 4406), we used the theoretical

Table 2. Journal of *IUE* observations.[a]

PN	Spectrum	Exp. Time (s)
NGC 2022	SWP 32732, 32729	4800, 5400
NGC 2440	SWP 07264, 14850, 17243	1800, 2100, 360
	SWP 32720	2400
NGC 3132	SWP 06160, 01745, 49629	7200, 1200, 7200
NGC 3242	SWP 5154, 5155	300, 330
NGC 3918	SWP 47514	300
NGC 5882	SWP 16349	1800
NGC 6302	SWP 05210, 05211	720, 5400
	SWP 30986, 33379	14400, 6600
IC 4406	SWP 23420, 36237	3600, 7200
	LWP 03725, 15490	3600, 7200
SMC N87	LWR 10043, SWP 13387	10500, 13387
LMC N141	SWP 13408	9000

[a]NGC 5315 and NGC 6818 line fluxes were taken from Feibelman (1998) and Hyung et al. (1999) respectively; for NGC 3918 the combined fluxes from SWP 47514 and those of Clegg et al. (1987) were used.

intensity ratio for He II λ1640/λ4686, calculated for the appropriate nebular temperatures and densities using the recombination theory predictions of Storey & Hummer (1995). In this way we scaled the UV spectra to $F(H\beta) = 100$ using our measurements of the dereddened $I(\lambda1640)$ and $I(\lambda4686)$ fluxes. In cases where the [O II] λ2470 doublet line was detected, as in NGC 6818 and IC 4406, we used instead the predicted intensity ratio [O II] $(\lambda7320 + \lambda7330)/\lambda2470 = 1.33$, which holds independently of nebular conditions as all lines involved arise from the same upper levels (*A*-values taken from Zeippen 1982). The method was found to be highly reliable; for instance in NGC 5315 whose angular diameter fits completely within the *IUE* large aperture – and there is thus no need for any aperture correction to be applied – the [O II] λ2470 intensity predicted using the optical [O II] λλ7320, 7330 intensities, is within 2 per cent of the actual UV measurement. For NGC 5315 and the three Cloud PNe (SMC N87, LMC N66 and LMC N141) the dereddened UV line fluxes were scaled directly to $F(H\beta) = 100$, with the use of total Hβ fluxes from CKS92 in the former case and from those listed by Barlow (1987) in the latter cases.

We proceeded with measuring the emission line fluxes from the UV and optical spectra using the MIDAS package. First we scrutinized the low-resolution *IUE* spectra in order to determine the nature of the emission lines, which in some cases can have a stellar and not nebular origin (e.g. N V λ1240, C IV λ1550, He II λ1640). The FWHM of the lines was compared against that of *IUE* low-resolution spectra which is ~6–7 Å. Lines with FWHM of $\gtrsim$ 8–9 Å were checked for blending or for the possible presence of P Cygni features that would betray their origin in the wind of a central star, as is the case for instance in NGC 5315 and NGC 5882.

Most of the line fluxes – and certainly all those of heavy element recombination lines – were derived using Gaussian line profile fitting techniques, apart from the strongest ones, for which their fluxes were measured by simply integrating over the lines. Gaussian line fitting within MIDAS is performed through least-squares fitting using the Newton–Raphson method.

Even in our 1.5-Å high-resolution optical spectra, blending of emission lines is evident throughout the wavelength range covered and it particularly affects weak features such as the ORLs of interest. The line broadening is dominated by instrumental broadening and not by nebular dynamics, as the typical FWHM of 1.5 Å translates to ~93 km s^{-1} at 4861 Å, whereas typical PN expansion velocities are $\lesssim$25 km s^{-1} (e.g. Kwok 1994). Therefore, in order to de-convolve

features affected by blending, multiple Gaussian fitting was employed. In such cases a successful estimate of the continuum emission level was deemed to be a very important first step. After subtracting the local continuum, line fluxes were retrieved by fitting multiple Gaussians of appropriate central wavelength and usually equal FWHM. The FWHM was taken to be the same as that of nearby unblended lines of similar strength to the ones fitted. Their relative wavelength spacing was constrained to that from laboratory wavelengths. This procedure assured accurate flux retrieval and aided line identification in the case of ambiguous features.

In rare instances where the fitting process was not adequately yielding unique fluxes for closely spaced lines, we made use of the theoretical intensity ratios of selected lines, assuming *LS*-coupling to hold for the ions in question (e.g. Kuhn 1969). As an example, in PNe of relatively high excitation class, such as NGC 5882, the [S II] λ4068 line is blended with the C III V 16 triplet, whose components at 4067.94, 4068.91 and 4070.26 Å have intensity ratios under pure *LS*-coupling of 1.00 : 1.31 : 1.71 (e.g. Allen 1973). Also present in this blend are the O II V 10 multiplet λλ4069.62, 4069.89 and 4072.16 lines. We therefore fitted six Gaussians to the 4069-Å complex, fixing the C III triplet relative intensities according to theory, while allowing the intensities of the other lines to vary independently. After reducing the number of free parameters in the minimization problem by two, convergence was more readily achieved. Of course in this way, the resulting flux for the C III triplet refers to the sum of its components only, while information on the true allocation of flux among them is lost. Individual fluxes, however, are retrieved for the [S II] and O II lines and the overall shape of the blend is accurately reproduced (see Fig. 2). As another example, the blend at 4650 Å can be fitted with five Gaussians, including the O II λλ4649.13, 4650.84 lines from multiplet V 1 and the C III V 1 triplet λλ4647.42, 4650.25
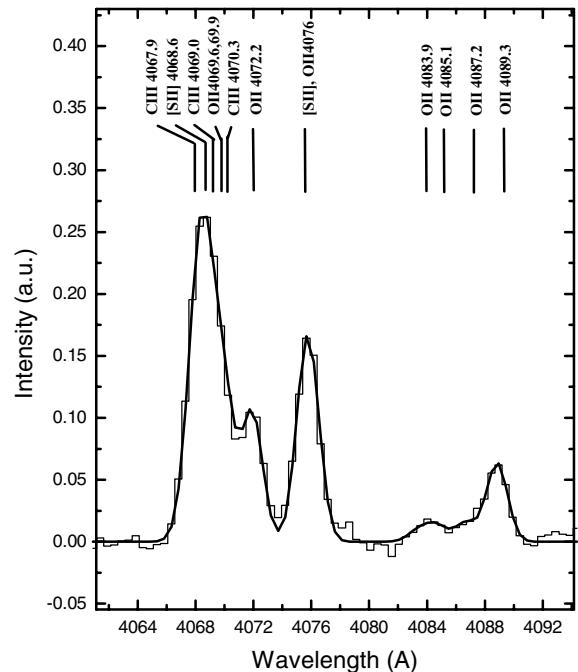

Figure 2. Medium-high resolution spectrum (1.5-Å FWHM) of the medium excitation PN NGC 5882: the blend of O II quartet V 10, C III triplet V 16 and [S II] doublet is well fitted by multiple Gaussians (*thick line*); also present are O II 4f–3d transitions of which λ4089.3 ($J = 11/2–9/2$) is the strongest predicted line. See text for more details.

and 4651.47 lines, the latter having relative intensities of 5 : 3 : 1, as predicted under *LS*-coupling. In general, apart from for the aforementioned cases, we avoided fixing the relative strengths of ORLs, because we were interested in comparing our observations with the predictions of current recombination theory, especially for O II.

Table 3 presents the observed optical relative line intensities for the 12 Galactic PNe in our sample, while Table 4 presents the observed optical and ultraviolet relative line intensities for the three Magellanic Cloud PNe. Table 5 presents the UV nebular line intensities for the 10 Galactic PNe in the sample which were observed by the *IUE*. Typical optical line flux errors are estimated to be less than 5 per cent for lines with observed fluxes $F(\lambda) \geqslant 0.2$ [in units of $F(H\beta) = 100$], 10 per cent for those with $0.1 \leqslant F(\lambda) \leqslant 0.2$, 20 per cent for $0.05 \leqslant F(\lambda) \leqslant 0.1$, and 30 per cent or more for lines with $F(\lambda) \leqslant 0.05$. For a given flux range, the errors for optical lines shortwards of 3400 Å are slightly larger, due to the decreasing CCD efficiency towards the end of the spectral coverage and the effects of ozone absorption.

3 INTERSTELLAR EXTINCTION

Before proceeding with any kind of formal analysis, nebular spectra have to be corrected for the effects of interstellar extinction caused by dust. In nebular studies the amount of interstellar reddening is most usually described by $c(H\beta)$, which is the logarithmic difference between observed and intrinsic (or else dereddened) Hβ fluxes. The reddening-corrected nebular fluxes [in units of $I(H\beta) = 100$] are then given by

$$I(\lambda) = 10^{c(H\beta)f(\lambda)}F(\lambda),$$

where $f(\lambda)$ is the adopted extinction curve normalized such that $f(H\beta) = 0$.

A common way to derive $c(H\beta)$ in optical studies of nebulae is from a comparison between the observed and predicted H I Balmer decrement, using the Hα/Hβ, Hγ/Hβ and Hδ/Hβ line ratios. This is the method we have adopted in order to deredden our optical spectra; three preliminary $c(H\beta)$ values were obtained from each of the above Balmer line ratios and then averaged with weights of 3 : 1 : 1, respectively, according to the wavelength separation of the lines. The comparison was against the theoretical ratios from Storey & Hummer (1995) for representative values of $T_e = 10\,000$ K and $N_e = 5000$ cm^{-3}. Subsequent iteration, once the true nebular temperatures and densities were derived, resulted in negligible changes for $c(H\beta)$, denoted as $c(H\beta)^{Ba}$ hereafter. The reddening correction applied using $c(H\beta)^{Ba}$ effectively compensates for errors introduced by the relative flux calibration of the spectra. The main disadvantage over other methods is the relatively small wavelength separation of the Balmer lines employed. The values of $c(H\beta)^{Ba}$ that were used to deredden each optical spectrum are given in Tables 3 and 4 under the heading of the line-list of each PNe. The two values listed for IC 4406 correspond to the scanned and fixed-slit spectra, respectively.

A more accurate estimate of $c(H\beta)$ is possible through a comparison of the observed (optically thin) radio free–free continuum radiation of the PN, e.g. at 5 GHz, with the observed total Hβ flux. As the wavelength baseline involved is large and the radio flux suffers virtually no extinction, this method gives highly reliable reddening estimates and is to be preferred when global nebular properties are studied. In this way we derived reddening values for our Galactic PNe using the formulae of Milne & Aller (1975), employing total Hβ and 5-GHz continuum fluxes taken from CKS92, along with

Table 3. Observed and dereddened relative line fluxes [$F(\lambda)$ and $I(\lambda)$, respectively], on a scale where Hβ = 100.

λ_{obs}	$F(\lambda)$	$I(\lambda)$	ID	λ_0	Mult
		NGC 2022			
		$c(H\beta)^{Ba} = 0.38$			
	*	*	[S III]	3721.63	F2
	*	*	H 14	3721.94	H14
	1.16(+1)	1.45(+1)	[O II]	3726.03	F1
	*	*	[O II]	3728.82	F1
	*	*	H 13	3734.37	H13
3750.89	3.78	4.71	H 12	3750.15	H12
3757.98	2.80	3.48	?		
3760.61	2.62	3.26	O III	3759.87	V2
3771.37	4.14	5.13	H 11	3770.63	H11
3797.88	5.41	6.68	H 10	3797.90	H10
3815.06	7.94(−1)	9.78(−1)	?		
3835.37	7.17	8.80	H 9	3835.39	H9
3869.16	4.55(+1)	5.56(+1)	[Ne III]	3868.75	F1
3889.46	1.08(+1)	1.32(+1)	He I	3888.65	V2
3922.34	6.26(−1)	7.57(−1)	He II	3923.48	4.15
3967.88	2.65(+1)	3.18(+1)	[Ne III]	3967.46	F1
4025.99	1.34	1.59	He I	4026.21	V18
4041.28	4.92(−2)	5.80(−2)	N II	4041.31	V39b
4060.39	1.56(−1)	1.84(−1)	[F IV]	4060.23	
4068.47	3.70(−1)	4.35(−1)	C III	4067.87	V16
4069.57	4.84(−1)	5.70(−1)	C III	4068.97	V16
4070.90	6.32(−1)	7.44(−1)	C III	4070.30	V16
4072.76	2.69(−1)	3.16(−1)	O II	4072.16	V10
4076.46	2.50(−1)	2.94(−1)	O II	4075.86	V10
4090.02	1.72(−1)	2.02(−1)	O II	4089.29	V48a
4098.09	1.04	1.22	N III	4097.33	V1
4102.21	2.39(+1)	2.80(+1)	H 6	4101.74	H6
4119.75	7.15(−2)	8.34(−2)	O II	4119.22	V20
	*	*	He I	4120.84	V16
4122.71	1.80(−1)	2.09(−1)	O II	4121.46	V19
4143.97	1.74(−1)	2.02(−1)	He I	4143.76	V53
4163.78	1.26(−1)	1.46(−1)	[K V]	4163.30	F1
4185.98	8.17(−2)	9.40(−2)	O II	4185.45	V36
4187.43	2.88(−1)	3.32(−1)	C III	4186.90	V18
4200.42	1.79	2.06	He II	4199.83	4.11
4228.17	5.16(−1)	5.89(−1)	[Fe V]	4227.74	F2
4267.78	7.24(−1)	8.20(−1)	C II	4267.15	V6
4276.62	1.64(−1)	1.85(−1)	O II	4276.75	V67b
4341.00	4.58(+1)	5.11(+1)	H 5	4340.47	H5
4350.13	1.04(−1)	1.16(−1)	O II	4349.43	V2
4363.78	1.29(+1)	1.43(+1)	[O III]	4363.21	F2
4367.46	2.50(−1)	2.77(−1)	O II	4366.89	V2
4370.43	1.31(−1)	1.45(−1)	Ne II	4369.86	V56
4377.24	1.74(−1)	1.92(−1)	?		
4379.98	4.26(−1)	4.72(−1)	N III	4379.11	V18
4388.50	7.54(−2)	8.33(−2)	He I	4387.93	V51
4409.86	4.61(−2)	5.07(−2)	Ne II	4409.30	V55e
4415.46	1.14(−1)	1.25(−1)	O II	4414.90	V5
4435.13	5.89(−2)	6.44(−2)	N III	4434.14	V2
4449.43	6.97(−2)	7.61(−2)	O II	4448.19	V35
4453.61	2.60(−1)	2.83(−1)	?		
4459.36	1.49(−1)	1.62(−1)	?		
4472.10	6.33(−1)	6.87(−1)	He I	4471.50	V14
4476.25	8.62(−2)	9.35(−2)	O II?	4477.90	V88
	*	*	Mg II	4481.21	V4
4511.52	1.48(−1)	1.59(−1)	N III	4510.91	V3
4517.74	6.85(−2)	7.37(−2)	N III	4518.15	V3
4535.41	6.51(−2)	6.97(−2)	N III	4534.58	V3
4542.22	3.54	3.79	He II	4541.59	4.9
4571.37	4.23(−2)	4.49(−2)	Mg I]	4571.10	
4607.24	1.06(−1)	1.12(−1)	N IV	4606.33	
4610.33	5.47(−2)	5.78(−2)	O II	4609.44	V92a

Table 3 – *continued*

λ_{obs}	$F(\lambda)$	$I(\lambda)$	ID	λ_0	Mult
			NGC 2022		
4621.81	3.08(−2)	3.24(−2)	N II	4621.81	V 5
4626.09	4.12(−2)	4.33(−2)	[Ar v]?	4624.54	
4631.50	3.18(−1)	3.34(−1)	O IV	4631.89	V1
4634.78	5.34(−1)	5.60(−1)	N III	4634.14	V2
4639.50	1.00(−1)	1.05(−1)	O II	4638.86	V1
4641.28	8.87(−1)	9.29(−1)	N III	4640.64	V2
4642.45	3.49(−1)	3.65(−1)	O II	4641.81	V1
4648.11	5.43(−1)	5.68(−1)	C III	4647.42	V1
4649.82	3.51(−1)	3.67(−1)	O II	4649.13	V1
4650.94	2.69(−1)	2.82(−1)	C III	4650.25	V1
4651.53	8.53(−2)	8.92(−2)	O II	4650.84	V1
4652.16	1.17(−1)	1.23(−1)	C III	4651.47	V1
4659.05	9.86(−1)	1.03	[Fe III]	4658.10	F3
	*	*	C IV	4658.30	V8
4662.20	1.04(−1)	1.09(−1)	O II	4661.63	V1
4677.18	7.36(−2)	7.71(−2)	O II	4676.24	V1
4681.24	2.12(−1)	2.20(−1)	?		
4686.41	1.08(+2)	1.12(+2)	He II	4685.68	3.4
4712.08	1.39(+1)	1.43(+1)	[Ar IV]	4711.37	F1
4715.20	1.04	1.07	He I	4713.17	V12
4724.92	1.03	1.07	[Ne IV]	4724.15	F1
4726.39	8.40(−1)	8.65(−1)	[Ne IV]	4725.62	F1
4740.91	1.21(+1)	1.24(+1)	[Ar IV]	4740.17	F1
4862.13	1.00(+2)	1.00(+2)	H 4	4861.33	H4
4922.81	2.28(−1)	2.25(−1)	He I	4921.93	V48
4932.04	1.35(−1)	1.33(−1)	[O III]	4931.80	F1
4959.16	2.51(+2)	2.46(+2)	[O III]	4958.91	F1
5007.09	7.58(+2)	7.35(+2)	[O III]	5006.84	F1
5147.34	3.81(−1)	3.59(−1)	[Fe VI]	5147.21	
5177.13	1.39(−1)	1.30(−1)	[Fe VI]	5177.0	
5345.87	1.49(−1)	1.34(−1)	?		
5411.95	9.73	8.67	He II	5411.52	4.7
5518.34	4.90(−1)	4.29(−1)	[Cl III]	5517.66	F1
5538.28	4.10(−1)	3.58(−1)	[Cl III]	5537.60	F1
5592.99	2.75(−1)	2.38(−1)	O III	5592.37	V5
5676.00	3.37(−2)	2.88(−2)	N II	5676.02	V3
5679.45	1.07(−1)	9.21(−2)	N II	5679.56	V3
5801.82	4.68(−1)	3.93(−1)	C IV	5801.51	V1
5812.45	2.83(−1)	2.37(−1)	C IV	5812.14	V1
5868.54	3.94(−1)	3.27(−1)	?		
5876.42	2.33	1.94	He I	5875.66	V11
5930.89	1.29(−1)	1.07(−1)	He II	5931.84	5.25
5953.59	1.80(−1)	1.48(−1)	He II	5952.94	5.24
5977.29	1.71(−1)	1.40(−1)	He II	5977.03	5.23
6006.09	2.16(−1)	1.76(−1)	?		
6037.45	2.30(−1)	1.87(−1)	He II	6036.70	5.21
6074.81	2.90(−1)	2.34(−1)	He II	6074.10	5.20
6102.86	8.17(−1)	6.58(−1)	[K IV]	6101.83	F1
6119.23	2.78(−1)	2.23(−1)	He II	6118.20	5.19
6172.20	3.14(−1)	2.51(−1)	He II	6170.60	5.18
6234.40	3.97(−1)	3.14(−1)	He II	6233.80	5.17
6313.08	2.40	1.88	[S III]	6312.10	F3
6407.30	6.35(−1)	4.91(−1)	He II	6406.30	5.15
6436.10	2.34	1.80	[Ar V]	6435.10	
6528.47	9.51(−1)	7.25(−1)	He II	6527.11	5.14
6549.22	1.39	1.06	[N II]	6548.10	F1
6563.89	3.96(+2)	3.00(+2)	H 3	6562.77	H3
6584.62	3.02	2.28	[N II]	6583.50	F1
6679.86	6.36(−1)	4.76(−1)	He I	6678.16	V46
6684.56	9.73(−1)	7.27(−1)	He II	6683.20	
6717.81	8.80(−1)	6.55(−1)	[S II]	6716.44	F2
6732.19	9.84(−1)	7.31(−1)	[S II]	6730.82	F2
6796.37	2.62(−1)	1.93(−1)	[K IV]	6795.00	F1

Table 3 – *continued*

λ_{obs}	$F(\lambda)$	$I(\lambda)$	ID	λ_0	Mult
			NGC 2022		
6828.16	9.75(−1)	7.16(−1)	?		
6862.86	2.91(−1)	2.13(−1)	?		
6892.24	1.06	7.76(−1)	He II	6890.88	
7007.02	5.06	3.64	[Ar V]	7005.67	
7066.61	6.42(−1)	4.59(−1)	He I	7065.25	V10
7136.82	1.33(+1)	9.51	[Ar III]	7135.80	F1
7171.65	7.22(−1)	5.11(−1)	[Ar IV]	7170.62	F2
7178.53	1.53	1.08	He II	7177.50	5.11
7238.48	7.96(−1)	5.59(−1)	[Ar IV]	7237.26	F2
7263.99	5.96(−1)	4.18(−1)	[Ar IV]	7262.76	F2
7320.46	4.98(−1)	3.47(−1)	[O II]	7318.92	F2
7331.22	5.17(−1)	3.59(−1)	[O II]	7329.67	F2
			NGC 2440 $c(H\beta)^{Ba} = 0.46$		
4004.83	4.75(−2)	5.87(−2)	N III	4003.58	V17
4010.20	1.35(−1)	1.67(−1)	He I	4009.26	V55
4026.89	1.92	2.37	He I	4026.21	V18
4042.29	5.03(−2)	6.18(−2)	N II	4041.31	V39b
4061.54	6.51(−2)	7.95(−2)	[F IV]	4060.00	
4069.36	1.99	2.43	[S II]	4068.60	F1
4070.52	4.74(−1)	5.78(−1)	O II	4069.62	V10
4072.92	1.24(−1)	1.51(−1)	O II	4072.16	V10
4077.11	6.98(−1)	8.50(−1)	[S II]	4076.35	F1
4098.23	2.34	2.84	N III	4097.33	V1
4102.57	2.28(+1)	2.76(+1)	H 6	4101.74	H6
4121.46	1.42(−1)	1.71(−1)	O II	4119.22	V20
4123.08	9.23(−2)	1.11(−1)	He I	4120.84	V16
4123.70	2.98(−2)	3.59(−2)	O II	4121.46	V19
4129.82	5.74(−2)	6.91(−2)	O II	4129.32	V19
4144.57	2.45(−1)	2.94(−1)	He I	4143.76	V53
	2.17(−2)	2.60(−2)	O II	4153.30	V19
4164.05	1.09(−1)	1.30(−1)	[K V]	4163.12	
4187.72	1.87(−1)	2.21(−1)	C III	4186.90	V18
4196.65	5.36(−2)	6.34(−2)	N III	4195.76	V6
4200.80	1.33	1.58	He II	4199.83	4.11
4228.22	1.58(−1)	1.85(−1)	N II	4227.74	V33
4237.63	4.22(−2)	4.95(−2)	N II	4237.05	V48b
4242.36	4.76(−2)	5.58(−2)	N II	4241.24	V48a
4268.02	3.46(−1)	4.03(−1)	C II	4267.15	V6
4341.36	4.26(+1)	4.87(+1)	H 5	4340.47	H5
4364.13	2.21(+1)	2.51(+1)	[O III]	4363.21	F2
4380.10	2.86(−1)	3.23(−1)	N III	4379.11	V18
	3.16(−1)	3.57(−1)	He I	4387.93	V51
4415.42	4.18(−2)	4.72(−2)	O II	4414.90	V5
4417.49	3.36(−2)	3.80(−2)	O II	4416.97	V5
4438.37	4.23(−2)	4.72(−2)	He I	4437.55	V50
4453.94	7.48(−2)	8.31(−2)	O II	4452.37	V5
4459.44	3.46(−2)	3.84(−2)	?		
4472.45	2.98	3.29	He I	4471.50	V14
4499.49	4.34(−2)	4.76(−2)	?	*	
4511.91	2.38(−1)	2.61(−1)	N III	4510.91	V3
4515.86	7.32(−2)	8.01(−2)	N III	4514.86	V3
4519.15	9.51(−2)	1.04(−1)	N III	4518.15	V3
4524.55	7.50(−2)	8.18(−2)	N III	4523.58	V3
4531.38	3.81(−2)	4.15(−2)	N II	4530.41	V58b
4535.55	8.19(−2)	8.91(−2)	N III	4534.58	V3
4542.56	2.30	2.50	He II	4541.59	4.9
4563.57	1.04(−1)	1.12(−1)	Mg I]	4562.60	
4572.06	2.06(−1)	2.22(−1)	Mg I]	4571.10	
4590.21	1.05(−1)	1.12(−1)	O II	4590.97	V15
4604.75	1.69(−1)	1.81(−1)	N V	4603.73	V1
4607.44	4.44(−1)	4.75(−1)	N IV	4606.33	

Table 3 – *continued*

λ_{obs}	$F(\lambda)$	$I(\lambda)$	ID	λ_0	Mult
			NGC 2440		
4620.02	2.38(−2)	2.54(−2)	N V	4619.98	V1
4621.31	5.21(−2)	5.54(−2)	N II	4621.39	V5
4626.41	8.99(−2)	9.55(−2)	?		
4632.99	2.82(−1)	3.00(−1)	O IV	4631.89	V1
4635.17	2.07	2.19	N III	4634.14	V2
4639.89	2.66(−1)	2.84(−1)	O II	4638.86	V1
4641.67	3.79	4.01	N III	4640.64	V2
4642.84	6.12(−1)	6.52(−1)	O II	4641.81	V1
4648.35	2.14(−1)	2.26(−1)	C III	4647.42	V1
4650.06	1.20(−1)	1.27(−1)	O II	4649.13	V1
4651.18	9.69(−2)	1.02(−1)	C III	4650.25	V1
4651.77	4.84(−2)	5.10(−2)	O II	4650.84	V1
4652.40	4.59(−2)	4.85(−2)	C III	4651.47	V1
4659.26	6.84(−1)	7.21(−1)	[Fe III]	4658.10	F3
	*	*	C IV	4658.30	V8
4662.55	3.28(−2)	3.46(−2)	O II	4661.63	V1
4666.59	2.90(−2)	3.05(−2)	?		
4677.19	6.74(−2)	7.10(−2)	O II	4676.24	V1
4686.76	6.91(+1)	7.23(+1)	He II	4685.68	3.4
4702.71	4.02(−2)	4.19(−2)	[Fe III]	4701.62	F3
4708.43	1.12(−1)	1.16(−1)	?		
4712.45	8.08	8.39	[Ar IV]	4711.37	F1
4714.25	1.23	1.27	He I	4713.17	V12
4725.26	8.67(−1)	8.99(−1)	[Ne IV]	4724.15	F1
4726.73	7.16(−1)	7.42(−1)	[Ne IV]	4725.62	F1
4741.34	9.13	9.42	[Ar IV]	4740.17	F1
4803.70	9.03(−2)	9.17(−2)	N II	4802.29	V20
4853.99	8.55(−2)	8.56(−2)	?		
4862.50	1.00(+2)	1.00(+2)	H4	4861.33	H4
4867.67	2.48(−1)	2.47(−1)	?		
4882.17	5.19(−2)	5.16(−2)	[Fe III]	4881.11	
4907.95	2.74(−2)	2.71(−2)	O II	4906.83	V28
4923.20	8.33(−1)	8.20(−1)	He I	4921.93	V48
4932.11	3.60(−1)	3.54(−1)	[O III]	4931.80	F1
4935.80	3.11(−2)	3.05(−2)	?		
4939.50	2.49(−2)	2.44(−2)	?		
4945.84	2.92(−1)	2.86(−1)	N V	4944.71	
4960.13	3.84(+2)	3.74(+2)	[O III]	4958.91	F1
			NGC 3132 $c(H\beta)^{Ba} = 0.20$		
	*	*	H 14	3721.94	
	*	*	[S III]	3721.63	
	4.90(+2)	5.51(+2)	[O II]	3726.03	
	*	*	[O II]	3728.82	
	*	*	H 13	3734.37	
3797.32	*	*	O III	3759.87	V2
3797.32	4.57	5.11	H 10	3797.90	H10
3867.99	1.06(+2)	1.18(+2)	[Ne III]	3868.75	F1
3888.03	2.23(+1)	2.47(+1)	He I	3888.65	V2
3967.30	4.60(+1)	5.06(+1)	[Ne III]	3967.46	F1
4009.21	2.80(−1)	3.07(−1)	He I	4009.26	V55
4025.89	2.66	2.91	He I	4026.21	V18
4068.20	5.76	6.28	[S II]	4068.60	F1
4069.36	3.74(−1)	4.09(−1)	O II	4069.62	V10
4072.07	1.36(−1)	1.48(−1)	O II	4072.16	V10
4075.46	3.29(−1)	3.59(−1)	O II	4075.86	V10
4075.95	1.75	1.91	[S II]	4076.35	F1
4084.95	3.97(−2)	4.33(−2)	O II	4085.11	V10
4096.95	3.33(−1)	3.62(−1)	N III	4097.33	V1
4101.33	2.37(+1)	2.58(+1)	H 6	4101.74	H6
4118.80	2.22(−2)	2.41(−2)	O II	4119.22	V20
	*	*	O II	4120.28	V20
	*	*	O II	4120.54	V20

Table 3 – *continued*

λ_{obs}	$F(\lambda)$	$I(\lambda)$	ID	λ_0	Mult
			NGC 3132		
4120.42	2.50(−1)	2.71(−1)	He I	4120.84	V16
	*	*	O II	4121.46	V19
4143.38	3.49(−1)	3.78(−1)	He I	4143.76	V53
4153.25	7.27(−2)	7.86(−2)	O II	4153.30	V19
4168.53	7.06(−2)	7.63(−2)	O II	4169.22	V19
4266.77	6.52(−1)	6.97(−1)	C II	4267.15	V6
4276.63	5.47(−2)	5.83(−2)	O II	4275.55	V67a
4303.36	9.51(−2)	1.01(−1)	O II	4303.61	V65a
4340.05	4.44(+1)	4.71(+1)	H 5	4340.47	H5
4345.32	7.47(−2)	7.92(−2)	O II	4345.56	V2
4349.19	5.41(−2)	5.73(−2)	O II	4349.43	V2
4362.82	4.06	4.30	[O III]	4363.21	F2
4365.91	4.10(−2)	4.33(−2)	O II	4366.89	V2
4371.84	3.04(−2)	3.21(−2)	O II	4371.62	V76b
4378.20	5.41(−2)	5.71(−2)	?		
4387.59	7.28(−1)	7.67(−1)	He I	4387.93	V51
4392.68	3.87(−2)	4.09(−2)	Ne II	4391.99	V55e
4436.95	6.27(−2)	6.57(−2)	He I	4437.55	V50
4438.30	4.30(−2)	4.51(−2)	?		
4471.10	5.88	6.14	He I	4471.50	V14
4491.12	5.07(−2)	5.29(−2)	O II	4491.23	V86a
4541.26	1.13(−1)	1.17(−1)	He II	4541.59	4.9
4562.25	3.33(−1)	3.44(−1)	Mg I]	4562.60	
4570.75	3.06(−1)	3.16(−1)	Mg I]	4571.10	
4599.08	4.98(−2)	5.13(−2)	?		
4621.36	3.21(−2)	3.30(−2)	N II	4621.39	
4630.61	4.00(−2)	4.11(−2)	N II	4630.54	V5
4633.11	5.98(−2)	6.14(−2)	?		
4712.90	6.01(−1)	6.17(−1)	N III	4634.14	V2
4638.39	1.01(−1)	1.04(−1)	O II	4638.86	V1
4640.17	2.37(−1)	2.43(−1)	N III	4640.64	V2
4641.36	1.68(−1)	1.71(−1)	O II	4641.81	V1
4648.91	1.62(−1)	1.65(−1)	O II	4649.13	V1
4650.62	1.19(−1)	1.22(−1)	O II	4650.84	V1
4658.09	1.99(−1)	2.03(−1)	[Fe III]	4658.10	F3
	*	*	C IV	4658.30	V8
4661.34	1.14(−1)	1.16(−1)	O II	4661.63	V1
4673.30	5.94(−2)	6.06(−2)	O II	4673.73	V1
4675.81	7.47(−2)	7.62(−2)	O II	4676.24	V1
4685.40	3.93	4.01	He II	4685.68	3.4
4695.78	2.82(−2)	2.88(−2)	O II	4696.35	V1
4701.45	4.91(−2)	5.00(−2)	[Fe III]	4701.62	F3
4711.10	4.49(−1)	4.57(−1)	[Ar IV]	4711.37	F1
4739.99	3.39(−1)	3.43(−1)	[Ar IV]	4740.17	F1
4755.26	3.69(−2)	3.74(−2)	[Fe III]	4754.83	
4769.16	3.35(−2)	3.38(−2)	[Fe III]	4769.40	3F
4777.53	3.50(−2)	3.53(−2)	[Fe III]	4777.88	V20
4861.13	1.00(+2)	1.00(+2)	H 4	4861.33	H4
4866.06	3.58(−2)	3.58(−2)	?		
4881.00	8.09(−2)	8.07(−2)	[Fe III]	4881.11	F2
4893.79	3.54(−2)	3.53(−2)	[Fe VII]	4893.90	F2
4910.55	4.45(−2)	4.43(−2)	?	*	
4921.78	1.56	1.55	He I	4921.93	V48
4924.38	7.12(−2)	7.07(−2)	O II	4924.53	V28
4930.70	8.98(−2)	8.91(−2)	[O III]	4931.80	F1
4932.31	5.00(−2)	4.97(−2)	?		
4958.07	2.70(+2)	2.67(+2)	[O III]	4958.91	F1
5005.99	8.03(+2)	7.89(+2)	[O III]	5006.84	F1
5190.28	7.08(−1)	6.82(−1)	[Ar III]	5191.82	F3
5198.30	1.08(+1)	1.04(+1)	[N I]	5199.84	F1
5282.08	3.70(−1)	3.53(−1)	ghost?		
5410.88	3.88(−1)	3.65(−1)	He II	5411.52	4.7
5517.08	1.19	1.11	[Cl III]	5517.66	F1

Table 3 – *continued*

λ_{obs}	$F(\lambda)$	$I(\lambda)$	ID	λ_0	Mult
			NGC 3132		
5537.01	9.73(−1)	9.05(−1)	[Cl III]	5537.60	F1
5576.60	7.37(−1)	6.83(−1)	[O I]	5577.34	F3
5676.01	2.70(−2)	2.49(−2)	N II	5676.02	V3
5678.50	8.68(−2)	7.99(−2)	N II	5679.56	V3
5754.04	8.91	8.15	[N II]	5754.60	F3
5875.09	1.80(+1)	1.63(+1)	He I	5875.66	V11
6300.10	4.21(+1)	3.70(+1)	[O I]	6300.34	F1
6311.86	2.73	2.40	[S III]	6312.10	F3
6363.54	1.47(+1)	1.28(+1)	[O I]	6363.78	F1
6547.80	2.37(+2)	2.05(+2)	[N II]	6548.10	F1
6562.47	3.32(+2)	2.86(+2)	H 3	6562.77	H3
6583.20	7.45(+2)	6.42(+2)	[N II]	6583.50	F1
6678.03	5.20	4.45	He I	6678.16	V46
6716.31	6.42(+1)	5.48(+1)	[S II]	6716.44	F2
6730.69	6.31(+1)	5.38(+1)	[S II]	6730.82	F2
7064.61	4.56(+0)	3.82	He I	7065.25	V10
7135.15	3.04(+1)	2.53(+1)	[Ar III]	7135.80	F1
7280.47	1.02(+0)	8.47(−1)	He I	7281.35	V45
7318.65	8.10(+0)	6.68	[O II]	7318.92	F2
7329.40	6.85(+0)	5.65	[O II]	7329.67	F2
			NGC 3242		
			$c(H\beta)^{Ba} = 0.10$		
	*	*	H 14	3721.94	
	*	*	[S III]	3721.63	
3726.73	1.36(+1)	1.44(+1)	[O II]	3726.03	
	*	*	[O II]	3728.82	
	*	*	H 13	3734.37	
3750.21	3.35	3.55	H 12	3750.15	H12
3757.30	1.43	1.51	O III	3759.87	V2
3759.93	2.36	2.50	O III	3759.87	V2
3770.69	4.05	4.28	H 11	3770.63	H11
3797.35	5.16	5.46	H 10	3797.90	H10
3819.00	1.04	1.09	He I	3819.62	V22
3834.91	7.03	7.43	H 9	3835.39	H9
3868.37	9.85(+1)	1.03(+2)	[Ne III]	3868.75	F1
3888.67	1.87(+1)	1.98(+1)	He I	3888.65	V2
3923.65	2.02(−1)	2.13(−1)	He II	3923.48	4.15
3967.07	4.30(+1)	4.51(+1)	[Ne III]	3967.46	F1
3998.55	1.94(−2)	2.03(−2)	N III	3998.63	V17
4003.60	2.26(−2)	2.37(−2)	N III	4003.58	V17
4009.20	1.65(−1)	1.73(−1)	He I	4009.26	V55
4012.03	1.52(−2)	1.59(−2)	?		
4026.02	2.16	2.26	He I	4026.21	V18
4041.28	1.21(−2)	1.28(−2)	N II	4041.31	V39b
4060.55	6.20(−3)	6.48(−3)	[F IV]	4060.00	
4067.67	1.79(−1)	1.87(−1)	C III	4067.94	V16
4068.40	2.29(−2)	2.40(−2)	[S II]	4068.60	F1
4068.77	2.35(−1)	2.45(−1)	C III	4068.91	V16
4069.56	1.75(−1)	1.83(−1)	O II	4069.62	V10
	*	*	O II	4069.89	V10
4070.10	3.07(−1)	3.21(−1)	C III	4070.26	
4071.96	2.06(−1)	2.15(−1)	O II	4072.16	V10
4075.66	1.59(−1)	1.66(−1)	O II	4075.86	V10
4076.15	7.55(−3)	7.89(−3)	[S II]	4076.35	F1
4078.58	2.03(−2)	2.13(−2)	O II	4078.84	V10
4080.84	1.33(−2)	1.39(−2)	O III	4081.10	
4083.59	2.02(−2)	2.11(−2)	O II	4083.90	V48b
4084.79	3.36(−2)	3.51(−2)	O II	4085.11	V10
4086.84	1.95(−2)	2.04(−2)	O II	4087.15	V48c
4088.97	1.06(−1)	1.11(−1)	O II	4089.29	V48a
4093.04	2.30(−2)	2.40(−2)	O II	4092.93	V10
4097.11	1.60	1.67	N III	4097.33	V1

λ_{obs}	$F(\lambda)$	$I(\lambda)$	ID	λ_0	Mult
			NGC 3242		
4101.52	2.55(+1)	2.66(+1)	H 6	4101.74	H6
4115.52	1.89(−2)	1.97(−2)	?		
4118.98	6.50(−2)	6.77(−2)	O II	4119.22	V20
4120.60	1.88(−1)	1.95(−1)	He I	4120.84	V16
4121.22	2.71(−2)	2.83(−2)	O II	4121.46	V19
4128.49	4.96(−2)	5.17(−2)	O II?	4129.32	V19
4131.97	2.02(−2)	2.10(−2)	O II	4132.80	V19
4143.51	3.04(−1)	3.16(−1)	He I	4143.76	V53
4152.93	2.92(−2)	3.04(−2)	O II	4153.30	V19
4156.16	3.58(−2)	3.73(−2)	O II?	4156.53	V19
4162.75	1.86(−2)	1.93(−2)	[K V]	4163.12	
4168.85	1.21(−2)	1.26(−2)	O II	4169.22	V19
4185.25	3.46(−2)	3.59(−2)	O II	4185.45	V36
4186.70	1.96(−1)	2.04(−1)	C III	4186.90	V18
4189.59	2.19(−2)	2.28(−2)	O II	4189.79	V36
4195.60	3.15(−2)	3.27(−2)	N III	4195.76	V6
4199.66	4.63(−1)	4.81(−1)	He II	4199.83	4.11
4215.64	1.07(−2)	1.11(−2)	?		
4219.32	1.75(−2)	1.82(−2)	Ne II	4219.37	V52a
	*	*	Ne II	4219.74	V52a
4227.32	1.03(−1)	1.07(−1)	N II	4227.74	V33
	*	*	N II	4236.91	V48a
4237.50	1.66(−2)	1.73(−2)	N II	4237.05	V48b
4253.67	1.62(−2)	1.67(−2)	O II	4254.00	V101
4266.96	6.00(−1)	6.20(−1)	C II	4267.15	V6
4275.31	3.00(−2)	3.10(−2)	O II	4275.55	V67a
	*	*	O II	4275.99	V67b
4276.16	2.66(−2)	2.76(−2)	O II	4276.28	V67b
	*	*	O II	4276.75	V67b
4277.41	1.66(−2)	1.72(−2)	O II	4277.43	V67c
	*	*	O II	4277.89	V67b
4282.78	8.37(−3)	8.65(−3)	O II	4282.96	V67c
4283.55	9.23(−3)	9.53(−3)	O II	4283.73	V67c
4285.51	1.16(−2)	1.20(−2)	O II	4285.69	V78b
4288.41	5.27(−3)	5.45(−3)	O II	4288.82	V53c
4291.21	1.56(−2)	1.62(−2)	O II	4291.25	V55
4292.17	8.29(−3)	8.55(−3)	O II	4292.21	V78c
4294.74	3.04(−2)	3.14(−2)	O II	4294.78	V53b
4303.64	5.64(−2)	5.82(−2)	O II	4303.61	V65a
4307.11	8.40(−3)	8.70(−3)	O II	4307.23	V53b
4313.14	8.30(−3)	8.56(−3)	O II	4313.44	V78a
4317.02	4.40(−2)	4.54(−2)	O II	4317.14	V2
	*	*	O II	4317.70	V53a
4319.23	2.20(−2)	2.27(−2)	O II	4319.63	V2
4325.54	3.01(−2)	3.11(−2)	O II	4325.76	V2
4340.25	4.61(+1)	4.74(+1)	H 5	4340.47	H5
4344.95	8.56(−2)	8.81(−2)	O II	4345.56	V2
4349.30	6.92(−2)	7.12(−2)	O II	4349.43	V2
4353.91	9.50(−3)	9.78(−3)	O II	4353.59	V76c
4357.57	1.76(−2)	1.82(−2)	O II	4357.25	V63a
4362.99	1.32(+1)	1.36(+1)	[O III]	4363.21	F2
4362.65	1.32(+1)	1.35(+1)	[O III]	4363.21	F2
4366.76	8.84(−2)	9.09(−2)	O II	4366.89	V2
4369.73	2.97(−2)	3.05(−2)	Ne II	4369.86	V56
4376.56	2.53(−2)	2.60(−2)	?		
4378.98	1.54(−1)	1.58(−1)	N III	4379.11	V18
4385.83	2.71(−2)	2.78(−2)	O II	4386.01	
4387.75	4.31(−1)	4.42(−1)	He I	4387.93	V51
4391.81	1.90(−2)	1.95(−2)	Ne II	4391.99	V55e
4409.03	1.81(−2)	1.86(−2)	Ne II	4409.30	V55e
4414.63	3.40(−2)	3.49(−2)	O II	4414.90	V5
4416.70	3.22(−2)	3.31(−2)	O II	4416.97	V5
4428.32	8.46(−3)	8.67(−3)	Ne II	4428.64	V60c
4430.74	9.13(−3)	9.35(−3)	Ne II	4430.94	V61a

Table 3 – *continued*

λ_{obs}	$F(\lambda)$	$I(\lambda)$	ID	λ_0	Mult
			NGC 3242		
4437.35	5.09(−2)	5.21(−2)	He I	4437.55	V50
4442.12	4.68(−3)	4.80(−3)	N II	4442.02	V55a
4448.11	1.18(−2)	1.21(−2)	O II	4448.19	V35
4453.50	1.74(−2)	1.79(−2)	O II	4452.37	V5
4458.18	1.78(−2)	1.82(−2)	Ne II	4457.24	V61d
4465.79	2.54(−2)	2.60(−2)	O II	4466.42	V86b
4471.29	4.03	4.12	He I	4471.50	V14
4477.70	1.41(−2)	1.45(−2)	O II	4477.90	V88
4481.01	2.18(−2)	2.22(−2)	Mg II	4481.21	V4
4488.05	9.83(−3)	1.00(−2)	O II	4488.20	V104
4489.34	5.39(−3)	5.51(−3)	O II	4489.49	V86b
4491.08	2.30(−2)	2.35(−2)	O II	4491.23	V86a
4510.76	7.98(−2)	8.14(−2)	N III	4510.91	V3
4514.71	2.18(−2)	2.22(−2)	N III	4514.86	V3
4518.00	2.04(−2)	2.08(−2)	N III	4518.15	V3
4523.39	1.76(−2)	1.79(−2)	N III	4523.58	V3
4534.39	2.59(−2)	2.63(−2)	N III	4534.58	V3
4541.40	8.40(−1)	8.55(−1)	He II	4541.59	4.9
4544.61	3.89(−2)	3.96(−2)	N III	4544.80	
4562.43	4.98(−2)	5.06(−2)	Mg I]	4562.60	
4570.93	8.34(−2)	8.48(−2)	Mg I]	4571.10	
4590.85	2.83(−2)	2.87(−2)	O II	4590.97	V15
4596.06	2.12(−2)	2.15(−2)	O II	4596.18	V15
4601.96	4.91(−3)	4.98(−3)	N II	4601.48	V5
4609.42	2.24(−2)	2.27(−2)	O II	4609.44	V92a
4610.18	2.30(−2)	2.33(−2)	O II	4610.20	V92c
4620.00	9.67(−3)	9.80(−3)	N II?	4621.39	V5
4630.69	1.76(−2)	1.79(−2)	N II	4630.54	V5
4633.96	8.23(−1)	8.34(−1)	N III	4634.14	V2
4638.68	1.67(−1)	1.69(−1)	O II	4638.86	V1
4640.46	1.55	1.57	N III	4640.64	V2
4641.63	2.12(−1)	2.15(−1)	O II	4641.81	V1
4647.27	3.24(−1)	3.27(−1)	C III	4647.42	V1
4648.98	2.20(−1)	2.23(−1)	O II	4649.13	V1
4650.10	1.94(−1)	1.96(−1)	C III	4650.25	V1
4650.69	9.66(−2)	9.79(−2)	O II	4650.84	V1
4651.32	6.48(−2)	6.55(−2)	C III	4651.47	V1
4658.01	7.64(−2)	7.73(−2)	[Fe III]	4658.10	F3
	*	*	C IV	4658.30	V8
4661.54	8.59(−2)	8.70(−2)	O II	4661.63	V1
4669.14	1.18(−2)	1.19(−2)	O II	4669.27	V89b
4673.60	3.00(−2)	3.04(−2)	O II	4673.73	V1
4676.11	5.67(−2)	5.74(−2)	O II	4676.24	V1
4685.59	2.55(+1)	2.57(+1)	He II	4685.68	3.4
4699.30	5.80(−3)	5.85(−3)	O II	4699.22	V25
4699.21	6.70(−3)	6.76(−3)	[Fe III]	4701.62	F3
4711.25	4.85	4.89	[Ar IV]	4711.37	F1
4713.05	5.62(−1)	5.67(−1)	He I	4713.17	V12
4724.05	4.89(−2)	4.93(−2)	[Ne IV]	4724.15	F1
4725.52	4.03(−2)	4.07(−2)	[Ne IV]	4725.62	F1
4740.12	4.49	4.52	[Ar IV]	4740.17	F1
4789.74	1.02(−2)	1.03(−2)	N II	4788.13	V20
4797.67	1.64(−2)	1.64(−2)	?		
4802.52	1.90(−2)	1.91(−2)	C II	4802.23	
4861.28	1.00(+2)	1.00(+2)	H 4	4861.33	H4
4906.89	1.86(−2)	1.86(−2)	O II	4906.83	V28
4921.91	1.02	1.02	He I	4921.93	V48
4931.28	1.77(−1)	1.76(−1)	[O III]	4931.80	F1
4934.63	1.19(−2)	1.18(−2)	?		
4958.37	4.29(+2)	4.27(+2)	[O III]	4958.91	F1
5006.30	1.30(+3)	1.28(+3)	[O III]	5006.84	F1
5130.26	5.31(−2)	5.23(−2)	?		
5190.80	1.23(−1)	1.21(−1)	[Ar III]	5191.82	F3

Table 3 – *continued*

λ_{obs}	$F(\lambda)$	$I(\lambda)$	ID	λ_0	Mult
			NGC 3242		
5303.80	3.70(−2)	3.61(−2)	?		
5342.19	4.15(−2)	4.03(−2)	C II		
5345.20	7.80(−2)	7.59(−2)	[Kr IV]	5345.90	
5411.06	1.97	1.91	He II	5411.52	4.7
5517.36	3.29(−1)	3.17(−1)	[Cl III]	5517.66	F1
5537.29	2.88(−1)	2.77(−1)	[Cl III]	5537.60	F1
5576.67	3.70(−2)	3.56(−2)	[O I]	5577.34	F3
5591.52	5.27(−2)	5.07(−2)	O III	5592.37	V5
5666.60	3.35(−2)	3.21(−2)	N II	5666.63	V3
5676.00	1.40(−2)	1.34(−2)	N II	5676.02	V3
5679.46	4.46(−2)	4.28(−2)	N II	5679.56	V3
5754.10	6.63(−2)	6.34(−2)	[N II]	5754.60	F3
5801.00	1.08(−1)	1.03(−1)	C IV	5801.51	V1
5811.63	9.16(−2)	8.74(−2)	C IV	5812.14	V1
5875.26	1.22(+1)	1.16(+1)	He I	5875.66	V11
5913.18	2.05(−2)	1.95(−2)	He II	5913.26	5.26
5931.76	1.15(−2)	1.09(−2)	He II	5931.84	5.25
5952.86	1.82(−2)	1.73(−2)	He II	5952.94	5.24
5975.14	2.00(−2)	1.90(−2)	?		
6004.90	4.85(−2)	4.59(−2)	He II	6004.73	5.22
6036.87	5.16(−2)	4.88(−2)	He II	6036.70	5.21
6074.27	5.01(−2)	4.73(−2)	He II	6074.10	5.20
6101.57	2.88(−1)	2.71(−1)	[K IV]	6101.83	F1
6118.37	6.34(−2)	5.98(−2)	He II	6118.20	5.19
6152.59	1.97(−2)	1.86(−2)	C II	6151.43	V16.04
6171.70	4.34(−2)	4.09(−2)	He II	6170.60	5.18
6234.91	7.54(−2)	7.09(−2)	He II	6233.80	5.17
6299.99	4.98(−2)	4.67(−2)	[O I]	6300.34	F1
6311.93	6.74(−1)	6.31(−1)	[S III]	6312.10	F3
6407.45	1.18(−1)	1.10(−1)	He II	6406.30	5.15
6435.37	4.43(−2)	4.13(−2)	[Ar v]	6435.09	
6461.46	6.79(−2)	6.32(−2)	C II	6461.95	
6527.18	1.56(−1)	1.45(−1)	He II	6527.11	5.14
6548.19	1.06	9.85(−1)	[N II]	6548.10	F1
6562.86	3.10(+2)	2.88(+2)	H 3	6562.77	H3
6583.59	2.83	2.63	[N II]	6583.50	F1
6678.41	3.44	3.19	He I	6678.16	V46
6716.69	3.00(−1)	2.78(−1)	[S II]	6716.44	F2
6731.07	4.24(−1)	3.92(−1)	[S II]	6730.82	F2
6780.76	2.56(−2)	2.36(−2)	?		
6794.47	6.72(−2)	6.20(−2)	[K IV]	6795.00	F1
6862.64	2.77(−1)	2.55(−1)	?		
6891.16	1.67(−1)	1.53(−1)	He II	6890.88	7
7006.03	9.12(−2)	8.35(−2)	[Ar v]	7005.74	
7065.03	3.23	2.95	He I	7065.25	V10
7135.58	7.66	6.99	[Ar III]	7135.80	F1
7170.23	1.17(−1)	1.07(−1)	[Ar IV]	7170.62	F2
7177.11	1.92(−1)	1.75(−1)	He II	7177.50	5.11
7236.27	2.89(−1)	2.63(−1)	C II	7236.42	V3
7262.61	1.37(−1)	1.24(−1)	[Ar IV]	7262.76	F2
7281.20	4.65(−1)	4.23(−1)	He I	7281.35	V45
7318.85	5.55(−1)	5.04(−1)	[O II]	7318.92	F2
7329.59	4.41(−1)	4.00(−1)	[O II]	7329.67	F2
			NGC 3918		
			$c(H\beta)^{Ba} = 0.44$		
	*	*	H 14	3721.94	H14
3726.46	7.30(+1)	9.45(+1)	[O II]	3726.03	F1
	*	*	[O II]	3728.82	F1
	*	*	H 13	3734.37	H13
3749.69	2.87	3.70	H 12	3750.15	H12
3759.41	3.97	5.11	O III	3759.87	V2
3770.07	3.17	4.07	H 11	3770.63	H11
3797.23	4.40	5.62	H 10	3797.90	H10
3819.14	5.50(−1)	7.00(−1)	He I	3819.62	V22

Table 3 – *continued*

λ_{obs}	$F(\lambda)$	$I(\lambda)$	ID	λ_0	Mult
			NGC 3918		
3834.62	6.09	7.73	H 9	3835.39	H9
3867.98	1.07(+2)	1.35(+2)	[Ne III]	3868.75	F1
3888.09	1.57(+1)	1.98(+1)	He I	3888.65	V2
3922.02	2.50(−1)	3.11(−1)	He II	3923.48	4.15
3967.20	4.65(+1)	5.75(+1)	[Ne III]	3967.46	F1
4008.79	1.10(−1)	1.34(−1)	He I	4009.26	V55
4025.64	1.86	2.27	He I	4026.21	V18
4040.83	1.10(−2)	1.34(−2)	N II	4041.31	V39b
4059.65	3.10(−2)	3.75(−2)	O II	4060.60	
4067.99	1.63	1.97	[S II]	4068.60	F1
4069.17	4.40(−1)	5.33(−1)	O II	4069.62	V10
4071.55	1.96(−1)	2.37(−1)	O II	4072.16	V10
4075.25	5.44(−2)	6.57(−2)	O II	4075.86	V10
4075.74	5.93(−1)	7.17(−1)	[S II]	4076.35	F1
4083.46	2.29(−2)	2.77(−2)	O II	4083.90	V48b
4084.67	1.60(−2)	1.93(−2)	O II	4085.11	V10
4087.12	1.98(−2)	2.39(−2)	O II	4087.15	V48c
4088.85	4.65(−2)	5.60(−2)	O II	4089.29	V48a
4096.84	1.80	2.16	N III	4097.33	V1
4101.20	2.33(+1)	2.79(+1)	H 6	4101.74	H6
4118.62	5.10(−2)	6.10(−2)	O II	4119.22	V20
	*	*	O II	4120.28	V20
4120.24	1.71(−1)	2.05(−1)	He I	4120.84	V16
4121.91	7.69(−2)	9.20(−2)	O II	4121.46	V19
4128.18	2.30(−2)	2.74(−2)	O II?	4129.32	V19
4131.76	1.51(−2)	1.80(−2)	O II	4132.80	V19
4143.18	2.80(−1)	3.33(−1)	He I	4143.76	V53
4152.63	2.19(−2)	2.60(−2)	O II	4153.30	V19
4155.84	3.12(−2)	3.70(−2)	O II	4156.53	V19
4162.78	5.70(−2)	6.74(−2)	[K V]	4163.30	F1
4168.17	3.81(−3)	4.50(−3)	O II	4169.22	V19
4184.89	3.18(−2)	3.74(−2)	O II	4185.45	V36
4186.34	1.29(−1)	1.51(−1)	C III	4186.90	V18
4189.23	3.27(−2)	3.84(−2)	O II	4189.79	V36
4195.17	1.70(−2)	1.99(−2)	N III	4195.76	V6
4199.32	6.90(−1)	8.10(−1)	He II	4199.83	4.11
4219.20	6.80(−3)	7.94(−3)	Ne II	4219.74	V52a
4226.95	2.20(−1)	2.56(−1)	N II	4227.74	V33
4237.30	1.40(−2)	1.63(−2)	N II	4237.05	V48b
4241.13	1.40(−2)	1.63(−2)	N II	4241.78	V48a
4253.53	1.10(−2)	1.27(−2)	O II	4254.00	V101
4266.62	4.30(−1)	4.97(−1)	C II	4267.15	V6
4275.21	2.63(−2)	3.03(−2)	O II	4275.55	V67a
	*	*	O II	4275.99	V67b
4276.19	1.19(−2)	1.37(−2)	O II	4276.75	V67b
4276.87	8.06(−3)	9.29(−3)	O II	4277.43	V67c
4291.09	2.12(−2)	2.43(−2)	O II	4291.25	V55
4294.62	2.21(−2)	2.53(−2)	O II	4294.78	V53b
4303.35	2.00(−2)	2.29(−2)	O II	4303.83	V53a
4316.71	3.65(−2)	4.17(−2)	O II	4317.14	V2
4319.20	1.49(−2)	1.70(−2)	O II	4319.63	V2
4325.33	1.24(−2)	1.41(−2)	O II	4325.76	V2
4339.89	4.33(+1)	4.92(+1)	H 5	4340.47	H5
4349.00	5.63(−2)	6.38(−2)	O II	4349.43	V2
4362.64	1.90(+1)	2.15(+1)	[O III]	4363.21	F2
4376.53	2.80(−2)	3.15(−2)	?		
4378.68	1.30(−1)	1.46(−1)	N III	4379.11	V18
4387.39	3.77(−1)	4.23(−1)	He I	4387.93	V51
4391.45	1.92(−2)	2.15(−2)	Ne II	4391.99	V55e
4408.70	2.23(−2)	2.49(−2)	Ne II	4409.30	V55e
4414.30	4.64(−2)	5.18(−2)	O II	4414.90	V5
4416.37	2.60(−2)	2.90(−2)	O II	4416.97	V5
4428.11	8.51(−3)	9.46(−3)	Ne II	4428.64	V60c
4434.28	2.70(−2)	3.00(−2)	N II	4433.48	V55b

Table 3 – *continued*

λ_{obs}	$F(\lambda)$	$I(\lambda)$	ID	λ_0	Mult
			NGC 3918		
4437.02	4.58(−2)	5.08(−2)	He I	4437.55	V50
4448.19	1.59(−2)	1.76(−2)	O II	4448.19	V35
4452.37	5.90(−2)	6.53(−2)	O II	4452.37	V5
4458.10	3.40(−2)	3.75(−2)	Ne II	4457.05	V61d
4465.13	2.20(−2)	2.42(−2)	O II	4466.42	V86b
4470.93	3.53	3.88	He I	4471.50	V14
4480.62	1.10(−2)	1.20(−2)	Mg II	4481.21	V4
4490.55	1.40(−2)	1.53(−2)	C II	4491.07	
4510.36	7.94(−2)	8.65(−2)	N III	4510.91	V3
4514.31	2.23(−2)	2.42(−2)	N III	4514.86	V3
4517.60	2.16(−2)	2.35(−2)	N III	4518.15	V3
4523.03	1.70(−2)	1.84(−2)	N III	4523.58	V3
4529.86	1.36(−2)	1.48(−2)	N II	4530.41	V58b
4534.03	2.99(−1)	3.24(−1)	N III	4534.58	V3
4541.03	1.40	1.51	He II	4541.59	4.9
4544.24	2.73(−2)	2.95(−2)	N III	4544.80	
4552.24	1.30(−2)	1.40(−2)	N II	4552.53	V58a
4562.01	1.24(−1)	1.33(−1)	Mg I]	4562.60	
4570.51	4.42(−1)	4.74(−1)	Mg I]	4571.10	
4590.54	3.81(−2)	4.08(−2)	O II	4590.97	V15
4595.75	2.57(−2)	2.75(−2)	O II	4596.18	V15
4606.04	6.20(−2)	6.60(−2)	N IV	4606.33	
4609.09	3.55(−2)	3.77(−2)	O II	4610.20	V92c
4619.68	1.60(−2)	1.69(−2)	N V	4619.98	V1
4624.75	4.40(−2)	4.66(−2)	[Ar V]	4624.54	
4629.97	6.88(−2)	7.28(−2)	N II	4630.54	V5
4631.71	1.41(−1)	1.50(−1)	O IV	4631.89	V1
4633.58	1.44	1.53	N III	4634.14	V2
4638.30	2.08(−1)	2.20(−1)	O II	4638.86	V1
4640.08	2.95	3.12	N III	4640.64	V2
4641.25	2.05(−1)	2.17(−1)	O II	4641.81	V1
4646.84	2.08(−1)	2.19(−1)	C III	4647.42	V1
4648.55	2.00(−1)	2.11(−1)	O II	4649.13	V1
4649.67	1.32(−1)	1.39(−1)	C III	4650.25	V1
4650.26	3.93(−2)	4.15(−2)	O II	4650.84	V1
4650.89	5.51(−2)	5.80(−2)	C III	4651.47	V1
4657.74	3.15(−1)	3.32(−1)	[Fe III]	4658.10	F3
	*	*	C IV	4658.30	V8
4661.07	7.07(−2)	7.43(−2)	O II	4661.63	V1
4665.25	1.35(−2)	1.41(−2)	C III	4665.90	
4668.90	1.16(−2)	1.21(−2)	O II	4669.27	V89b
4673.36	2.96(−2)	3.10(−2)	O II	4673.73	V1
4675.87	6.26(−2)	6.56(−2)	O II	4676.24	V1
4679.81	6.40(−2)	6.69(−2)	?		
4685.21	3.98(+1)	4.16(+1)	He II	4685.68	3.4
4701.14	1.70(−2)	1.76(−2)	[Fe III]	4701.62	F3
4710.86	5.94	6.16	[Ar IV]	4711.37	F1
4712.66	8.40(−1)	8.71(−1)	He I	4713.17	V12
4723.60	5.60(−1)	5.79(−1)	[Ne IV]	4724.15	F1
4725.07	4.83(−1)	4.99(−1)	[Ne IV]	4725.62	F1
4739.73	7.40	7.62	[Ar IV]	4740.17	F1
4754.27	8.20(−3)	8.41(−3)	[Fe III]	4754.83	
4769.28	2.10(−2)	2.14(−2)	?		
4802.99	2.60(−2)	2.63(−2)	C II	4802.23	
4860.89	1.00(+2)	1.00(+2)	H 4	4861.33	H4
4880.60	3.20(−2)	3.18(−2)	[Fe III]	4881.11	F2
4905.88	9.80(−3)	9.69(−3)	O II	4906.83	V28
4921.52	9.50(−1)	9.35(−1)	He I	4921.93	V48
4930.85	2.10(−1)	2.06(−1)	[O III]	4931.80	F1
4958.00	5.62(+2)	5.48(+2)	[O III]	4958.91	F1
5005.93	1.71(+3)	1.65(+3)	[O III]	5006.84	F1
5189.94	2.62(−1)	2.41(−1)	[Ar III]	5191.82	F3
5197.96	6.83(−1)	6.28(−1)	[N I]	5199.84	F1

Table 3 – *continued*

λ_{obs}	$F(\lambda)$	$I(\lambda)$	ID	λ_0	Mult
			NGC 3918		
5410.60	3.48	3.04	He II	5411.52	4.7
5516.79	6.40(−1)	5.48(−1)	[Cl III]	5517.66	F1
5536.98	9.20(−1)	7.85(−1)	[Cl III]	5537.60	F1
5591.58	7.60(−2)	6.42(−2)	O III	5592.37	V5
5753.69	2.11	1.73	[N II]	5754.60	F3
5800.81	1.20(−1)	9.78(−1)	C IV	5801.51	V1
5874.81	1.34(+1)	1.08(+1)	He I	5875.66	V11
6086.35	1.40(−1)	1.09(−1)	[Fe VII]	6086.90	
6101.17	4.50(−1)	3.49(−1)	[K IV]	6101.83	F1
6170.07	9.50(−2)	7.30(−2)	He II	6170.60	5.18
6233.27	1.20(−1)	9.13(−2)	He II	6233.80	5.17
6299.76	6.96	5.24	[O I]	6300.34	F1
6311.44	3.02	2.27	[S III]	6312.10	F3
6363.34	2.38	1.77	[O I]	6363.78	F1
6406.11	2.30(−1)	1.70(−1)	He II	6406.30	5.15
6434.64	1.07	7.89(−1)	[Ar V]	6435.10	
6527.11	2.10(−1)	1.53(−1)	He II	6527.11	5.14
6547.62	3.64(+1)	2.64(+1)	[N II]	6548.10	F1
6562.27	4.19(+2)	3.04(+2)	H 3	6562.77	H3
6583.00	1.15(+2)	8.36(+1)	[N II]	6583.50	F1
6678.00	4.03	2.87	He I	6678.16	V46
6716.04	4.08	2.89	[S II]	6716.44	F2
6730.41	7.12	5.03	[S II]	6730.82	F2
7005.19	2.21	1.50	[Ar V]	7005.67	
7064.61	5.69	3.85	He I	7065.25	V10
7134.99	2.59(+1)	1.74(+1)	[Ar III]	7135.80	F1
7169.84	4.62(−1)	3.08(−1)	[Ar IV]	7170.62	F2
7176.65	5.33(−1)	3.55(−1)	He II	7177.50	5.11
7236.26	5.50(−1)	3.64(−1)	C II	7236.42	V3
7262.28	3.10(−1)	2.04(−1)	[Ar IV]	7262.76	F2
7280.48	6.80(−1)	4.48(−1)	He I	7281.35	V45
7318.44	5.99	3.93	[O II]	7318.92	F2
7329.28	5.30	3.47	[O II]	7329.67	F2
			NGC 5315		
			$c(H\beta)^{Ba} = 0.70$		
	*	*	[S III]	3721.63	F2
	*	*	H 14	3721.94	H14
3725.79	4.01(+1)	6.06(+1)	[O II]	3726.03	F1
	*	*	[O II]	3728.82	F1
	*	*	H 13	3734.37	H13
3749.33	1.88	2.82	H 12	3750.15	H12
3769.57	2.85	4.25	H 11	3770.63	H11
3797.03	3.47	5.14	H 10	3797.90	H10
3817.43	1.03	1.51	He I	3819.62	V22
3834.04	6.16	9.02	H 9	3835.39	H9
3867.55	4.73(+1)	6.86(+1)	[Ne III]	3868.75	F1
3887.64	1.26(+1)	1.82(+1)	He I	3888.65	V2
3967.15	2.60(+1)	3.65(+1)	[Ne III]	3967.46	F1
4008.44	1.92(−1)	2.66(−1)	He I	4009.26	V55
4025.38	2.26	3.11	He I	4026.21	V18
4040.42	4.18(−2)	5.73(−2)	N II	4041.31	V39b
4067.63	4.20	5.69	[S II]	4068.60	F1
4068.79	3.14(−1)	4.26(−1)	O II	4069.62	V10
4071.19	1.38(−1)	1.88(−1)	O II	4072.16	V10
4074.89	1.04(−1)	1.41(−1)	O II	4075.86	V10
4075.38	1.51	2.04	[S II]	4076.35	F1
4082.97	1.78(−2)	2.41(−2)	O II	4083.90	V48b
4084.18	3.24(−2)	4.37(−2)	O II	4085.11	V10
4086.22	2.36(−2)	3.19(−2)	O II	4087.15	V48c
4088.36	6.67(−2)	8.99(−2)	O II	4089.29	V48a
4096.68	2.30(−1)	3.08(−1)	N III	4097.33	V1
4100.80	1.97(+1)	2.65(+1)	H 6	4101.74	H6
4109.04	1.06(−2)	1.41(−2)	O II	4110.78	V20

Table 3 – *continued*

λ_{obs}	$F(\lambda)$	$I(\lambda)$	ID	λ_0	Mult
			NGC 5315		
4119.70	2.48(−1)	3.30(−1)	O II	4119.22	V20
	*	*	O II	4120.28	V20
	*	*	O II	4120.54	V20
4121.32	3.90(−2)	5.20(−2)	He I	4120.84	V16
	*	*	O II	4121.46	V19
4131.68	5.50(−2)	7.29(−2)	O II	4132.80	V19
4142.89	3.80(−1)	5.01(−1)	He I	4143.76	V53
4152.27	6.92(−2)	9.10(−2)	O II	4153.30	V19
4155.50	6.36(−2)	8.36(−2)	O II	4156.53	V19
4167.97	7.09(−2)	9.27(−2)	O II	4169.22	V19
4184.47	4.04(−2)	5.25(−2)	O II	4185.45	V36
4185.92	8.24(−3)	1.07(−2)	C III	4186.90	V18
4188.81	5.16(−2)	6.70(−2)	O II	4189.79	V36
4218.93	1.10(−2)	1.41(−2)	Ne II	4219.74	V52a
4236.04	1.30(−2)	1.66(−2)	N II	4237.05	V48b
4240.99	3.30(−2)	4.22(−2)	N II	4241.24	V48a
	*	*	N II	4241.78	V48a
4252.87	2.50(−2)	3.16(−2)	O II	4254.00	V101
4266.15	5.59(−1)	7.06(−1)	C II	4267.15	V6
4274.54	8.37(−2)	1.01(−1)	O II	4275.55	V67a
4302.82	2.65(−2)	3.31(−2)	O II	4303.82	V53a
4316.19	5.60(−2)	6.94(−2)	O II	4317.14	V2
	*	*	O II	4317.70	V53a
4318.68	3.97(−2)	4.91(−2)	O II	4319.63	V2
4324.96	1.54(−2)	1.91(−2)	O II	4325.76	V2
4339.50	3.95(+1)	4.85(+1)	H 5	4340.47	H5
4344.58	5.18(−2)	6.35(−2)	O II	4345.56	V2
4348.45	6.08(−2)	7.44(−2)	O II	4349.43	V2
4362.26	3.21	3.91	[O III]	4363.21	F2
4366.73	4.84(−2)	5.89(−2)	O II	4366.89	V2
4386.98	6.30(−1)	7.58(−1)	He I	4387.93	V51
4390.89	1.40(−2)	1.68(−2)	Ne II	4391.99	V55e
4396.89	1.60(−2)	1.92(−2)	Ne II	4397.99	V57b
4408.71	1.00(−2)	1.19(−2)	Ne II	4409.30	V55e
4412.18	2.05(−2)	2.45(−2)	Ne II	4413.22	V65
4413.86	6.04(−2)	7.21(−2)	O II	4414.90	V5
4415.93	5.20(−2)	6.20(−2)	O II	4416.97	V5
4436.61	5.40(−2)	6.38(−2)	He I	4437.55	V50
4324.76	1.23(−2)	1.46(−2)	O II	4452.37	V5
4470.52	5.57	6.49	He I	4471.50	V14
4480.30	1.80(−2)	2.09(−2)	Mg II	4481.21	V4
4490.40	1.40(−2)	1.62(−2)	C II	4491.07	
4529.05	4.80(−2)	5.47(−2)	N II	4530.41	V58b
4551.59	2.38(−2)	2.69(−2)	N II	4552.53	V58a
4570.07	2.05(−1)	2.30(−1)	Mg I]	4571.10	
4590.06	7.13(−2)	7.93(−2)	O II	4590.97	V15
4595.27	5.26(−2)	5.84(−2)	O II	4596.18	V15
4600.59	5.10(−2)	5.65(−2)	N II	4601.48	V5
4606.27	4.81(−2)	5.32(−2)	N II	4607.16	V5
4608.54	4.31(−2)	4.76(−2)	O II	4609.44	V92a
	*		O II	4610.20	V92c
4624.96	3.26(−2)	3.59(−2)	[Ar V]	4624.54	
4629.65	1.10(−1)	1.20(−1)	N II	4630.54	V5
4633.32	1.13(−1)	1.24(−1)	N III	4634.14	V2
4638.04	1.59(−1)	1.74(−1)	O II	4638.86	V1
4639.82	2.37(−1)	2.59(−1)	N III	4640.64	V2
4640.99	2.18(−1)	2.37(−1)	O II	4641.81	V1
	*		N III	4641.84	V2
4648.17	3.28(−1)	3.57(−1)	O II	4649.13	V1
4649.88	8.28(−2)	9.00(−2)	O II	4650.84	V1
4657.05	2.91(−1)	3.15(−1)	[Fe III]	4658.10	F3
	*	*	C IV	4658.30	V8
4660.58	8.28(−2)	8.97(−2)	O II	4661.63	V1

Table 3 – *continued*

λ_{obs}	$F(\lambda)$	$I(\lambda)$	ID	λ_0	Mult
			NGC 5315		
4672.77	1.26(−2)	1.37(−2)	O II	4673.73	V1
4675.28	7.33(−2)	7.89(−2)	O II	4676.24	V1
4677.18	2.90(−2)	3.12(−2)	N II	4678.14	V61b
4684.78	4.70(−2)	5.04(−2)	He II	4685.68	3.4
4698.92	2.34(−2)	2.49(−2)	O II	4699.22	V25
4700.66	6.72(−2)	7.15(−2)	[Fe III]	4701.62	F3
4712.20	7.90(−1)	8.38(−1)	[Ar IV]	4711.37	F1
4732.86	3.70(−2)	3.89(−2)	?		
4739.46	1.80(−1)	1.88(−1)	[Ar IV]	4740.17	F1
4753.58	4.50(−3)	4.69(−3)	[Fe III]	4754.83	
4768.69	2.00(−2)	2.07(−2)	?		
4802.07	1.34(−2)	1.37(−2)	C II	4802.23	
4803.15	2.64(−2)	2.71(−2)	N II	4803.29	V20
4814.15	1.90(−2)	1.93(−2)	S II	4815.55	V9
4860.43	1.00(+2)	1.00(+2)	H 4	4861.33	H4
4880.05	1.20(−1)	1.19(−1)	[Fe III]	4881.11	F2
4889.81	2.30(−2)	2.27(−2)	O II	4890.86	V28
4905.90	3.43(−2)	3.37(−2)	O II	4906.83	V28
4921.06	1.69	1.65	He I	4921.93	V48
4930.28	9.50(−2)	9.23(−2)	[O III]	4931.80	F1
4957.55	2.72(+2)	2.62(+2)	[O III]	4958.91	F1
5005.47	8.41(+2)	7.94(+2)	[O III]	5006.84	F1
5189.23	1.65(−1)	1.44(−1)	[Ar III]	5191.82	F3
5197.25	1.26	1.10	[N I]	5199.84	F1
5516.32	3.50(−1)	2.73(−1)	[Cl III]	5517.66	F1
5536.25	9.49(−1)	7.36(−1)	[Cl III]	5537.60	F1
5269.97	1.80(−1)	1.53(−1)	?		
5665.14	1.20(−1)	8.98(−2)	N II	5666.63	V3
5678.13	3.20(−1)	2.38(−1)	N II	5679.56	V3
5753.23	6.18	4.51	[N II]	5754.60	F3
5874.26	2.67(+1)	1.89(+1)	He I	5875.66	V11
6299.16	8.45	5.36	[O I]	6300.34	F1
6310.96	5.03	3.18	[S III]	6312.10	F3
6345.67	9.90(−2)	6.21(−2)	Si II	6347.10	V2
6362.69	2.90	1.81	[O I]	6363.78	F1
6460.91	1.10(−1)	6.72(−2)	C II	6461.95	
6546.94	1.09(+2)	6.52(+1)	[N II]	6548.10	F1
6561.73	4.95(+2)	2.95(+2)	H 3	6562.77	H3
6582.46	3.44(+2)	2.04(+2)	[N II]	6583.50	F1
6677.00	8.66	5.03	He I	6678.16	V46
6715.28	9.20	5.30	[S II]	6716.44	F2
6729.66	1.74(+1)	1.00(+1)	[S II]	6730.82	F2
7063.78	1.52(+1)	8.17	He I	7065.25	V10
7134.31	5.31(+1)	2.80(+1)	[Ar III]	7135.80	F1
7153.35	2.40(−1)	1.26(−1)	?		
7233.23	7.90(−1)	4.09(−1)	C II	7236.42	V3
7279.63	1.46	7.49(−1)	He I	7281.35	V45
7317.73	1.22(+1)	6.25	[O II]	7318.92	F2
7328.48	1.10(+1)	5.62	[O II]	7329.67	F2
			NGC 5882		
			$c(H\beta)^{Ba} = 0.52$		
3671.78	3.35(−1)	4.62(−1)	H 24	3671.48	H24
3674.04	3.54(−1)	4.88(−1)	H 23	3673.74	H23
3676.66	3.81(−1)	5.25(−1)	H 22	3676.36	H22
3679.66	4.22(−1)	5.81(−1)	H 21	3679.36	H21
3683.12	4.56(−1)	6.28(−1)	?		
3683.12	4.56(−1)	6.28(−1)	H 20	3682.81	H20
3687.14	5.39(−1)	7.41(−1)	H 19	3686.83	H19
3691.87	6.13(−1)	8.41(−1)	H 18	3691.56	H18
3697.46	6.98(−1)	9.57(−1)	H 17	3697.15	H17
3703.89	9.03(−1)	1.23	H 16	3703.86	H16
3705.05	7.42(−1)	1.01	He I	3705.02	V25
3707.28	2.39(−1)	3.27(−1)	O III	3707.25	V14

Table 3 – *continued*

λ_{obs}	$F(\lambda)$	$I(\lambda)$	ID	λ_0	Mult
			NGC 5882		
3712.33	1.17	1.61	H 15	3711.97	H15
3715.44	1.81(−1)	2.47(−1)	O III	3715.08	V14
	*	*	[S III]	3721.63	F2
3722.16	2.15	2.94	H 14	3721.94	H14
3726.41	7.49	1.02(+1)	[O II]	3726.03	F1
3729.20	3.65	4.98	[O II]	3728.82	F1
3734.75	1.68	2.29	H 13	3734.37	H13
3750.50	2.24	3.04	H 12	3750.15	H12
3755.09	2.89(−1)	3.92(−1)	O III	3754.69	V2
3757.59	1.91(−1)	2.59(−1)	O III	3757.24	V2
3760.22	5.14(−1)	6.95(−1)	O III	3759.87	V2
3770.98	2.71	3.66	H 11	3770.63	H11
3774.28	7.53(−2)	1.01(−1)	O III	3774.02	V2
3791.65	9.25(−2)	1.24(−1)	O III	3791.27	V2
3798.29	3.71	4.99	H 10	3797.90	H10
3806.38	7.71(−2)	1.03(−1)	He I	3805.74	V58
3820.05	1.12	1.49	He I	3819.62	V22
3835.82	5.26	7.01	H 9	3835.39	H9
3869.20	7.05(+1)	9.31(+1)	[Ne III]	3868.75	F1
3889.09	5.19	6.83	He I	3888.65	V2
3889.49	8.68	1.14(+1)	H 8	3889.05	V2
3927.14	2.29(+1)	2.98(+1)	He I	3926.54	V58
3967.90	2.17(+1)	2.81(+1)	[Ne III]	3967.46	F1
3970.51	1.18(+1)	1.53(+1)	H 7	3970.07	
4009.06	1.92(−1)	2.45(−1)	He I	4009.26	V55
4026.02	2.12	2.69	He I	4026.21	V18
4026.02	2.12	2.69	He I	4026.21	V18
4041.24	2.15(−2)	2.73(−2)	N II	4041.31	V39b
4067.63	8.15(−2)	1.02(−1)	C III	4067.94	V16
4068.36	3.02(−1)	3.79(−1)	[S II]	4068.60	F1
4068.73	1.06(−1)	1.34(−1)	C III	4068.91	V16
4069.52	1.08(−1)	1.36(−1)	O II	4069.78	V10
4070.06	1.39(−1)	1.75(−1)	C III	4070.26	V16
4071.92	1.90(−1)	2.39(−1)	O II	4072.16	V10
4075.62	2.19(−1)	2.75(−1)	O II	4075.86	V10
4076.11	9.93(−2)	1.24(−1)	[S II]	4076.35	F1
4083.45	1.68(−2)	2.10(−2)	O II	4083.90	V48b
4084.66	2.31(−2)	2.90(−2)	O II	4085.11	V10
4086.70	2.87(−2)	3.59(−2)	O II	4087.15	V48c
4088.84	1.16(−1)	1.45(−1)	O II	4089.29	V48a
4093.00	1.71(−2)	2.12(−2)	O II	4092.93	V10
4097.07	1.05	1.31	N III	4097.33	V1
4101.48	2.14(+1)	2.66(+1)	H 6	4101.74	H6
4110.48	2.89(−2)	3.59(−2)	O II	4110.78	V20
4115.79	2.26(−2)	2.80(−2)	Si IV	4116.10	
4118.94	7.41(−2)	9.19(−2)	O II	4119.22	V20
4120.56	2.05(−1)	2.54(−1)	He I	4120.84	V16
4121.18	2.33(−2)	2.89(−2)	O II	4121.46	V19
4132.54	4.33(−2)	5.35(−2)	O II	4132.80	V19
4143.49	3.31(−1)	4.08(−1)	He I	4143.76	V53
4153.00	7.77(−2)	9.55(−2)	O II	4153.30	V19
4156.23	5.93(−2)	7.28(−2)	O II	4156.53	V19
4168.91	2.29(−2)	2.79(−2)	O II	4169.22	V19
4185.16	3.49(−2)	4.25(−2)	O II	4185.45	V36
4186.61	3.09(−2)	3.76(−2)	C III	4186.90	V18
4189.50	5.38(−2)	6.54(−2)	O II	4189.79	V36
4195.59	5.30(−2)	6.43(−2)	N III	4195.76	V6
4199.66	1.01(−1)	1.23(−1)	He II	4199.83	4.11
4215.51	1.65(−2)	1.99(−2)	N III	4215.69	
4219.38	3.11(−2)	3.75(−2)	Ne II	4219.74	V52a
4227.38	2.32(−2)	2.80(−2)	N II	4227.74	V33
4231.78	1.20(−2)	1.44(−2)	Ne II	4231.64	V52b
4237.05	1.16(−2)	1.39(−2)	N II	4237.05	V48b
4241.38	2.55(−2)	3.06(−2)	N II	4241.78	V48a

Table 3 – *continued*

λ_{obs}	$F(\lambda)$	$I(\lambda)$	ID	λ_0	Mult
		NGC 5882			
4253.59	2.15(−2)	2.57(−2)	O II	4254.00	V101
4266.91	3.35(−1)	3.99(−1)	C II	4267.15	V6
4275.38	4.87(−2)	5.79(−2)	O II	4275.55	V67a
4276.23	1.98(−2)	2.36(−2)	O II	4276.75	V67b
4277.48	2.22(−2)	2.65(−2)	O II	4277.43	V67c
4291.14	1.87(−2)	2.21(−2)	O II	4291.25	V55
4292.10	6.59(−3)	7.79(−3)	O II	4292.21	V18c
4294.67	1.32(−2)	1.56(−2)	O II	4294.78	V53b
4303.51	4.86(−2)	5.73(−2)	O II	4303.61	V65a
4317.11	5.43(−2)	6.38(−2)	O II	4317.14	V2
4319.32	2.84(−2)	3.33(−2)	O II	4319.63	V2
4340.19	4.10(+1)	4.77(+1)	H 5	4340.47	H5
4345.19	9.45(−2)	1.10(−1)	O II	4345.56	V2
4349.06	7.83(−2)	9.11(−2)	O II	4349.43	V2
4353.18	1.28(−2)	1.49(−2)	O II	4353.59	V76c
4362.95	4.81	5.56	[O III]	4363.21	F2
4366.54	5.22(−2)	6.04(−2)	O II	4366.89	V2
4378.86	1.18(−1)	1.36(−1)	N III	4379.11	V18
4385.79	4.61(−2)	5.31(−2)	O II	4386.01	
4387.71	5.22(−1)	6.00(−1)	He I	4387.93	V51
4391.77	2.99(−2)	3.44(−2)	Ne II	4391.99	V55e
4409.02	2.03(−2)	2.32(−2)	Ne II	4409.30	V55e
4414.62	3.84(−2)	4.39(−2)	O II	4414.90	V5
4416.69	3.49(−2)	3.99(−2)	O II	4416.97	V5
4437.33	5.09(−2)	5.77(−2)	He I	4437.55	V50
4465.38	2.71(−2)	3.05(−2)	O II	4466.42	V86b
4471.23	5.03	5.65	He I	4471.50	V14
4491.10	1.82(−2)	2.03(−2)	O II	4491.23	V86a
4510.71	7.09(−2)	7.87(−2)	N III	4510.91	V3
4514.66	2.32(−2)	2.57(−2)	N III	4514.86	V3
4517.95	2.69(−2)	2.98(−2)	N III	4518.15	V3
4523.38	2.16(−2)	2.39(−2)	N III	4523.58	V3
4530.21	1.62(−2)	1.80(−2)	N II	4530.41	V58b
4534.38	1.77(−2)	1.95(−2)	N III	4534.58	V3
4541.31	5.90(−2)	6.48(−2)	He II	4541.59	4.9
4544.52	3.01(−2)	3.31(−2)	N III	4544.80	
4570.81	2.66(−2)	2.90(−2)	Mg I]	4571.10	
4590.89	5.26(−2)	5.70(−2)	O II	4590.97	V15
4596.10	3.90(−2)	4.22(−2)	O II	4596.18	V15
4601.56	1.91(−2)	2.06(−2)	N II	4601.48	V5
4609.52	5.64(−2)	6.08(−2)	O II	4609.44	V92a
	*	*	O II	4610.20	V92c
4620.48	2.68(−2)	2.88(−2)	N II	4621.39	V5
	*	*	N II	4621.39	V5
4630.55	3.56(−2)	3.81(−2)	N II	4630.54	V5
4633.91	5.36(−1)	5.73(−1)	N III	4634.14	V2
4638.63	1.58(−1)	1.69(−1)	O II	4638.86	V1
4640.41	1.05	1.12	N III	4640.64	V2
4641.58	2.37(−1)	2.52(−1)	O II	4641.81	V1
4647.21	9.00(−2)	9.59(−2)	C III	4647.42	V1
4648.92	3.23(−1)	3.45(−1)	O II	4649.13	V1
4650.04	5.40(−2)	5.75(−2)	C III	4650.25	V1
4650.63	1.07(−1)	1.14(−1)	O II	4650.84	V1
4651.26	1.80(−2)	1.91(−2)	C III	4651.47	V1
4657.92	1.47(−1)	1.56(−1)	[Fe III]	4658.10	F3
	*	*	C IV	4658.30	V8
4661.45	1.11(−1)	1.19(−1)	O II	4661.63	V1
4673.59	1.77(−2)	1.89(−2)	O II	4673.73	V1
4676.10	8.57(−2)	9.06(−2)	O II	4676.24	V1
4685.54	2.61	2.75	He II	4685.68	3.4
4688.69	3.58(−2)	3.77(−2)	?		
4701.45	3.52(−2)	3.69(−2)	[Fe III]	4701.62	F3
4711.18	2.49	2.60	[Ar IV]	4711.37	F1

Table 3 – *continued*

λ_{obs}	$F(\lambda)$	$I(\lambda)$	ID	λ_0	Mult
		NGC 5882			
4712.98	6.33(−1)	6.61(−1)	He I	4713.17	v12
4733.83	2.17(−2)	2.25(−2)	[Fe III]	4733.93	
4740.05	2.88	2.99	[Ar IV]	4740.17	F1
4754.60	2.63(−2)	2.71(−2)	[Fe III]	4754.83	
4769.49	1.69(−2)	1.74(−2)	[Fe III]	4769.60	
4802.00	9.80(−3)	9.98(−3)	C II	4802.23	
4803.15	1.80(−2)	1.83(−2)	N II	4803.29	V20
4860.80	1.00(+2)	1.00(+2)	H 4	4861.33	H4
4881.03	6.38(−2)	6.34(−2)	[Fe III]	4881.11	F2
4891.60	8.74(−3)	8.66(−3)	O II	4890.86	V28
4899.28	8.78(−3)	8.68(−3)	Fe IV?		
4902.59	2.88(−2)	2.84(−2)	Si II	4902.65	
4906.53	3.67(−2)	3.62(−2)	O II	4906.83	V28
4921.84	1.43	1.40	He I	4921.93	V48
4924.44	6.68(−2)	6.56(−2)	O II	4924.53	V28
4931.02	1.40(−1)	1.37(−1)	[O III]	4931.80	F1
4958.41	3.63(+2)	3.53(+2)	[O III]	4958.91	F1
5006.33	1.10(+3)	1.05(+3)	[O III]	5006.84	F1
5411.19	1.97(−1)	1.68(−1)	He II	5411.52	4.7
5517.46	5.09(−1)	4.22(−1)	[Cl III]	5517.66	F1
5537.40	6.19(−1)	5.12(−1)	[Cl III]	5537.60	F1
5676.05	2.34(−2)	1.89(−2)	N II	5676.02	V3
5679.32	7.47(−2)	6.04(−2)	N II	5679.56	V3
5754.21	3.39(−1)	2.68(−1)	[N II]	5754.60	F3
5800.76	1.97(−1)	1.54(−1)	C IV	5801.51	V1
5811.39	1.50(−1)	1.17(−1)	C IV	5812.14	V1
5875.26	2.07(+1)	1.60(+1)	He I	5875.66	V11
6101.74	1.62(−1)	1.20(−1)	[K IV]	6101.83	F1
6300.31	5.37(−1)	3.82(−1)	[O I]	6300.34	F1
6312.07	1.69	1.20	[S III]	6312.10	F3
6364.00	2.25(−1)	1.58(−1)	[O I]	6363.78	F1
6462.90	8.80(−2)	6.09(−2)	C II	6461.95	
6548.22	7.15	4.87	[N II]	6548.10	F1
6562.85	4.35(+2)	2.95(+2)	H 3	6562.77	H3
6583.40	2.13(+1)	1.44(+1)	[N II]	6583.50	F1
6678.27	6.47	4.31	He I	6678.16	V46
6716.55	1.69	1.11	[S II]	6716.44	F2
6730.93	2.89	1.91	[S II]	6730.82	F2
7064.98	7.85	4.92	He I	7065.25	V10
7111.38	6.76(−2)	4.20(−2)	C I	7111.50	
7135.52	2.29(+1)	1.42(+1)	[Ar III]	7135.80	F1
7229.89	1.24(−1)	7.60(−2)	?		
7236.02	2.70(−1)	1.65(−1)	C II	7236.42	V3
7262.36	1.35(−1)	8.25(−2)	[Ar IV]	7262.76	F2
7280.95	1.00	6.09(−1)	He I	7281.35	V45
7318.96	1.55	9.38(−1)	[O II]	7318.92	F2
7329.71	1.42	8.56(−1)	[O II]	7329.67	F2
		NGC 6302			
		$c(H\beta)^{Ba} = 1.44$			
3118.22	1.16	5.24		*	
3120.54	1.31	5.86	O III	3121.71	V12
3131.16	1.66	7.33	O III	3132.79	V12
3184.38	1.21(−1)	4.96(−1)	Si III	3185.12	V8
3187.00	8.32(−1)	3.38	He I	3187.74	V3
3202.37	7.10	2.82(+1)	He II	3203.10	3.5
3239.26	7.04(−2)	2.67(−1)	?		
3241.15	3.95(−1)	1.49	Si III	3241.62	V6
3298.89	8.16(−1)	2.86	O III	3299.36	V3
3311.83	2.27	7.87	O III	3312.30	V3
3334.52	3.68(−2)	1.22(−1)	Ne II	3334.84	V2
3340.26	3.73	1.24(+1)	O III	3340.74	V3
3345.38	2.51(+1)	8.33(+1)	[Ne V]	3345.86	
3354.22	5.61(−2)	1.84(−1)	?		

Table 3 – *continued*

λ_obs	F(λ)	I(λ)	ID	λ_0	Mult
			NGC 6302		
3361.83	1.49(−1)	4.86(−1)	[Na IV]	3362.20	
3380.59	7.55(−2)	2.40(−1)	O IV	3381.21	
3384.90	5.80(−2)	1.83(−1)	O IV	3385.52	
3405.33	1.41(−1)	4.38(−1)	?		
3411.35	6.41(−2)	1.97(−1)	O IV	3411.69	
3414.92	2.67(−1)	8.21(−1)	O III	3415.31	
3425.45	7.69(+1)	2.33(+2)	[Ne V]	3425.86	
3429.65	6.25(−1)	1.88	O III	3428.65	V15
3432.71	1.12(−1)	3.37(−1)	?		
3443.66	6.90	2.05(+1)	O III	3444.07	V15
3466.13	4.04(−1)	1.17	He I	3467.54	
3478.27	6.33(−2)	1.81(−1)	He I	3478.97	V43
3553.98	8.45(−2)	2.24(−1)	He I	3554.20	V34
3567.92	8.19(−2)	2.14(−1)	Ne II	3568.50	V9
3586.70	1.69(−1)	4.35(−1)	He I	3587.28	V31
3613.18	1.20(−1)	3.02(−1)	He I	3613.64	V6
3633.66	1.69(−1)	4.17(−1)	He I	3634.25	V28
3671.16	7.20(−2)	1.73(−1)	H 24	3671.48	H24
3673.38	1.40(−1)	3.37(−1)	H 23	3673.74	H23
3676.03	2.00(−1)	4.81(−1)	H 22	3676.36	H22
3678.99	2.60(−1)	6.25(−1)	H 21	3679.36	H21
3682.46	3.10(−1)	7.43(−1)	H 20	3682.81	H20
3686.46	3.90(−1)	9.33(−1)	H 19	3686.83	H19
3691.18	4.50(−1)	1.07	H 18	3691.56	H18
3696.81	6.50(−1)	1.54	H 17	3697.15	H17
3703.62	1.20	2.84	H 16	3703.86	H16
	*	*	He I	3705.02	V25
3711.64	1.07	2.52	H 15	3711.97	H15
3714.54	9.50(−2)	2.23(−1)	O III	3715.08	V14
	*	*	H 14	3721.94	H14
3721.14	2.11	4.96	[S III]	3721.63	F2
3725.54	1.28(+1)	3.00(+1)	[O II]	3726.03	F1
3728.33	6.00	1.40(+1)	[O II]	3728.82	F1
3733.88	7.71(−1)	1.79	H 13	3734.37	H13
3749.69	1.00	2.32	H 12	3750.15	H12
3754.19	3.03(−1)	6.99(−1)	O III	3754.69	V2
3756.74	2.24(−1)	5.16(−1)	O III	3757.24	V2
3759.37	1.63	3.76	O III	3759.87	V2
3770.17	1.25	2.86	H 11	3770.63	H11
3773.31	3.63(−2)	8.26(−2)	O III	3774.02	V2
3777.81	3.79(−3)	8.54(−2)	Ne II	3777.14	V1
3781.28	5.90(−2)	1.33(−1)	He II	*	
3790.86	8.03(−2)	1.81(−1)	O III	3791.27	V2
3797.46	1.78	4.00	H 10	3797.90	H10
3805.53	2.48(−2)	5.54(−2)	He I	3805.74	V58
3813.12	9.30(−2)	2.06(−1)	He II	3813.50	4.19
3819.27	4.97(−1)	1.10	He I	3819.62	V22
3834.98	2.85	6.27	H 9	3835.39	H9
3839.10	2.32(−2)	5.07(−2)	[Fe V]	3839.27	
3855.83	1.49(−1)	3.22(−1)	?		
3857.65	1.52(−1)	3.28(−1)	He II	3858.07	4.17
3888.47	8.57	1.81(+1)	He I	3888.65	V2
3895.42	1.01(−2)	2.13(−2)	?		
3923.18	2.15(−1)	4.45(−1)	He II	3923.48	4.15
3926.23	5.07(−1)	1.04	He I	3926.54	V58
3967.11	2.76(+1)	5.56(+1)	[Ne III]	3967.46	F1
3975.44	2.24(−2)	4.47(−2)	?		
4008.91	9.36(−2)	1.82(−1)	He I	4009.26	V55
4025.65	1.55	3.00	He I	4026.21	V18
4059.90	3.60(−2)	6.77(−2)	O II	4060.60	
4068.23	7.76	1.45(+1)	[S II]	4068.60	F1
4075.98	2.58	4.80	[S II]	4076.35	F1
4096.89	1.68	3.09	N III	4097.33	V1
4101.31	1.47(+1)	2.68(+1)	H 6	4101.74	H6
	*	*	O II	4119.22	V20
	*	*	O II	4120.28	V20
	*	*	O II	4120.54	V20
4120.43	2.24(−1)	4.03(−1)	He I	4120.84	V16
4122.08	2.12(−1)	3.82(−1)	?		
4143.35	1.95(−1)	3.46(−1)	He I	4143.76	V53
4162.88	2.33(−1)	4.07(−1)	[K V]	4163.30	
4199.43	8.73(−1)	1.48	He II	4199.83	4.11
4226.98	1.01(−1)	1.71(−)2	N II	4227.74	V33
4266.67	1.00(−1)	1.63(−1)	C II	4267.15	V6
4335.09	8.27(−2)	1.26(−1)	O II	4334.09	V63b
4340.01	3.17(+1)	4.83(+1)	H 5	4340.47	H5
4362.75	2.65(+1)	3.96(+1)	[O III]	4363.21	F2
4366.39	7.62(−2)	1.13(−1)	O II	4366.89	V2
4378.63	1.23(−1)	1.81(−1)	N III	4379.11	V18
4387.45	4.25(−1)	6.23(−1)	He I	4387.93	V51
4415.15	9.53(−2)	1.36(−1)	O II	4414.90	V5
4468.12	4.32	5.92	He I	4471.50	V14
4510.45	1.31(−1)	1.74(−1)	N III	4510.91	V3
4519.30	1.09(−1)	1.44(−1)	N III	4518.15	V3
4541.20	2.18	2.83	He II	4541.59	4.9
4562.43	1.95(−1)	2.48(−1)	Mg I]	4562.60	
4570.71	1.95(−1)	2.47(−1)	Mg I]	4571.10	
4590.91	3.40(−2)	4.23(−2)	O II	4590.97	V15
4603.52	1.34(−1)	1.65(−1)	N V	4603.74	V1
4606.06	5.42(−1)	6.68(−1)	N IV	4606.33	
4606.72	4.93(−2)	6.07(−2)	N II?	4607.16	V5
4625.04	3.43(−1)	4.16(−1)	[Ar V]	4624.54	
4629.68	6.16(−2)	7.43(−2)	N II	4630.54	V5
4631.93	1.89(−1)	2.28(−1)	O IV	4631.89	V1
4633.79	2.40	2.89	N III	4634.14	V2
4638.49	3.81(−1)	4.57(−1)	O II	4638.49	V1
4640.27	4.56	5.46	N III	4640.64	V2
4641.44	6.31(−1)	7.55(−1)	O II	4641.44	V1
4647.24	6.33(−2)	7.54(−2)	C III	4647.42	V1
4648.95	1.29(−1)	1.54(−1)	O II	4649.13	V1
4650.63	5.11(−2)	6.09(−2)	O II	4650.84	V1
4675.41	4.71(−2)	5.56(−2)	[Fe III]	4658.10	F3
	*	*	C IV	4658.30	V8
4661.45	2.96(−2)	3.53(−2)	O II	4661.63	V1
4675.82	9.87(−2)	1.14(−1)	O II	4676.24	V1
4685.42	6.52(+1)	7.53(+1)	He II	4685.68	3.4
4701.28	4.76(−2)	5.42(−2)	[Fe III]	4701.62	F3
4707.10	1.48(−1)	1.68(−1)	?		
4711.05	1.12(+1)	1.26(+1)	[Ar IV]	4711.37	F1
4713.65	2.62	2.96	He I	4713.17	V12
4723.85	1.86	2.08	[Ne IV]	4724.15	F1
4725.32	1.63	1.82	[Ne IV]	4725.62	F1
4739.93	1.89(+1)	2.09(+1)	[Ar IV]	4740.17	F1
4802.41	6.23(−2)	6.54(−2)	C II	4802.23	
4831.07	2.70(−2)	2.76(−2)	?		
4861.11	1.00(+2)	1.00(+2)	H 4	4861.33	H4
4880.73	9.12(−2)	8.97(−2)	[Fe III]	4881.11	F2
4893.40	5.44(−2)	5.30(−2)	?		
4921.75	1.52	1.45	He I	4921.93	V48
4930.63	5.59(−1)	5.28(−1)	O III	4931.80	F1
4934.69	5.91(−2)	5.56(−2)	?		
4944.42	2.40(−1)	2.25(−1)	O II	4943.00	V33
4957.76	4.65(+2)	4.29(+2)	[O III]	4958.91	F1
5005.68	1.45(+3)	1.29(+3)	[O III]	5006.84	F1
5039.66	3.53	3.06	Si II	5039.66	
5054.61	1.53	1.31	Si II	5054.61	

Table 3 – *continued*

λ_{obs}	$F(\lambda)$	$I(\lambda)$	ID	λ_0	Mult
			NGC 6302		
5190.01	1.98	1.52	[Ar III]	5191.82	F3
5198.03	1.42(+1)	1.08(+1)	[N I]	5199.84	F1
5409.63	9.41	6.04	He II	5411.52	4.7
5516.74	5.65(−1)	3.39(−1)	[Cl III]	5517.66	F1
5536.67	1.45	8.61(−1)	[Cl III]	5537.60	F1
5576.41	4.01(−1)	2.32(−1)	[O I]	5577.34	F3
5668.07	1.33(−1)	7.35(−2)	N II?	5666.63	V3
5677.46	2.88(−1)	1.58(−1)	[Fe VI]	5677.00	
5700.47	1.42(−1)	7.72(−2)	?		
5720.00	4.51(−1)	2.41(−1)	[Fe VII]	5720.00	
5753.69	3.83(+1)	2.01(+1)	[N II]	5754.60	F3
5874.74	3.57(+1)	1.75(+1)	He I	5875.66	V11
5912.59	1.48(−1)	7.14(−2)	He II	5913.26	5.26
5927.13	4.29(−2)	2.05(−2)	N II	5927.81	V28
5931.10	7.55(−2)	3.61(−2)	N II	5931.78	V28
5952.26	2.07(−1)	9.77(−2)	He II	5952.94	5.24
5976.35	2.53(−1)	1.17(−1)	He II	5977.03	5.23
6004.77	2.47	1.13	He II	6004.73	5.22
6037.15	4.29(−1)	1.93(−1)	He II	6036.70	5.21
6046.60	7.82(−1)	3.50(−1)	?		
6074.62	8.52(−1)	3.76(−1)	He II	6074.10	5.20
6085.33	1.18	5.22(−1)	[Fe VII]	6086.90	
6100.80	2.00	8.73(−1)	[K IV]	6101.83	F1
6117.65	4.05(−1)	1.75(−1)	He II	6118.20	5.19
6169.79	4.82(−1)	2.02(−1)	He II	6170.60	5.18
6200.27	1.40(−1)	5.81(−2)	?		
6227.73	5.27(−1)	2.15(−1)	[K IV]	6228.40	
6232.99	5.72(−1)	2.32(−1)	He II	6233.80	5.17
6299.93	6.18(+1)	2.43(+1)	[O I]	6300.34	F1
6311.69	1.49(+1)	5.84	[S III]	6312.10	F3
6346.73	9.77(−1)	3.71(−1)	Si II	6347.10	V2
6363.41	2.09(+1)	7.97	[O I]	6363.78	F1
6371.01	2.29	8.71(−1)	Si II	6371.38	V2
6393.32	1.10(−1)	4.16(−2)	[Mn V]	6393.60	
6406.02	9.63(−1)	3.59(−1)	He II	6406.30	5.15
6434.52	1.36(+1)	5.02	[Ar V]	6435.10	
6476.86	2.49(−1)	8.99(−2)	?		
6499.95	2.28(−1)	8.12(−2)	?		
6516.44	2.15(−1)	7.62(−2)	?		
6526.80	1.49	5.27(−1)	He II	6527.11	5.14
6547.73	4.99(+2)	1.74(+2)	[N II]	6548.10	F1
6562.40	8.20(+2)	2.83(+2)	H 3	6562.77	H3
6583.13	1.52(+3)	5.22(+2)	[N II]	6583.50	F1
6677.97	3.13	1.02	He I	6678.16	V46
6716.15	3.13(+1)	1.01(+1)	[S II]	6716.44	F2
6730.53	6.21(+1)	1.98(+1)	[S II]	6730.82	F2
6744.88	2.18(−1)	6.94(−2)	?		
6794.58	3.87(−1)	1.20(−1)	[K IV]	6795.00	F1
6826.21	1.31	4.04(−1)			
6890.67	1.84	5.51(−1)	He II	6890.88	7
7005.26	3.41(+1)	9.67	[Ar V]	7005.67	
7064.85	2.97(+1)	8.22	He I	7065.25	V10
7135.26	8.82(+1)	2.37(+1)	[Ar III]	7135.80	F1
7154.48	5.82(−1)	1.55(−1)	[Fe II]	7154.98	
7170.06	4.73	1.25	[Ar IV]	7170.62	F2
7176.94	2.81	7.44(−1)	He II	7177.50	5.11
7236.17	3.40	8.77(−1)	C II	7236.42	V3
	*	*	[Ar IV]	7237.40	F2
7262.51	3.79	9.68(−1)	[Ar IV]	7262.76	F2
7281.09	3.52	8.93(−1)	He I	7281.35	V45
7319.04	3.43(+1)	8.57	[O II]	7318.92	F2
7329.79	2.92(+1)	7.28	[O II]	7329.67	F2

Table 3 – *continued*

λ_{obs}	$F(\lambda)$	$I(\lambda)$	ID	λ_0	Mult
			NGC 6818		
		$c(\mathrm{H}\beta)^{\mathrm{Ba}} = 0.47$			
3120.58	1.10	1.79	O III	3121.71	V12
3131.91	5.15(+1)	8.37(+1)	O III	3132.79	V12
3187.11	1.39	2.20	He I	3187.74	V3
3202.55	1.93(+1)	3.04(+1)	He II	3203.10	3.5
3241.35	3.80(−1)	5.87(−1)	Si III	3241.62	V6
3299.06	1.82	2.75	O III	3299.36	V3
3312.03	5.23	7.86	O III	3312.30	V3
3340.55	8.09	1.20(+1)	O III	3340.74	V3
3345.54	1.08(+1)	1.61(+1)	[Ne V]	3345.86	
3380.95	2.10(−1)	3.07(−1)	O IV	3381.21	
3385.40	1.70(−1)	2.48(−1)	O IV	3385.52	
3411.40	1.20(−1)	1.73(−1)	O IV	3411.69	
3425.59	3.47(+1)	5.00(+1)	[Ne V]	3425.86	
3428.20	2.01	2.89	O III	3428.65	V15
3443.77	1.64(+1)	2.34(+1)	O III	3444.07	V15
3568.12	1.40(−1)	1.92(−1)	Ne II	3568.50	V9
3586.73	1.20(−1)	1.63(−1)	He I	3587.28	V31
3633.91	1.30(−1)	1.74(−1)	He I	3634.25	V28
3671.13	3.74(−1)	5.00(−1)	H 24	3671.48	H24
3673.39	3.91(−1)	5.22(−1)	H 23	3673.74	H23
3676.01	4.26(−1)	5.69(−1)	H 22	3676.36	H22
3679.01	4.65(−1)	6.21(−1)	H 21	3679.36	H21
3682.46	4.90(−1)	6.54(−1)	H 20	3682.81	H20
3686.48	5.40(−1)	7.20(−1)	H 19	3686.83	H19
3691.21	6.10(−1)	8.11(−1)	H 18	3691.56	H18
3696.72	7.93(−1)	9.66(−1)	H 17	3697.15	H17
3703.43	9.55(−1)	1.59	H 16	3703.86	H16
3704.59	3.57(−1)	5.94(−2)	He I	3705.02	V25
3711.62	1.23	1.64	H 15	3711.97	H15
3714.73	1.99(−1)	2.64(−1)	O III	3715.08	V14
3721.47	4.11	5.44	H 14	3721.94	H14
3725.70	3.36(+1)	4.45(+1)	[O II]	3726.03	F1
3728.49	2.27(+1)	3.01(+1)	[O II]	3728.82	F1
3734.04	1.84	2.43	H 13	3734.37	H13
3749.78	2.40	3.17	H 12	3750.15	H12
3754.33	9.67(−1)	1.27	O III	3754.69	V2
3756.88	7.33(−1)	9.63(−1)	O III	3757.24	V2
3759.51	3.14	4.12	O III	3759.87	V2
3770.29	3.05	4.00	H 11	3770.63	H11
3773.66	2.80(−1)	3.66(−1)	O III	3774.02	V2
3781.40	1.10(−1)	1.44(−1)	He II	3781.76	
3791.02	2.80(−1)	3.65(−1)	O III	3791.27	V2
3797.58	4.17	5.43	H 10	3797.90	H10
3811.24	5.90(−2)	7.67(−2)	O VI	3811.35	
3813.24	1.90(−1)	2.47(−1)	He II	3813.50	4.19
3819.38	4.50(−1)	5.84(−1)	He I	3819.62	V22
3835.11	5.41	7.01	H 9	3835.39	H9
3839.13	4.60(−2)	5.95(−2)	[Fe V]	3839.27	
3857.86	2.20(−1)	2.83(−1)	He II	3858.07	4.17
3868.51	1.10(+2)	1.42(+2)	[Ne III]	3868.75	F1
3888.36	3.84	4.91	He I	3888.65	V2
3888.76	9.49	1.21(+1)	H 8	3889.05	H8
3923.29	3.00(−1)	3.81(−1)	He II	3923.48	4.15
3967.23	4.78(+1)	6.01(+1)	[Ne III]	3967.46	F1
4008.82	7.40(−2)	9.21(−2)	He I	4009.26	V55
4025.71	1.52	1.88	He I	4026.21	V18
4059.90	3.60(−2)	4.43(−2)	[F IV]	4060.23	
4067.64	1.93(−1)	2.38(−1)	C III	4067.94	V16
4068.37	8.59(−1)	1.05	[S II]	4068.60	F1
4068.74	2.53(−1)	3.11(−1)	C III	4068.91	V16
4069.52	1.08(−1)	1.32(−1)	O II	4069.78	V10

Table 3 – *continued*

λ_{obs}	$F(\lambda)$	$I(\lambda)$	ID	λ_0	Mult
		NGC 6818			
4070.07	3.31(−1)	4.06(−1)	C III	4070.26	V16
4071.93	1.43(−1)	1.75(−1)	O II	4072.16	V10
4075.63	3.57(−1)	4.38(−1)	O II	4075.86	V10
4076.12	2.60(−1)	3.19(−1)	[S II]	4076.35	F1
4078.61	5.10(−2)	6.25(−2)	S II	4078.84	V10
4083.46	5.67(−2)	6.94(−2)	O II	4083.90	V48b
4085.05	5.90(−2)	7.22(−2)	O II	4085.11	V10
4086.71	3.22(−2)	3.94(−2)	O II	4087.15	V48c
4088.84	8.05(−2)	9.84(−2)	O II	4089.29	V48a
4097.01	1.38	1.68	N III	4097.33	V1
4101.40	2.09(+1)	2.55(+1)	H 6	4101.74	H6
	*	*	O II	4120.28	V20
	*	*	O II	4120.54	V20
4120.45	1.29(−1)	1.57(−1)	He I	4120.84	V16
4122.14	5.40(−2)	6.55(−2)	O II	4121.46	V19
4143.24	1.79(−1)	2.15(−1)	He I	4143.76	V53
4185.06	4.38(−2)	5.23(−2)	O II	4185.45	V36
4186.51	9.92(−2)	1.18(−1)	C III	4186.90	V18
4195.91	2.50(−2)	2.97(−2)	N III	4195.76	V6
4199.50	9.30(−1)	1.10	He II	4199.83	4.11
4219.16	4.24(−2)	5.02(−2)	Ne II	4219.74	V52a
4227.32	2.38(−1)	2.81(−1)	N II	4227.74	V33
4250.98	2.89(−2)	3.40(−2)	Ne II	4250.65	
4266.89	3.83(−1)	4.49(−1)	C II	4267.15	V6
4340.13	4.08(+1)	4.68(+1)	H 5	4340.47	H5
4362.87	2.03(+1)	2.32(+1)	[O III]	4363.21	F2
4366.81	8.74(−2)	9.97(−2)	O II	4366.89	V2
4368.89	6.13(−2)	6.99(−2)	Ne II	4369.86	V56
4378.87	1.78(−1)	2.02(−1)	N III	4379.11	V18
4387.69	2.80(−1)	3.18(−1)	He I	4387.93	V51
4414.82	5.27(−2)	5.94(−2)	O II	4414.90	V5
4452.67	5.76(−2)	6.43(−2)	O II?	4452.37	V5
4471.20	2.32	2.58	He I	4471.50	V14
4510.69	9.10(−2)	9.99(−2)	N III	4510.91	V3
4534.44	4.43(−2)	4.83(−2)	N III	4534.58	V3
4541.35	1.92	2.09	He II	4541.59	4.9
4562.43	1.95(−1)	2.11(−1)	Mg I]	4562.60	
4570.94	2.90(−1)	3.13(−1)	Mg I]	4571.10	
4590.86	5.03(−2)	5.40(−2)	O II	4590.97	V15
4606.52	4.30(−2)	4.60(−2)	N IV	4606.33	
4633.92	1.07	1.13	N III	4634.14	V2
4632.05	1.30(−1)	1.38(−1)	N III	4634.14	
4638.64	2.03(−1)	2.16(−1)	O II	4638.86	V1
4640.42	2.12	2.25	N III	4640.64	V2
4641.59	4.67(−1)	4.96(−1)	O II	4641.81	V1
4647.21	1.76(−1)	1.87(−1)	C III	4647.42	V1
4648.92	1.59(−1)	1.69(−1)	O II	4649.13	V1
4650.04	1.16(−1)	1.23(−1)	C III	4650.25	V1
4650.63	2.47(−2)	2.62(−2)	O II	4650.84	V1
4651.26	7.42(−2)	7.85(−2)	C III	4651.47	V1
4657.29	1.48(−1)	1.57(−1)	?	4657.29	
4658.45	1.70(−1)	1.80(−1)	[Fe III]	4658.10	F3
	*	*	C IV	4658.30	V8
4661.36	8.06(−2)	8.51(−2)	O II	4661.63	V1
4676.20	2.30(−2)	2.41(−2)	O II	4676.24	V1
4685.60	5.83(+1)	6.11(+1)	He II	4685.68	3.4
4711.25	7.91	8.23	[Ar IV]	4711.37	F1
4713.85	7.90(−1)	8.22(−1)	He I	4713.17	V12
4724.04	6.48(−1)	6.72(−1)	[Ne IV]	4724.15	F1
4725.51	5.19(−1)	5.38(−1)	[Ne IV]	4725.62	F1
4740.12	7.10	7.33	[Ar IV]	4740.17	F1
4796.03	4.10(−2)	4.17(−2)	?		
4831.07	2.70(−2)	2.72(−2)	?		

Table 3 – *continued*

λ_{obs}	$F(\lambda)$	$I(\lambda)$	ID	λ_0	Mult
		NGC 6818			
4861.31	1.00(+2)	1.00(+2)	H 4	4861.33	H4
4921.97	7.00(−1)	6.88(−1)	He I	4921.93	V48
4931.48	1.60(−1)	1.57(−1)	[O III]	4931.80	F1
4935.82	1.20(−1)	1.17(−1)	?		
4958.92	5.71(+2)	5.56(+2)	[O III]	4958.91	F1
	5.62(+2)	5.48(+2)	[O III]	4958.91	F1
5006.10	1.60(+3)	1.54(+3)	[O III]	5006.84	F1
5190.37	3.39(−1)	3.10(−1)	[Ar III]	5191.82	F3
5198.39	3.52(−1)	3.21(−1)	[N I]	5199.84	F1
5410.75	4.99	4.31	He II	5411.52	4.7
5517.02	9.80(−1)	8.28(−1)	[Cl III]	5517.66	F1
5537.15	1.03	8.67(−1)	[Cl III]	5537.60	F1
5592.33	2.50(−1)	2.08(−1)	O III	5592.37	V5
5676.05	3.94(−2)	3.22(−2)	N II	5676.02	V3
5679.51	1.26(−1)	1.03(−1)	N II	5679.56	V3
5753.99	1.53	1.23	[N II]	5754.60	F3
5801.33	7.00(−2)	5.61(−2)	C IV	5801.51	V1
5875.16	9.43	7.46	He I	5875.66	V11
6004.63	1.40(−1)	1.08(−1)	He II	6004.73	5.22
6046.22	3.60(−1)	2.76(−1)	?		
6101.26	4.60(−1)	3.50(−1)	[K IV]	6101.83	F1
6117.41	1.00(−1)	7.58(−2)	He II	6118.20	5.19
6170.06	1.70(−1)	1.27(−1)	He II	6170.60	5.18
6233.58	2.70(−1)	2.00(−1)	He II	6233.80	5.17
6300.23	3.01	2.21	[O I]	6300.34	F1
6311.85	4.50	3.30	[S III]	6312.10	F3
6363.78	1.00	7.28(−1)	[O I]	6363.78	F1
6406.33	3.80(−1)	2.74(−1)	He II	6406.30	5.15
6435.08	1.00	7.20(−1)	[Ar V]	6435.10	
6527.32	4.70(−1)	3.33(−1)	He II	6527.11	5.14
6548.22	2.88(+1)	2.03(+1)	[N II]	6548.10	F1
6562.79	3.88(+2)	2.74(+2)	H 3	6562.77	H3
6583.55	8.89(+1)	6.25(+1)	[N II]	6583.50	F1
6678.45	3.13	2.17	He I	6678.16	V46
6716.64	7.69	5.30	[S II]	6716.44	F2
6730.99	1.02(+1)	7.07	[S II]	6730.82	F2
6825.87	2.70(−1)	1.83(−1)	?		
6890.92	6.40(−1)	4.30(−1)	He II	6890.88	7
7005.89	2.07	1.36	[Ar V]	7005.67	
7065.08	2.86	1.87	He I	7065.25	V10
7135.66	2.80(+1)	1.82(+1)	[Ar III]	7135.80	F1
7170.72	4.06(−1)	2.62(−1)	[Ar IV]	7170.62	F2
7177.60	8.06(−1)	5.20(−1)	He II	7177.50	5.11
7236.26	4.60(−1)	2.94(−1)	C II	7236.42	V3
7262.79	3.60(−1)	2.29(−1)	[Ar IV]	7262.76	F2
7281.29	4.00(−1)	2.54(−1)	He I	7281.35	V45
7319.74	3.43	2.17	[O II]	7318.92	F2
7329.94	2.87	1.81	[O II]	7329.67	F2
		IC 4191 (fixed-slit)			
		$c(H\beta)^{Ba} = 0.61$			
3704.18	7.17(−1)	1.03	He I	3705.02	
3711.95	6.00(−1)	8.63(−1)	H 15	3711.97	
	*	*	H 14	3721.94	H14
	*	*	[S III]	3721.63	F2
3726.19	3.24(+1)	4.65(+1)	[O II]	3726.03	F1
	*	*	[O II]	3728.82	F1
	*	*	H 13	3734.37	H13
3749.91	2.06	2.94	H 12	3750.15	H12
3757.00	4.33(−1)	6.16(−1)	O III	3757.24	V2
3759.63	1.14	1.63	O III	3759.87	V2
3770.39	2.37	3.36	H 11	3770.63	H11
3797.47	3.36	4.73	H 10	3797.90	H10
3819.19	8.93(−1)	1.25	He I	3819.62	
3834.96	4.81	6.72	H 9	3835.39	H9

Table 3 – *continued*

λ_obs	F(λ)	I(λ)	ID	λ₀	Mult
			IC 4191 (fixed-slit)		
3868.41	9.46(+1)	1.30(+2)	[Ne III]	3868.75	F1
3888.71	1.20(+1)	1.66(+1)	He I	3888.65	V2
3967.11	3.85(+1)	5.18(+1)	[Ne III]	3967.46	F1
4009.04	1.58(−1)	2.10(−1)	He I	4009.26	V55
4025.97	2.00	2.65	He I	4026.21	V18
4068.35	3.16	4.12	[S II]	4068.60	
	*	*	O II	4069.62	V10
	*	*	O II	4069.89	V10
4069.51	4.60(−1)	6.00(−1)	O II	4069.78	
4071.91	2.73(−1)	3.57(−1)	O II	4072.16	V10
4075.61	2.65(−1)	3.45(−1)	O II	4075.86	V10
4076.10	1.14	1.48	[S II]	4076.35	F1
4083.71	5.39(−2)	7.01(−2)	O II	4083.90	V48b
4084.92	2.04(−2)	2.66(−2)	O II	4085.11	V10
4086.96	5.27(−2)	6.85(−2)	O II	4087.15	V48c
4089.10	1.59(−1)	2.06(−1)	O II	4089.29	V48a
4097.11	1.27	1.64	N III	4097.33	V1
4101.52	1.92(+1)	2.48(+1)	H 6	4101.74	H6
4119.16	1.21(−1)	1.56(−1)	O II	4119.22	V20
4120.78	2.00(−1)	2.57(−1)	He I	4120.84	V16
4143.48	2.91(−1)	3.71(−1)	He I	4143.76	V53
4185.26	5.02(−2)	6.31(−2)	O II	4185.45	V36
4186.71	7.85(−2)	9.86(−2)	C III	4186.90	V18
4189.60	7.35(−2)	9.22(−2)	O II	4189.79	V36
4199.73	2.35(−1)	2.95(−1)	He II	4199.83	4.11
4219.75	5.53(−2)	6.87(−2)	Ne II	4219.74	V52a
4267.00	4.65(−1)	5.69(−1)	C II	4267.15	V6
4275.40	1.20(−1)	1.47(−1)	O II	4275.55	V67a
	*	*	O II	4275.99	V67b
4276.60	7.89(−2)	9.63(−2)	O II	4276.75	
	*	*	O II	4303.61	V65a
4303.63	5.65(−2)	6.84(−2)	O II	4303.82	V53a
4317.01	5.60(−2)	6.76(−2)	O II	4317.14	V2
4319.50	4.57(−2)	5.51(−2)	O II	4319.63	V2
4340.27	3.92(+1)	4.69(+1)	H 5	4340.47	H5
4345.40	1.01(−1)	1.21(−1)	O II	4345.56	V2
4349.27	1.95(−1)	2.32(−1)	O II	4349.43	V2
4363.01	9.14	1.08(+1)	[O III]	4363.21	F2
4366.78	8.98(−2)	1.06(−1)	O II	4366.89	V2
4378.94	2.34(−1)	2.76(−1)	N III	4379.11	V18
4387.76	4.76(−1)	5.59(−1)	He I	4387.93	V51
4391.63	4.70(−2)	5.52(−2)	Ne II	4391.99	V55e
4414.81	4.68(−2)	5.46(−2)	O II	4414.90	V5
4416.88	3.81(−2)	4.44(−2)	O II	4416.97	V5
4437.40	3.98(−2)	4.60(−2)	He I	4437.55	V50
4465.51	3.37(−2)	3.87(−2)	O II?		
4471.33	4.39	5.01	He I	4471.50	V14
4510.78	1.08(−1)	1.22(−1)	N III	4510.91	
4541.46	4.31(−1)	4.81(−1)	He II	4541.59	
4570.97	1.36(−1)	1.51(−1)	Mg I]	4571.10	
4590.82	7.32(−2)	8.04(−2)	O II	4590.97	
4596.03	5.63(−2)	6.17(−2)	O II	4596.18	V15
4609.75	5.52(−2)	6.03(−2)	O II	4609.44	V92a
	*	*	O II	4610.20	V92c
4631.93	7.53(−2)	8.15(−2)	N II	4630.54	V5
4634.03	9.33(−1)	1.01	N III	4634.14	V2
4638.75	2.24(−1)	2.43(−1)	O II	4638.49	V1
4640.53	1.82	1.97	N III	4640.64	V2
4641.70	1.88(−1)	2.02(−1)	O II	4641.44	V1
4647.30	1.60(−1)	1.72(−1)	C III	4647.42	V1
4649.01	5.35(−1)	5.76(−1)	O II	4649.13	V1
4650.13	1.13(−1)	1.22(−1)	C III	4650.25	V1
4650.72	1.08(−1)	1.17(−1)	O II	4650.84	V1

Table 3 – *continued*

λ_obs	F(λ)	I(λ)	ID	λ₀	Mult
			IC 4191 (fixed-slit)		
4651.35	1.44(−2)	1.55(−2)	C III	4651.47	V1
4658.06	7.88(−2)	8.45(−2)	[Fe III]	4658.10	F3
	*	*	C IV	4658.30	V8
4661.59	1.34(−1)	1.44(−1)	O II	4661.63	V1
4676.20	1.01(−1)	1.08(−1)	O II	4676.24	V1
4685.64	1.36(+1)	1.45(+1)	He II	4685.68	3.4
4711.32	2.97	3.12	[Ar IV]	4711.37	F1
4713.12	9.40(−1)	9.90(−1)	He I	4713.17	V12
4724.14	1.84(−1)	1.93(−1)	[Ne IV]	4724.15	F1
4725.61	1.46(−1)	1.53(−1)	[Ne IV]	4725.62	F1
4740.17	5.38	5.61	[Ar IV]	4740.17	F1
4861.30	1.00(+2)	1.00(+2)	H 4	4861.33	H4
4921.95	1.43	1.40	He I	4921.93	V48
4924.55	4.76(−2)	4.66(−2)	O II	4924.53	V28
4931.29	1.85(−1)	1.81(−1)	[O III]	4931.80	F1
4958.88	4.55(+2)	4.40(+2)	[O III]	4958.91	F1
4958.20	5.01(+2)	4.84(+2)	[O III]	4958.91	F1
5006.12	1.57(+3)	1.50(+3)	[O III]	5006.84	F1
5041.04	1.74(−1)	1.64(−1)	Si II	5041.03	V5
5047.73	1.48(−1)	1.39(−1)	He I	5047.74	V47
5055.99	1.88(−1)	1.75(−1)	Si II	5055.98	V5
5190.21	1.74(−1)	1.55(−1)	[Ar III]	5191.82	F3
5198.23	4.61(−1)	4.10(−1)	[N I]	5199.84	F1
5343.41	3.78(−2)	3.21(−2)	C II	5342.38	
5411.18	1.48	1.23	He II	5411.52	4.7
5517.43	5.06(−1)	4.07(−1)	[Cl III]	5517.66	F1
5537.37	1.06	8.54(−1)	[Cl III]	5537.60	F1
5577.11	1.66(−1)	1.32(−1)	[O I]	5577.34	F3
5591.89	1.23(−1)	9.77(−2)	O III	5592.37	V5
5666.14	1.18(−1)	9.20(−2)	N II	5666.63	V3
5679.07	2.17(−1)	1.68(−1)	N II	5679.56	V3
5701.48	8.18(−2)	6.31(−2)	[Mn v]?	5703	
5754.43	2.81	2.13	[N II]	5754.60	F3
5801.53	1.21(−1)	9.14(−2)	C IV	5801.51	V1
5812.16	1.11(−1)	8.36(−2)	C IV	5812.14	V1
5861.49	8.52(−2)	6.33(−2)	[Mn v]?	5862	
5875.49	2.26(+1)	1.67(+1)	He I	5875.66	V11
5930.58	8.12(−2)	5.93(−2)	He II	5930.58	
5953.67	6.22(−2)	4.52(−2)	He II	5952.94	5.24
5977.58	4.80(−2)	3.47(−2)	He II	5977.03	5.23
6004.34	1.81(−1)	1.30(−1)			
6045.58	6.57(−1)	4.68(−1)			
6074.35	7.62(−2)	5.39(−2)	He II	6074.19	5.20
6083.53	6.32(−2)	4.46(−2)	[Mn v]?	6084	
6101.77	4.45(−1)	3.13(−1)	[K IV]	6101.83	F1
6117.67	6.22(−2)	4.35(−2)	He II	6118.20	5.19
6151.97	4.50(−2)	3.13(−2)	C II	6151.43	V16.04
6158.15	5.30(−2)	3.68(−2)	[Mn v]	6157.60	
6170.35	7.79(−2)	5.39(−2)	He II	6170.69	5.18
6234.02	9.84(−2)	6.72(−2)	He II	6233.80	5.17
6300.39	1.19(+1)	8.03	[O I]	6300.34	F1
6312.15	3.94	2.65	[S III]	6312.10	F3
6347.23	2.76(−1)	1.84(−1)	Si II	6347.10	V2
6363.91	4.07	2.70	[O I]	6363.78	F1
6371.51	2.23(−1)	1.48(−1)	Si II	6371.38	V2
6393.98	1.17(−1)	7.78(−2)	[Mn v]	6393.60	
6401.95	9.58(−2)	6.31(−2)	?		
6406.68	1.26(−1)	8.33(−2)	He II	6406.30	5.15
6435.11	5.40(−1)	3.53(−1)	[Ar v]	6435.10	
6461.96	1.26(−1)	8.22(−2)	C II	6461.95	
6527.29	2.09(−1)	1.34(−1)	He II	6527.11	5.14
6547.97	3.81(+1)	2.43(+1)	[N II]	6548.10	F1
6562.64	4.33(+2)	2.76(+2)	H 3	6562.77	H3

Table 3 – *continued*

λ_{obs}	$F(\lambda)$	$I(\lambda)$	ID	λ_0	Mult
			IC 4191 (fixed-slit)		
6583.37	1.19(+2)	7.55(+1)	[N II]	6583.50	F1
6678.24	7.30	4.55	He I	6678.16	V46
6716.52	6.09	3.77	[S II]	6716.44	F2
6730.91	1.21(+1)	7.49	[S II]	6730.82	F2
6794.84	9.86(−2)	6.01(−2)	[K IV]	6795.00	F1
6891.13	2.39(−1)	1.43(−1)	He II	6890.90	
7005.74	1.13	6.63(−1)	[Ar V]	7005.74	
7109.63	6.78(−2)	3.94(−2)	He I	7065.25	V10
7135.79	3.31(+1)	1.89(+1)	[Ar III]	7135.80	F1
7170.70	3.08(−1)	1.75(−1)	[Ar IV]	7170.62	F2
7177.58	2.80(−1)	1.59(−1)	He II	7177.50	5.11
7231.56	1.31(−1)	7.40(−2)	C II	7231.32	V3
7236.60	4.79(−1)	2.70(−1)	C II	7236.42	V3
7262.94	2.38(−1)	1.23(−1)	[Ar IV]	7762.76	F2
7281.53	1.19	6.66(−1)	He I	7281.35	V45
7297.49	5.52(−2)	3.08(−2)	He I	7298.04	
7319.82	1.04(+1)	5.79	[O II]	7318.92	F2
7330.57	8.63	4.78	[O II]	7329.67	F2
			IC 4191 (scanning-slit) $c(H\beta)^{Ba} = 0.58$		
	*	*	H 14	3721.94	H14
	*	*	[S III]	3721.63	F2
3726.10	4.20(+1)	5.91(+1)	[O II]	3726.03	F1
	*	*	[O II]	3728.82	F1
	*	*	H 13	3734.37	H13
3749.66	2.43	3.41	H 12	3750.15	H12
3756.75	4.54(−1)	6.35(−1)	O III	3757.24	V2
3759.38	1.27	1.78	O III	3759.87	V2
3770.14	2.82	3.93	H 11	3770.63	H11
3796.95	3.94	5.46	H 10	3797.90	H10
3818.67	1.09	1.50	He I	3819.62	V22
3834.43	5.39	7.40	H 9	3835.39	H9
3867.88	1.01(+2)	1.38(+2)	[Ne III]	3868.75	F1
3888.18	1.24(+1)	1.69(+1)	He I	3888.65	V2
3966.57	4.08(+1)	5.40(+1)	[Ne III]	3967.46	F1
4008.59	1.58(−1)	2.07(−1)	He I	4009.26	V55
4025.59	1.88	2.46	He I	4026.21	V18
4040.99	4.97(−2)	6.39(−2)	N II	4041.31	V39b
4067.88	3.08	3.96	[S II]	4068.60	F1
	*	*	O II	4069.62	V10
	*	*	O II	4069.89	V10
4069.04	5.48(−1)	7.06(−1)	O II	4069.78	V10
4071.44	2.84(−1)	3.65(−1)	O II	4072.16	V10
4075.14	2.24(−1)	2.88(−1)	O II	4075.86	V10
4075.63	1.09	1.40	[S II]	4076.35	F1
4083.14	3.25(−2)	4.18(−2)	O II	4083.90	V48b
4084.35	3.92(−2)	5.03(−2)	O II	4085.11	V10
4086.39	4.52(−2)	5.80(−2)	O II	4087.15	V48c
4088.52	1.15(−1)	1.48(−1)	O II	4089.29	V48a
4096.64	1.20	1.54	N III	4097.33	V1
4101.05	1.92(+1)	2.45(+1)	H 6	4101.74	H6
4118.70	1.14(−1)	1.44(−1)	O II	4119.22	V20
4120.32	1.95(−1)	2.48(−1)	He I	4120.84	V16
4143.07	3.17(−1)	3.99(−1)	He I	4143.76	V53
4184.56	3.60(−2)	4.48(−2)	O II	4185.45	V36
4186.01	5.72(−2)	7.11(−2)	C III	4186.90	V18
4188.90	5.71(−2)	7.09(−2)	O II	4189.79	V36
4199.27	2.23(−1)	2.76(−1)	He II	4199.83	4.11
4266.49	4.50(−1)	5.46(−1)	C II	4267.15	V6
4274.89	5.98(−2)	7.23(−2)	O II	4275.55	V67a
	*	*	O II	4275.99	V67b
4276.09	7.67(−2)	9.27(−2)	O II	4276.75	V67b
4282.49	4.86(−2)	5.87(−2)	O II	4282.96	V67c

Table 3 – *continued*

λ_{obs}	$F(\lambda)$	$I(\lambda)$	ID	λ_0	Mult
			IC 4191 (scanning-slit)		
4284.45	6.59(−2)	7.94(−2)	O II	4283.73	V67c
4303.26	7.75(−2)	9.30(−2)	O II	4303.61	V65a
	6.93(−2)	8.26(−2)	O II	4317.14	V2
4339.73	3.95(+1)	4.68(+1)	H 5	4340.47	H5
4348.84	1.40(−1)	1.66(−1)	O II	4349.43	V2
4362.46	8.62	1.01(+1)	[O III]	4363.21	F2
4378.43	2.30(−1)	2.70(−1)	N III	4379.11	V18
4387.25	4.88(−1)	5.70(−1)	He I	4387.93	V51
4391.03	3.70(−2)	4.31(−2)	Ne II	4391.99	V55e
4414.17	6.54(−2)	7.57(−2)	O II	4414.90	V5
4416.24	4.59(−2)	5.31(−2)	O II	4416.97	V5
4436.83	4.09(−2)	4.69(−2)	He I	4437.55	V50
4470.78	4.42	5.02	He I	4471.50	V14
4510.22	1.07(−1)	1.20(−1)	N III	4510.91	
4540.90	4.01(−1)	4.45(−1)	He II	4541.59	4.9
4570.40	1.48(−1)	1.63(−1)	Mg I]	4571.10	
4590.35	6.93(−2)	7.57(−2)	O II	4590.97	V15
4595.56	5.37(−2)	5.85(−2)	O II	4596.18	V15
4608.91	7.84(−2)	8.52(−2)	O II	4609.44	V92a
	*	*	OII	4610.20	V92c
4630.10	5.09(−2)	5.49(−2)	N II	4630.54	V5
4633.47	8.52(−1)	9.18(−1)	N III	4634.14	V2
4638.19	1.77(−1)	1.91(−1)	O II	4638.49	V1
4639.97	1.74	1.87	N III	4640.64	V2
4641.14	3.01(−1)	3.22(−1)	O II	4641.44	V1
4646.76	1.46(−1)	1.56(−1)	C III	4647.42	V1
4648.47	5.07(−1)	5.44(−1)	O II	4649.13	V1
4649.59	1.19(−1)	1.28(−1)	C III	4650.25	V1
4650.18	9.30(−2)	9.97(−2)	O II	4650.84	V1
4650.81	6.91(−2)	7.40(−2)	C III	4651.47	V1
4657.49	9.92(−2)	1.06(−1)	[Fe III]	4658.10	F3
	*	*	C IV	4658.30	V8
4661.02	1.44(−1)	1.54(−1)	O II	4661.63	V1
4675.63	1.15(−1)	1.23(−1)	O II	4676.24	V1
4685.07	1.24(+1)	1.32(+1)	He II	4685.68	3.4
4704.93	1.67(−2)	1.76(−2)	O II	4705.35	V25
4710.74	2.78	2.92	[Ar IV]	4711.37	F1
4712.54	7.96(−1)	8.36(−1)	He I	4713.17	V12
4723.61	1.62(−1)	1.70(−1)	[Ne IV]	4724.15	F1
4725.08	1.19(−1)	1.25(−1)	[Ne IV]	4725.62	F1
4739.61	4.87	5.07	[Ar IV]	4740.17	F1
4860.62	1.00(+2)	1.00(+2)	H 4	4861.33	H4
4905.89	4.10(−2)	4.04(−2)	?		
4907.15	3.40(−2)	3.35(−2)	O II	4906.83	V28
4921.39	1.29	1.27	He I	4921.93	V48
4923.98	6.99(−2)	6.85(−2)	O II	4924.53	V28
4930.73	1.61(−1)	1.57(−1)	[O III]	4931.80	F1
4958.22	5.23(+2)	5.06(+2)	[O III]	4958.91	F1
5006.14	1.58(+3)	1.50(+3)	[O III]	5006.84	F1
5189.59	1.92(−1)	1.72(−1)	[Ar III]	5191.82	F3
5197.61	6.52(−1)	5.84(−1)	[N I]	5199.84	F1
5410.44	1.29	1.08	He II	5411.52	4.7
5516.71	5.48(−1)	4.46(−1)	[Cl III]	5517.66	F1
5536.64	1.05	8.57(−1)	[Cl III]	5537.60	F1
5576.38	1.82(−1)	1.46(−1)	[O I]	5577.34	F3
5666.55	1.17(−1)	9.21(−2)	N II	5666.63	V3
5677.93	5.08(−2)	4.00(−2)	N II	5676.02	V3
5679.41	1.63(−1)	1.28(−1)	N II	5679.56	V3
5753.56	3.01	2.32	[N II]	5754.60	F3
5874.60	2.29(+1)	1.72(+1)	He I	5875.66	V11
5930.99	6.15(−2)	4.60(−2)	N II	5931.78	V3
6101.07	3.70(−1)	2.64(−1)	[K IV]	6101.83	F1
6299.58	1.30(+1)	8.92	[O I]	6300.34	F1

Table 3 – *continued*

λ_{obs}	$F(\lambda)$	$I(\lambda)$	ID	λ_0	Mult
			IC 4191 (scanning-slit)		
6311.34	3.78	2.59	[S III]	6312.10	F3
6346.41	1.49(−1)	1.01(−1)	Si II	6347.10	V2
6363.09	4.45	3.02	[O I]	6363.78	F1
6370.69	2.76(−1)	1.86(−1)	Si II	6371.38	V2
6434.24	4.53(−1)	3.03(−1)	[Ar V]	6435.10	
6461.32	1.36(−1)	9.09(−2)	C II	6461.95	
6501.68	8.31(−2)	5.48(−2)	?		
6526.50	2.52(−1)	1.66(−1)	He II	6527.11	5.14
6547.75	4.09(+1)	2.68(+1)	[N II]	6548.10	F1
6562.42	4.22(+2)	2.75(+2)	H 3	6562.77	H3
6583.15	1.26(+2)	8.22(+1)	[N II]	6583.50	F1
6677.51	7.20	4.60	He I	6678.16	V46
6715.79	7.81	4.95	[S II]	6716.44	F2
6730.17	1.47(+1)	9.29	[S II]	6730.82	F2
6794.17	9.40(−2)	5.87(−2)	[K IV]	6795.00	F1
7064.20	1.36(+1)	8.12	He I	7065.25	V10
7134.74	3.63(+1)	2.14(+1)	[Ar III]	7135.80	F1
7169.45	2.84(−1)	1.66(−1)	[Ar IV]	7170.62	F2
7176.32	1.96(−1)	1.14(−1)	He II	7177.50	5.11
7235.22	5.45(−1)	3.16(−1)	C II	7236.42	V3
7261.56	2.73(−1)	1.46(−1)	[Ar IV]	7262.76	F2
7280.14	1.36	7.84(−1)	He I	7281.35	V45
7318.17	1.17(+1)	6.73	[O II]	7318.92	F2
7328.92	1.05(+1)	5.99	[O II]	7329.67	F2
			IC 4406		
			$c(H\beta)^{Ba} = 0.26/0.44$		
3721.14	*	*	[S III]	3721.63	F2
	*	*	H 14	3721.94	H14
3726.29	3.25(+2)	4.22(+2)	[O II]	3726.03	F1
3728.33	*	*	[O II]	3728.82	F1
3749.18	3.30	4.26	H 12	3750.15	H12
3756.27	1.18	1.52	O III	3757.24	V2
3758.90	1.69	2.18	O III	3759.87	V2
3769.66	3.55	4.57	H 11	3770.63	H11
3797.28	4.78	6.12	H 10	3797.90	H10
3835.34	6.11	7.77	H 9	3835.39	H9
3867.94	1.02(+2)	1.29(+2)	[Ne III]	3868.75	F1
3888.24	1.82(+1)	2.29(+1)	He I	3888.65	V2
3966.63	4.19(+1)	5.19(+1)	[Ne III]	3967.46	F1
4008.78	1.46(−1)	1.79(−1)	He I	4009.26	V55
4025.88	2.11	2.58	He I	4026.21	V18
4068.18	1.18	1.43	[S II]	4068.60	F1
	*	*	O II	4069.62	V10
	*	*	O II	4069.89	V10
4069.34	3.39(−1)	4.11(−1)	O II	4069.78	V10
4071.74	3.12(−1)	3.78(−1)	O II	4072.16	V10
4075.44	2.09(−1)	2.53(−1)	O II	4075.86	V10
4075.93	4.29(−1)	5.18(−1)	[S II]	4076.35	F1
4096.97	8.28(−1)	9.97(−1)	N III	4097.33	V1
4101.38	2.00(+1)	2.40(+1)	H 6	4101.74	H6
	*	*	O II	4119.22	V20
4120.68	2.27(−1)	2.71(−1)	He I	4120.84	V16
4143.37	3.06(−1)	3.65(−1)	He I	4143.76	V53
4186.73	7.73(−2)	9.12(−2)	C III	4186.90	V18
4199.56	3.02(−1)	3.55(−1)	He II	4199.83	4.11
4266.82	6.96(−1)	8.05(−1)	C II	4267.15	V6
4325.24	1.07(−1)	1.23(−1)	O II	4325.76	V2
4340.09	4.02(+1)	4.57(+1)	H 5	4340.47	H5
4362.83	6.00	6.79	[O III]	4363.21	F2
4378.89	1.52(−1)	1.71(−1)	N III	4379.11	V18
4387.53	6.22(−1)	6.99(−1)	He I	4387.93	V51
4391.23	8.30(−2)	9.33(−2)	Ne II	4391.99	V55e
4471.12	4.25	4.68	He I	4471.50	V14

Table 3 – *continued*

λ_{obs}	$F(\lambda)$	$I(\lambda)$	ID	λ_0	Mult
			IC 4406		
4541.25	4.56(−1)	4.94(−1)	He II	4541.59	4.39
4562.26	2.94(−1)	3.17(−1)	Mg I]	4562.60	
4570.75	2.98(−1)	3.20(−1)	Mg I]	4571.10	
4631.29	2.18(−2)	2.32(−1)	N II	4630.54	V5
4633.83	4.25(−1)	4.50(−1)	N III	4634.14	V2
4638.55	1.71(−1)	1.82(−1)	O II	4638.49	V1
4640.33	7.61(−1)	8.04(−1)	N III	4640.64	V2
4641.50	2.49(−1)	2.63(−1)	O II	4641.44	V1
4647.08	1.07(−1)	1.13(−1)	C III	4647.42	V1
4648.79	2.45(−1)	2.59(−1)	O II	4649.13	V1
4649.91	9.64(−2)	1.01(−1)	C III	4650.25	V1
4650.50	9.10(−2)	9.59(−2)	O II	4650.84	V1
4651.13	2.10(−2)	2.21(−2)	C III	4651.47	V1
4661.37	9.40(−2)	9.88(−2)	O II	4661.63	V1
4675.89	4.59(−2)	4.81(−2)	O II	4676.24	V1
4685.43	1.40(+1)	1.46(+1)	He II	4685.68	3.4
4711.13	1.40	1.45	[Ar IV]	4711.37	F1
4712.93	5.14(−1)	5.33(−1)	He I	4713.17	V12
4739.92	1.15	1.18	[Ar IV]	4740.17	F1
4861.07	1.00(+2)	1.00(+2)	H 4	4861.33	H4
4921.68	1.36	1.34	He I	4921.93	V48
4931.02	1.46(−1)	1.43(−1)	O III	4931.80	F1
4934.52	1.10(−1)	1.08(−1)	?	4934.52	
4958.16	3.73(+2)	3.64(+2)	[O III]	4958.91	
5006.09	1.08(+3)	1.04(+3)	[O III]	5006.84	F1
5198.10	7.06	6.50	[N I]	5199.84	F1
5410.55	1.20	1.05	He II	5411.52	4.7
5517.28	6.13(−1)	5.24(−1)	[Cl III]	5517.66	F1
5537.22	7.51(−1)	6.40(−1)	[Cl III]	5537.60	F1
5576.96	4.37(−1)	3.70(−1)	[O I]	5577.34	F3
5753.81	7.03	5.77	[N II]	5754.60	F3
5875.01	1.75(+1)	1.40(+1)	He I	5875.66	V11
6299.99	4.25(+1)	3.19(+1)	[O I]	6300.34	F1
6311.75	8.95(−1)	6.72(−1)	[S III]	6312.10	F3
6363.41	2.09(+1)	1.55(+1)	[O I]	6363.78	F1
6547.95	1.73(+2)	1.26(+2)	[N II]	6548.10	F1
6562.62	3.68(+2)	2.66(+2)	H 3	6562.77	H3
6583.35	5.22(+2)	3.76(+2)	[N II]	6583.50	F1
6678.03	5.24	3.73	He I	6678.16	V46
6716.41	1.16(+1)	8.21	[S II]	6716.44	F2
6730.79	1.31(+1)	9.27	[S II]	6730.82	F2
7064.96	4.62	3.12	He I	7065.25	V10
7135.47	2.94(+1)	1.97(+1)	[Ar III]	7135.80	F1
7281.53	7.94(−1)	5.22(−1)	He I	7281.35	V45
7319.11	9.81	6.42	[O II]	7318.92	F2
7329.86	7.89	5.16	[O II]	7329.67	F2
			My Cn 18		
			$c(H\beta)^{Ba} = 1.24$		
	*	*	H 14	3721.94	H14
	*	*	[S III]	3721.63	F2
3724.96	3.05(+1)	6.36(+1)	[O II]	3726.03	F1
	*	*	[O II]	3728.82	F1
	*	*	H 13	3734.37	H13
3833.28	2.13	4.19	H 9	3835.39	H9
3866.32	5.47	1.05(+1)	[Ne III]	3868.75	F1
3886.40	6.82	1.30(+1)	He I	3888.65	V2
3967.24	8.36	1.52(+1)	[Ne III]	3967.46	F1
4025.33	1.15	2.03	He I	4026.21	V18
4040.83	2.95(−2)	5.14(−2)	N II	4041.31	V39b
4056.61	8.23(−2)	1.42(−1)	?	4056.61	
4067.73	1.30	2.23	[S II]	4068.60	F1
4075.48	4.47(−1)	7.63(−1)	[S II]	4076.35	F1
4087.91	1.11(−1)	1.89(−1)	O II	4087.15	V48c
4100.84	1.26(+1)	2.12(+1)	H 6	4101.74	H6

Table 3 – *continued*

λ_{obs}	$F(\lambda)$	$I(\lambda)$	ID	λ_0	Mult
			My Cn 18		
4119.95	8.33(−2)	1.38(−1)	O II	4119.22	V20
*	*	*	He I	4120.84	V16
4142.60	1.99(−1)	3.26(−1)	He I	4143.76	V53
4238.12	3.63(−2)	5.58(−2)	N II	4238.12	
4266.22	1.67(−1)	2.52(−1)	C II	4267.15	V6
4339.51	2.89(+1)	4.16(+1)	H 5	4340.47	H5
4362.22	4.03(−1)	5.70(−1)	[O III]	4363.21	F2
4386.93	3.89(−1)	5.41(−1)	He I	4387.93	V51
4470.54	4.18	5.49	He I	4471.50	V14
4570.24	7.20(−2)	8.83(−2)	Mg I]	4571.10	
4606.37	7.04(−2)	8.42(−2)	N II	4607.16	V5
4620.60	6.17(−2)	7.31(−2)	N II	4621.39	V5
4629.75	1.78(−1)	2.10(−1)	N II	4630.54	V5
4638.77	9.24(−2)	1.08(−1)	O II	4638.49	V1
4640.55	2.05(−1)	2.39(−1)	N III	4640.64	V2
4641.72	1.00(−1)	1.16(−1)	O II	4641.44	V1
4648.09	1.97(−1)	2.29(−1)	O II	4649.13	V1
4649.79	1.32(−1)	1.53(−1)	O II	4650.84	V1
4657.32	5.35(−1)	6.18(−1)	[Fe III]	4658.10	F3
*	*	*	C IV	4658.30	V8
4685.46	5.07(−1)	5.74(−1)	He II	4685.68	3.4
4700.83	1.64(−1)	1.83(−1)	[Fe III]	4701.62	
4712.38	5.81(−1)	6.45(−1)	He I	4713.17	V12
4733.12	4.52(−2)	4.95(−2)	[Fe III]	4733.90	
4754.05	1.25(−1)	1.35(−1)	[Fe III]	4754.80	
4860.61	1.00(+2)	1.00(+2)	H 4	4861.33	H4
4880.22	2.84(−1)	2.80(−1)	[Fe III]	4881.11	
4905.77	7.77(−2)	7.53(−2)	?		
4921.23	1.52	1.46	He I	4921.93	V48
4923.96	4.87(−2)	4.66(−2)	?		
4930.21	5.98(−2)	5.70(−2)	?		
4958.19	9.67(+1)	9.03(+1)	[O III]	4958.91	F1
4956.96	1.05(+2)	9.80(+1)	[O III]	4958.91	
5004.88	3.19(+2)	2.88(+2)	[O III]	5006.84	F1
5099.97	2.33(+1)	1.97(+1)	?		
5196.78	9.33(−1)	7.38(−1)	[N I]	5197.88	
5268.56	6.13(−1)	4.61(−1)	[Fe III]	5270.40	
5515.94	4.90(−1)	3.16(−1)	[Cl III]	5517.66	F1
5535.87	9.48(−1)	6.04(−1)	[Cl III]	5537.60	F1
5677.11	5.98(−1)	3.56(−1)	N II	5679.56	V3
5752.91	5.52	3.17	[N II]	5754.60	F3
5873.93	2.82(+1)	1.53(+1)	He I	5875.66	V11
6006.39	4.50(−1)	2.29(−1)	?		
6048.71	8.79(−1)	4.39(−1)	?		
6299.13	3.51	1.57	[O I]	6300.34	F1
6310.89	3.04	1.35	[S III]	6312.10	F3
6346.02	2.67(−1)	1.17(−1)	Si II	6347.10	V2
6362.70	1.12	4.91(−1)	[O I]	6363.78	F1
6547.09	1.43(+2)	5.79(+1)	[N II]	6548.10	F1
6561.75	5.73(+2)	2.29(+2)	H 3	6562.77	H3
6582.48	4.42(+2)	1.76(+2)	[N II]	6583.50	F1
6677.03	9.92	3.79	He I	6678.16	V46
6715.42	7.58	2.86	[S II]	6716.44	F2
6729.80	1.34(+1)	5.04	[S II]	6730.82	F2
7063.98	1.54(+1)	5.11	He I	7065.25	V10
7134.51	3.43(+1)	1.10(+1)	[Ar III]	7135.80	F1
7176.65	1.01	3.23(−1)	He II	7177.50	5.11
7230.02	2.47(−1)	7.71(−2)	C II	7231.32	V3
7235.12	6.20(−1)	1.93(−1)	C II	7236.42	V3
7279.85	1.65	5.08(−1)	He I	7281.35	V45
7318.18	1.19(+1)	3.61	[O II]	7318.92	F2
7328.93	1.00(+1)	3.02	[O II]	7329.67	F2

Table 4. Observed and dereddened relative line fluxes [$F(\lambda)$ and $I(\lambda)$, respectively], on a scale where Hβ = 100.

λ_{obs}	$F(\lambda)$	$I(\lambda)$	ID	λ_0	Mult
			SMC N87		
			$c(H\beta)^{Ba} = 0.03$ (Gal), 0.02 (SMC)		
1549	49.7	62.4	C IV	1549	
1663	19.3	23.8	O III]	1663	
1908	451	550	C III]	1908	
2426	52.1	62.4	C II]	2426	
3721.72	1.26	1.61	H 14	3721.94	H14
*	*	*	[S III]	3721.63	[S III]
3725.79	3.74	4.79	[O II]	3726.03	F1
3728.58	2.14	2.73	[O II]	3728.82	F1
3734.06	9.41(−1)	1.20	H 13	3734.37	H13
3749.98	1.41	1.79	H 12	3750.15	H12
3770.46	1.52	1.93	H 11	3770.63	H11
3797.73	2.39	3.00	H 10	3797.90	H10
3835.22	3.83	4.76	H 9	3835.39	H9
3868.47	1.70(+1)	2.10(+1)	[Ne III]	3868.75	F1
3888.77	1.00(+1)	1.22(+1)	He I	3888.65	V2
3967.17	6.55	7.88	[Ne III]	3967.46	F1
3969.78	9.71	1.16(+1)	H 7	3970.07	H7
4025.99	1.91	2.26	He I	4026.21	V18
4070.30	3.08(−1)	3.61(−1)	[S II]	4068.60	F1
4071.46	1.45(−1)	1.71(−1)	O II	4069.62	V10
*	*	*	O II	4069.89	V10
4073.86	5.52(−2)	6.48(−2)	O II	4072.16	V10
*	*	*	O II	4075.86	V10
4078.06	1.39(−1)	1.63(−1)	[S II]	4076.35	F1
4080.55	2.29(−2)	2.69(−2)	O II	4078.84	V10
4086.82	3.09(−2)	3.61(−2)	O II	4083.90	V48b
4088.03	1.08(−2)	1.27(−2)	O II	4085.11	V10
4090.07	2.45(−2)	2.86(−2)	O II	4087.15	V48c
*	*	*	O II	4089.29	V48a
4103.46	2.28(+1)	2.65(+1)	H 6	4101.74	H6
*	*	*	O II	4120.54	V20
4122.46	2.59(−1)	3.01(−1)	He I	4120.84	V16
4145.37	3.09(−1)	3.56(−1)	He I	4143.76	V53
4188.46	9.46(−2)	1.08(−1)	C III	4186.90	V18
4268.66	5.98(−1)	6.72(−1)	C II	4267.15	V6
4294.11	4.16(−2)	4.65(−2)	O II	4292.21	V78c
4327.58	5.66(−2)	6.27(−2)	O II	4325.76	V2
4342.02	4.20(+1)	4.64(+1)	H 5	4340.47	H5
4351.07	4.53(−2)	5.00(−2)	O II	4349.43	V2
4359.53	3.54(−2)	3.89(−2)	O II	4357.25	V63a
4364.79	6.16	6.78	[O III]	4363.21	F2
4389.55	5.70(−1)	6.23(−1)	He I	4387.93	V51
4439.03	1.15(−1)	1.24(−1)	He I	4437.55	V50
4458.31	2.33(−2)	2.51(−2)	Ne II	4457.24	V61d
4473.10	4.96	5.33	He I	4471.50	V14
4641.10	7.99(−2)	8.32(−2)	O II	4638.86	V1
4643.26	1.29(−2)	1.34(−2)	N III	4640.64	V2
4644.06	7.99(−2)	8.31(−2)	O II	4641.81	V1
4649.59	7.52(−2)	7.81(−2)	C III	4647.42	V1
4651.30	7.52(−2)	7.81(−2)	O II	4649.13	V1
4652.42	4.51(−2)	4.68(−2)	C III	4650.25	V1
4653.01	7.52(−2)	7.81(−2)	O II	4650.84	V1
4653.64	1.50(−2)	1.56(−2)	C III	4651.47	V1
4675.16	7.95(−3)	8.25(−3)	[Fe III]	4658.10	F3
*	*	*	C IV	4658.30	V8
4677.67	2.34(−2)	2.43(−2)	O II	4661.63	V1
4677.66	2.40(−2)	2.48(−2)	O II	4676.24	V1
4713.41	2.65(−1)	2.72(−1)	[Ar IV]	4711.37	F1
4715.22	9.08(−1)	9.32(−1)	He I	4713.17	V12
4742.22	3.97(−1)	4.05(−1)	[Ar IV]	4740.17	F1
4755.96	2.78(−2)	2.83(−2)	[Fe III]	4754.83	

Table 4 – *continued*

λ_{obs}	$F(\lambda)$	$I(\lambda)$	ID	λ_0	Mult
		SMC N87			
4758.33	1.34(−2)	1.37(−2)	?		
4802.77	2.80(−2)	2.83(−2)	?		
4804.79	3.47(−2)	3.50(−2)	N II	4802.29	V20
4861.30	1.00(+2)	1.00(+2)	H 4	4861.33	H4
4923.89	1.30	1.28	He I	4921.93	V48
4926.49	6.55(−2)	6.48(−2)	O II	4924.53	V28
4933.09	5.84(−2)	5.79(−2)	[O III]	4931.80	F1
4960.99	1.93(+2)	1.90(+2)	[O III]	4958.91	F1
6557.81	2.52	2.03	[N II]	6548.10	F1
6571.25	3.55(+2)	2.85(+2)	H 3	6562.77	H3
6590.48	6.86	5.49	[N II]	6583.50	F1
7068.72	5.22	4.14	He I	6678.16	V46
6717.16	3.76(−1)	4.43(−1)	[S II]	6716.44	F2
6731.54	8.07(−1)	7.18(−1)	[S II]	6730.82	F2
7068.72	1.36(+1)	1.04(+1)	He I	7065.25	V10
7141.32	4.28	3.26	[Ar III]	7135.80	F1
7291.42	1.57	1.18	He I	7281.35	V45
7330.40	3.17	2.38	[O II]	7318.92	F2
7341.16	2.55	1.92	[O II]	7329.67	F2
		LMC N141			
		$c(H\beta)^{Ba} = 0.11$ (Gal), 0.03 (LMC)			
1549	33.9	52.2	C IV	1549	
1640	14.3	21.4	He II	1640	
1908	136	205	C III]	1908	
3727.44	8.51	1.06(+1)	[O II]	3726.03	F1
3730.23	5.22	6.52	[O II]	3728.82	F1
3751.71	1.50	1.86	H 12	3750.15	H12
3772.20	1.36	1.68	H 11	3770.63	H11
3799.48	1.99	2.45	H 10	3797.90	H10
3836.99	4.36	5.32	H 9	3835.39	H9
3870.33	3.53(+1)	4.27(+1)	[Ne III]	3868.75	F1
3890.64	9.18	1.10(+1)	He I	3888.65	V2
3969.08	1.29(+1)	1.53(+1)	[Ne III]	3967.46	F1
3971.69	1.03(+1)	1.22(+1)	H 7	3970.07	H7
4027.91	2.43	2.85	He I	4026.21	V18
4072.63	1.12	1.30	[S II]	4068.60	F1
4073.79	1.62(−1)	1.88(−1)	O II	4069.62	V10
4076.19	1.06(−1)	1.24(−1)	O II	4072.16	V10
4079.90	2.18(−1)	2.54(−1)	O II	4075.86	V10
4080.39	2.79(−1)	3.23(−1)	[S II]	4076.35	F1
4101.60	2.83(−1)	3.26(−1)	N III	4097.33	V1
4105.78	2.53(+1)	2.91(+1)	H 6	4101.74	H6
4125.03	3.10(−1)	3.56(−1)	He I	4120.84	V16
4147.69	3.47(−1)	3.97(−1)	He I	4143.76	V53
4190.46	4.60(−2)	5.22(−2)	C III	4186.90	V18
4193.36	5.90(−2)	6.67(−2)	O II	4189.79	V36
4271.09	6.12(−1)	6.83(−1)	C II	4267.15	V6
4344.45	4.87(+1)	5.35(+1)	H 5	4340.47	H5
4367.25	9.35	1.02(+1)	[O III]	4363.21	F2
4391.96	6.39(−1)	6.96(−1)	He I	4387.93	V51
4442.17	9.42(−2)	1.01(−1)	He I	4437.55	V50
4475.61	5.38	5.77	He I	4471.50	V14
4556.98	1.81(−1)	1.91(−1)	N II	4552.53	V58a
4566.39	2.98(−1)	3.14(−1)	Mg I]	4562.60	
4574.90	1.16	1.22	Mg I]	4571.10	
4594.73	1.66(−1)	1.74(−1)	O II	4590.97	V15
4638.01	9.06(−2)	9.42(−2)	N III	4634.14	V2
4642.74	2.45(−2)	2.55(−2)	O II	4638.86	V1
4644.52	1.80(−1)	1.87(−1)	N III	4640.64	V2
4645.69	1.15(−1)	1.20(−1)	O II	4641.81	V1
4651.05	7.41(−2)	7.68(−2)	C III	4647.42	V1
4652.76	1.22(−1)	1.27(−1)	O II	4649.13	V1
4653.88	6.69(−2)	6.93(−2)	C III	4650.25	V1

Table 4 – *continued*

λ_{obs}	$F(\lambda)$	$I(\lambda)$	ID	λ_0	Mult
		LMC N141			
4654.47	8.06(−2)	8.36(−2)	O II	4650.84	V1
4655.10	3.35(−2)	3.47(−2)	C III	4651.47	V1
4662.12	1.00(−1)	1.04(−1)	[Fe III]	4658.10	F3
	*	*	C IV	4658.30	V8
4665.65	5.00(−2)	5.18(−2)	O II	4661.63	V1
4680.62	4.50(−2)	4.65(−2)	O II	4676.24	V1
4689.66	3.03(−1)	3.13(−1)	He II	4685.68	3.4
4705.54	5.63(−2)	5.78(−2)	[Fe III]	4701.62	F3
4715.34	8.29(−1)	8.51(−1)	[Ar IV]	4711.37	F1
4717.14	8.59(−1)	8.81(−1)	He I	4713.17	v12
4744.05	1.19	1.22	[Ar IV]	4740.17	F1
4818.38	3.16(−2)	3.18(−2)	S II?	4815.55	V9
4865.49	1.00(+2)	1.00(+2)	H 4	4861.33	H4
4884.98	7.78(−2)	7.75(−2)	[Fe III]	4881.11	F2
4894.31	3.72(−2)	3.70(−2)	O II	4890.86	V28
4925.79	1.42	1.40	He I	4921.93	V48
4935.06	1.04(−1)	1.03(−1)	[O III]	4931.80	F1
4963.05	3.20(+2)	3.15(+2)	[O III]	4958.91	F1
6560.35	7.31	5.91	[N II]	6548.10	F1
6574.07	3.52(+2)	2.85(+2)	H 3	6562.77	H3
6593.29	2.17(+1)	1.75(+1)	[N II]	6583.50	F1
6683.36	5.88	4.70	He I	6678.16	V46
6720.29	1.85	1.47	[S II]	6716.44	F2
6734.37	3.41	2.71	[S II]	6730.82	F2
7071.99	1.36(+1)	1.05(+1)	He I	7065.25	V10
7144.58	1.45(+1)	1.11(+1)	[Ar III]	7135.80	F1
7294.46	1.37	1.03	He I	7281.35	V45
7333.61	5.77	4.35	[O II]	7318.92	F2
7344.37	4.81	3.62	[O II]	7329.67	F2
7752.96	3.32	2.42	C IV?	7736.00	
		LMC N66			
		$c(H\beta)^{1640} = 0.09$ (Gal), 0.05 (LMC)			
1240	187	318	N V	1240	
1486	119	177	N IV]	1486	
1549	188	276	C IV	1549	
1574	30.6	44.6	Ne V	1574	
1640	345	498	He II	1640	
1663	37.8	54.4	O III]	1663	
1750	65.1	93.4	N III]	1750	
1908	62.2	92.5	C III]	1908	
3727.04	1.13(+1)		[O II]	3726.03	F1
3729.83	1.94(+1)		[O II]	3728.82	F1
3870.43	1.09(+2)		[Ne III]	3868.75	F1
3890.74	1.96(+1)		He I	3888.65	V2
3969.18	4.59(+1)		[Ne III]	3967.46	F1
3971.79	1.31(+1)		H 7	3970.07	H7
4105.68	3.14(+1)		H 6	4101.74	H6
4231.02	4.23(+0)		[Fe V]	4227.20	F2
4344.38	4.96(+1)		H 5	4340.47	H5
4367.17	3.35(+1)		[O III]	4363.21	F2
4475.38	3.72(+0)		He I	4471.50	V14
4545.70	2.15(+0)		He II	4541.59	4.9
4559.22	2.95(−1)		[Fe II]	4555.00	
4600.94	2.99(−1)		O II	4596.18	V15
4616.38	3.41(−1)		?		
4618.55	1.54(−1)		N II	4613.87	V5
4637.28	1.98(−1)		O IV	4631.89	V19
4638.96	3.63(−1)		N III	4634.14	V2
4645.05	3.80(−1)		N III	4640.64	V2
4646.25	3.80(−1)		O II	4641.81	V1
4653.47	2.27(−1)		O II	4649.13	V1
4655.18	2.27(−1)		O II	4650.84	V1
4662.13	4.31(−1)		[Fe III]	4658.10	F3

Table 4 – *continued*

λ_{obs}	$F(\lambda)$	$I(\lambda)$	ID	λ_0	Mult
			LMC N66		
	*		C IV	4658.30	V8
4665.04	1.70(−1)		O II	4661.63	V1
4669.65	5.25(−1)		[Fe III]	4667.01	F3
4673.60	2.98(−1)		O II	4669.27	V89b
4676.74	4.67(−1)		O II	4673.73	V1
4679.25	4.67(−1)		O II	4676.24	V1
4681.15	2.74(−1)		N II	4678.14	V61b
4690.02	6.73(+1)		He II	4685.68	3.4
4701.92	2.93(+0)		?		
4703.74	6.44(−1)		[Fe VII]	4698.25	
4707.11	5.47(−1)		[Fe III]	4701.62	F3
4715.37	1.18(+1)		[Ar IV]	4711.37	F1
4717.18	4.18(+0)		He I	4713.17	V12
4728.12	9.64(−1)		[Ne IV]	4724.15	F1
4729.59	1.50(+0)		[Ne IV]	4725.62	F1
4737.79	3.23(−1)		[Fe III]	4733.93	F3
4744.47	1.29(+1)		[Ar IV]	4740.17	F1
4759.58	1.34(−1)		[Fe III]	4754.83	
4761.27	1.72(−1)		?		
4769.48	2.18(−1)		?		
4772.56	1.69(−1)		[Fe III]	4769.40	F3
4777.70	1.90(−1)		Ne II	4772.93	
4782.65	2.08(−1)		[Fe III]	4777.88	V20
4800.75	3.74(−1)		?		
4865.50	1.00(+2)		H4	4861.33	H4
4898.94	5.60(−1)		[Fe VII]	4893.90	
4926.32	9.15(−1)		He I	4921.93	V48
4992.32	3.79(+2)		[O III]	4958.91	F1
5040.29	1.12(+3)		[O III]	5006.84	F1
5444.24	5.04(+0)		He II	5411.52	4.7
5786.96	1.98(+0)		[N II]	5754.60	F3
5907.72	7.71(+0)		He I	5875.66	V11
6335.11	7.23(+0)		[O I]	6300.34	F1
6395.70	1.47(+0)		[O I]	6363.78	F1
6560.37	2.63(+1)		[N II]	6548.10	F1
6574.10	2.78(+2)		H 3	6562.77	H3
6593.34	7.51(+1)		[N II]	6583.50	F1
6683.88	3.30(+0)		HeI	6678.16	V46
6720.26	5.91(+0)		[S II]	6716.44	F2
6734.37	7.53(+0)		[S II]	6730.82	F2
7011.20	3.37(+0)		[Ar V]	7005.74	
7072.05	3.83(+0)		He I	7065.25	V10
7144.66	1.56(+1)		[Ar III]	7135.80	F1
7333.53	3.35(+0)		[O II]	7318.92	F2
7344.02	3.66(+0)		[O II]	7329.67	F2

He^+/H^+ and He^{2+}/H^+ fractions deduced from our optical observations (see Section 5.1). Similarly, one can also derive $c(H\beta)$ from a comparison between the He II $\lambda1640$ and $\lambda4686$ or [O II] $\lambda2470$ and $\lambda\lambda7320, 7330$ integrated line fluxes.

In this work we used the value of $c(H\beta)$ derived from the radio-$H\beta$ method, denoted $c(H\beta)^{radio}$ (as listed in column 3 of Table 1), to deredden the UV line fluxes in cases where the apparent PN diameter was larger than the *IUE* large aperture. All UV fluxes were then scaled to the optical spectra as described previously in Section 4. In our sample, apart from NGC 5315 and the Cloud nebulae, the PNe angular diameters are larger than the *IUE* large aperture, so the derived $c(H\beta)^{1640}$ values are consistently greater than the one given by $c(H\beta)^{rad}$, as the derivation involves a comparison between a

fraction of the He II $\lambda1640$ line flux with the total nebular He II $\lambda4686$ flux; therefore $c(H\beta)^{1640}$ values were not used in our analysis.

The Magellanic Cloud PN spectra were dereddened in a two-step process. First the contribution from Galactic foreground reddening was removed; this was estimated from the reddening maps of Burstein & Heiles (1982), using the extinction law of Howarth (1983) in all cases. The remaining extinction due to the interstellar medium of the Magellanic Clouds was taken from Barlow (1987) in the case of the UV data, and from the observed Balmer decrement in the case of the optical data. The SMC extinction law of Prévot et al. (1984) was used in the case of SMC N87, while the mean LMC extinction law of Howarth (1983) was used for LMC N141. For the directions to SMC N87 and LMC N141, $c(H\beta) = 0.03$ and 0.11 through the Milky Way were found, respectively. From the foreground-corrected Balmer decrements, values of $c(H\beta) = 0.02$ and 0.03, respectively, were found for the remaining Magellanic Cloud extinction. For LMC N66, the observed optical Balmer line ratios were already consistent with Case B values, so no extinction correction was applied to the optical line fluxes. We corrected the observed *IUE* line fluxes of Peña & Ruiz (1988) by comparing the observed He II $\lambda1640/\lambda4686$ flux ratio of 5.1 with the theoretical Case B value of 7.4 for $T_e = 2 \times 10^4$ K. This yielded $c(H\beta) = 0.14$ (0.09 Galactic; 0.05 LMC), which was applied to deredden the UV line fluxes.

Another kind of correction had to be applied for high-excitation objects with a high He II $\lambda4686$ flux [e.g. $\gtrsim 65$ when $F(H\beta) = 100$]; in such nebulae the He II Pickering series (transitions $n \to 4$) begins to contribute significantly to the H I Balmer series. Relevant cases include NGC 2022, NGC 2440, NGC 6302 and LMC N66, where the contribution to $H\beta$ from He II Pi 8 was estimated using the observed He II $\lambda4686$ flux and emissivities from Storey & Hummer (1995). Fluxes of the contaminating He II $\lambda4859$ ($n = 8 \to 4$) amounted to ~3–5 per cent and were subtracted from the $H\beta$ fluxes before any further analysis was performed.

Throughout the above analysis we used total nebular $F(H\beta)$ and 5-GHz continuum fluxes for the Galactic PNe, as listed by CKS92; from them total nebular He II $\lambda4686$ fluxes were derived, using the observed $I(\lambda4686)/I(H\beta)$ ratios from our scanned nebular spectra. In the case of nebulae that were observed only with a fixed-slit we proceeded as follows: for NGC 6302 we used the total nebular He II flux from CKS92 directly, without resorting to our fixed-slit $I(\lambda4686)/I(H\beta)$ ratio, while for NGC 6818 the above optical ratio was assumed to be representative of the whole PN.

4 NEBULAR DIAGNOSTICS

Nebular electron temperatures and densities were derived from several CEL diagnostic ratios by solving the equations of statistical equilibrium for multi-level ($\geqslant5$) atomic models using the program EQUIB (originally written by I.D. Howarth and S. Adams). The following diagnostic ratios were used:

$T_e(O\ III)$: $I(\lambda4959 + \lambda5007)/I(\lambda4363)$

$T_e(O\ III)_{IR}$: $I(\lambda4959 + \lambda5007)/I(52\ \mu m + 88\ \mu m)$

$T_e(N\ II)$: $I(\lambda6548 + \lambda6584)/I(\lambda5754)$

$T_e(O\ II)$: $I(\lambda3727)/I(\lambda7320 + \lambda7330)$

$T_e(S\ II)$: $I(\lambda4068)/I(\lambda6731 + \lambda6716)$

$T_e(BJ)$: $I_c(\lambda3646^- - \lambda3646^+)/I(H\ 11)$

$N_e(Ar\ IV)$: $I(\lambda4740)/I(\lambda4711)$

$N_e(Cl\ III)$: $I(\lambda5537/I(\lambda5517)$

$N_e(S\ II)$: $I(\lambda6731)/I(\lambda6716)$

$N_e(O\ II)$: $I(\lambda3729)/I(\lambda3726)$

The procedure to derive temperatures and densities from CEL line ratios is as follows: we assumed a representative initial electron temperature of 10 000 K to derive N_e(Cl III) and N_e(Ar IV). We then used the mean density from these diagnostics to derive T_e(O III) and iterated once to get the final values. In a similar manner, T_e(N II) was derived in conjunction with N_e(O II) and N_e(S II). The atomic data used for the purpose of this analysis, but also throughout this work, are those used by Liu et al. (2000) in their case study of NGC 6153.

4.1 Electron densities

The derived electron densities for our sample of PNe are listed in Table 6. In all spectra the [Ar IV] $\lambda4711$ line is blended with the He I $\lambda4713$ line; individual fluxes for the two lines were thus derived by means of Gaussian profile fitting, as described previously in Section 2.3. Both of the [Ar IV] $\lambda\lambda4711, 4740$ fluxes were measured on high-resolution spectra (1.5 Å for the Galactic PNe and 2 Å for the Magellanic Cloud PNe) in all cases; they were then used to derive the N_e(Ar IV) values listed in Table 6.

We were able to derive N_e values using the [O II] $\lambda3729/\lambda3726$ ratio only for NGC 5882, 6302 and 6818, for which the [O II] $\lambda\lambda3726$, 3729 doublet was resolved in the high-resolution 3040–4040 Å spectra. For the remaining PNe the [O II] doublet is covered in lower resolution only and is blended with the H 14 $\lambda3721.9$, [S III] $\lambda3721.6$ and H 13 $\lambda3734.4$ lines; the overall [O II] flux was derived as follows: the [S III] $\lambda3721$ flux was estimated from a comparison with the dereddened flux of the [S III] $\lambda6312.1$ line, which originates from the same upper level. The latter line is often blended with He II $\lambda6310.8$ in high excitation objects and that flux was retrieved via its theoretical ratio relative to He II $\lambda4686$. Finally, the $I(H13)/I(H\beta)$ and $I(H14)/I(H\beta)$ intensity ratios were estimated using H I line emissivities from Storey & Hummer (1995). The deconvolved $\lambda3727$ flux was then used to derive N_e values for the remaining PNe of Table 6 from the [O II] $I(\lambda3727)/I(\lambda7320 + \lambda7330)$ ratio.

Electron densities were also derived from the [O III] 52 μm/ 88 μm *ISO* LWS line flux ratios measured for eight of our sample PNe by Liu et al. (2001a).[2]

It should be borne in mind that the derived densities correspond to mean values, as the employed line ratios have been taken from scanned nebular spectra in most cases. In addition, all observations sampled lines of sight throughout the nebular volumes as well. It is thus quite probable that localized density variations on a small scale have been effectively smoothed out, or that they are not even seen due to the relatively low spatial resolution of our observations.

On the other hand, the N_e(S II) values for the whole sample are consistently lower than the N_e(Ar IV) values, by about ∼30 per cent. This behaviour is consistent with the presence of strong density variations in the nebulae, so that the diagnostic line ratios with higher critical densities (e.g. the [Cl III] and [Ar IV] diagnostics) yield higher derived nebular electron densities.[3] The effect is shown to be more pronounced from a comparison between the [O III] 52-μm/88-μm and [Cl III] and [Ar IV] densities. For the eight PNe for which values from all three of these ratios have been derived, the latter diagnostics yield N_e values that are on average a factor of 6 higher than those

---

[2] Liu et al. adopted a constant electron temperature of 10^4 K to derive electron densities from their 52 μm/88 μm flux ratios and compared their values to those derived from the [Cl III] and [Ar IV] optical doublet ratios.
[3] [Cl III] $\lambda\lambda5517$, 5537, $N_{cr} = 6400$, 34 000 cm^{-3}; [Ar IV] $\lambda\lambda4711$, 4740, $N_{cr} = 14 000$, 130 000 cm^{-3}; [S II] $\lambda\lambda6716$, 6730, $N_{cr} = 1200$, 3300 cm^{-3} respectively.

obtained from the far-IR ratio (see Rubin 1989; Liu et al. 2001a). This effect will be discussed further in Section 5.2.

4.2 Electron temperatures

We derived T_e values using ionic CEL ratios of nebular to transauroral [S II] transitions, nebular to auroral transitions of [N II], [O II] and [O III], and nebular to IR fine-structure transitions of [O III] (the latter designated as T_e(O III)^{IR}). We adopted the *ISO* Long Wavelength Spectrometer (LWS) fluxes listed by Liu et al. (2001a) for the [O III] 52- and 88-μm lines. The LWS aperture size of ∼80 arcsec included all of the emission from these nebulae. The results are presented in Table 7. We were able to derive values of T_e(O III) for all 15 PNe; values of T_e(N II) for 12 PNe, excluding NGC 2440, SMC N87 and LMC N141, for which the auroral $\lambda5754$ line did not fall within our wavelength coverage; and values of T_e(O III)^{IR} for eight PNe. The correct choice of electron temperature is crucial when deriving abundances from forbidden lines, so in what follows we discuss the pattern of N_e values for the current sample of 15 PNe, as measured from the above ionic ratios.

4.2.1 Recombination excitation of the N II and O II auroral lines

The mean T_e(O III) for the whole sample is 12 300 K, while the mean T_e(N II) is 11 700 K. For 12 PNe where both T_e values were measured, the values differ by about 3 per cent, T_e(O III) being only slightly higher than T_e(N II). It could be argued that generally in PNe, N$^+$ is present in a lower ionization zone than O^{2+}, and that the temperature should be lower too. However, for eight PNe where both T_e(O III) and T_e(O II) can be measured, it is found that on average, T_e(O III) = 11 500 K, while T_e(O II) = 13 400 K, i.e. *higher* by 1900 K. The disagreement between [O II] and [O III] electron temperatures, as derived from the nebular to auroral line ratios $I(\lambda3727)/I(\lambda7320 + \lambda7330)$ and $I(\lambda4959 + \lambda5007)/I(\lambda4363)$, respectively, is at its most extreme in the cases of NGC 3242, NGC 5882 and My Cn 18. In these objects the derived T_e(O II) values are higher than the T_e(O III) values by 7850, 5900 and 4980 K, respectively.

A variety of hypotheses can be invoked in order to explain the difference of electron temperatures in these three nebulae. Radiation hardening in the nebular volumes where singly ionized species are expected to exist could result in higher temperatures than those of the O^{2+} zone, but the effect should be similar for both T_e(N II) and T_e(O II), as the ionization potentials of N$^+$ and O$^+$ are very comparable.

An alternative proposition is as follows: in NGC 3242, NGC 5882 and My Cn 18 most of the N and O atoms are in their doubly ionized stages (O^{2+}/O = 0.85, 0.96 and 0.63, while N^{2+}/N = 0.65, 0.72 and 0.63, respectively; cf. Section 5). Thus, as discussed by Rubin (1986) and Liu et al. (2000), recombination of N^{2+} and O^{2+} can be important in contributing to the excitation of the [N II] nebular and [O II] nebular and auroral lines.

We will attempt to quantify this effect for these three extreme cases, using the expressions of Liu et al. (2000). They employed radiative recombination coefficients from Péquignot, Petitjean & Boisson (1991) and dielectronic recombination coefficients from Nussbaumer & Storey (1984), to show that the intensity of the [N II] $\lambda5754$ auroral line due to recombination excitation can be fitted by

$$\frac{I_R(\lambda5754)}{I(H\beta)} = 3.19t^{0.30}\frac{N^{2+}}{H^+}, \quad (1)$$

where $t \equiv T_e/10^4$ and $0.5 \leqslant t \leqslant 2.0$. Also, Liu et al. (2000) calculated new recombination coefficients for the metastable

Table 5. *IUE* fluxes of Galactic PNe[a].

| Line | NGC 2022 | | NGC 2440 | | NGC 3132 | | NGC 3242 | | NGC 3918 | |
	$F(\lambda)$ (10^{-14})	$I(\lambda)$ $c = 0.55$	$F(\lambda)$ (10^{-13})	$I(\lambda)$ $c = 0.52$	$F(\lambda)$ (10^{-13})	$I(\lambda)$ $c = 0.33$	$F(\lambda)$ (10^{-13})	$I(\lambda)$ $c = 0.20$	$F(\lambda)^b$ (10^{-12})	$I(\lambda)$ $c = 0.40$
N v λ1240	*	*	28.3	105	*	*	*	*	6.70	41.1
O iv] λ1401	47.8	124	21.3	52.9	*	*	*	*	10.8	48.9
N iv] λ1486	38.3	90.1	82.2	186	*	*	*	*	11.0	46.4
C iv λ1549	367	814	309	659	49.3	7.40	*	*	113	458
[Ne v] λ1574	9.78	21.3	5.83	12.2	*	*	*	*	*	*
[Ne iv] λ1601	6.94	14.8	*	*	*	*	*	*	1.50	5.90
He ii λ1640	378	790	255	514	17.8	25.9	890	172	73.3	284
O iii] λ1663	8.58	17.7	19.6	39.2	2.08	3.00	43.9	8.50	8.20	31.5
N iii] λ1750	*	*	70.6	140	3.18	4.60	28.7	5.50	7.00	26.7
C iii] λ1908	224	526	410	924	26.4	41.1	741	150	117	493

| Line | NGC 5315 | | NGC 5882 | | NGC 6302 | | NGC 6818 | | IC 4406 | |
	$F(\lambda)^c$ (10^{-13})	$I(\lambda)$ $c = 0.57$	$F(\lambda)$ (10^{-13})	$I(\lambda)$ $c = 0.43$	$F(\lambda)$ (10^{-13})	$I(\lambda)$ $c = 1.47$	$F(\lambda)^e$ (10^{-12})	$I(\lambda)$ $c = 0.36$	$F(\lambda)$ (10^{-13})	$I(\lambda)$ $c = 0.30$
N v λ1240	*	*	*	*	3.01	1382	7.90	15.9	*	*
O iv] λ1401	3.54	.679	*	*	1.46	112	21.5	32.6	*	*
N iv] λ1486	1.95	2.58	*	*	6.96	534	22.2	31.6	*	*
C iv λ1549	*	*	*	*	8.39	552	70.8	96.7	4.84	19.9
[Ne v] λ1574	6.21	7.41	*	*	*	*	7.30:	9.84:	*	*
[Ne iv] λ1601	2.06	2.41	*	*	0.30[d]	26.6	5.20	6.94	*	*
He ii λ1640	*	*	15.3	17.8	7.24	409	242	318	21.0	83.8
O iii] λ1663	3.9	4.42	4.25	4.90	2.34	129	22.8	29.8	1.97	7.80
N iii] λ1750	4.7	5.26	3.90	4.50	7.61	408	16.4	21.2	1.99	7.80
C iii] λ1908	24.7	31.9	24.7	31.4	6.09	463	319	453	40.6	140
C ii] λ2326	6.20	9.46	*	*	*	*	16.5	26.0	14.9	68.9
[Ne iv] λ2423	1.72	1.92	*	*	10.1[d]	795	39.2	50.7	2.38	9.30
[O ii] λ2470	9.05	8.93	*	*	*	*	2.50	3.00	2.83	10.4

[a]Notes: $F(\lambda)$ in units of erg cm^{-2} s^{-1}, $I(\lambda)$ in units such that $I(H\beta) = 100$. The quoted reddening constants are from the ratio of the 5 GHz free–free continuum to Hβ. For those PNe observed at ESO with a scanning slit the percentages of total nebular $F(\lambda1640)$ in IUE's large aperture are: 27 per cent (NGC 2022), 60 per cent (NGC 2440), 46 per cent (NGC 3132), 53 per cent (NGC 3242), 80 per cent (NGC 3918), 65 per cent (NGC 5882) and 48 per cent (IC 4406);
[b]From Clegg et al. (1987) combined with fluxes from spectrum SWP 47514;
[c]From Feibelman (1998);
[d]From Feibelman (2001);
[e]From Hyung et al. (1999).

Table 6. Electron densities.

PN	[O ii][a] λ3727/(λ7320 + λ7330)	[S ii] λ6731/λ6716	[Cl iii] λ5537/λ5517 N_e (cm^{-3})	[Ar iv] λ4740/λ4711	[O iii][b] 52 μm/88 μm
NGC 2022	1970	1050	850	2150	*
NGC 3132	*	550	720	530	355
NGC 3242	*	1970	1200	3040	775
NGC 3918	*	4600	5500	6900	1380
NGC 5315	13040	8200	22825	12300	2290
NGC 5882	4750	4000	2700	5000	1175
NGC 6302	5750	12900	22450	14900	1380
NGC 6818	1800	1700	2400	2350	*
IC 4191[c]	13530	12750	12375	13750	*
IC 4191[d]	11930	7900	10150	12800	1700
IC 4406	*	950	3500	1250	540
My Cn 18	*	5025	9420	6300	*
SMC N87	2850	3950	*	9500	*
LMC N66	⩽200	1900	*	5700	*
LMC N141	2300	7400	*	9500	*

[a]For NGC 5882, 6302, 6818 and LMC N66 quoted values were derived from the λ3729/λ3726 ratio;
[b]From the *ISO* LWS line-fluxes of Liu et al. (2001a);
[c]Values from the fixed-slit spectrum of the nebula;
[d]Values for the whole nebula from a scanned spectrum.

Table 7. Electron temperatures.

PN	[S II]	[O II]	[N II]	[O III]	BJ	[O III]^{IR}	[O III]$^{IR}_{ClIII}$	O II ORLs[a]
				T_e (K)				
NGC 2022	*	*	14700	15000	13200	*	*	400
NGC 2440	*	*	*	16150	14000	*	*	*
NGC 3132	8120	*	9350	9530	10780	9900	9000	*
NGC 3242	4800	19550	13400	11700	10200	13800	12400	1000
NGC 3918	9350	10400	10800	12600	12300	19900	12400	*
NGC 5315	11400	*	10800	9000	8600	18500	7800	8100
NGC 5882	6900	15300	10800	9400	7800	11400	9400	800
NGC 6302	10000	20200	14225	18400	16400	>50000	10900	*
NGC 6818	5750	11200	11100	13300	12140	*	*	≲2900
IC 4191[b]	7750	*	11575	10700	10500	*	*	*
IC 4191[c]	8550	*	12225	10000	9200	16700	8900	4300
IC 4406	8650	9000	9900	10000	9350	9900	7100	*
My Cn 18	12825	12300	10225	7325	*	*	*	*
SMC N87	>20000	*	*	12250	*	*	*	*
LMC N66	*	*	12700	18150	*	*	*	*
LMC N141	10100	*	*	11850	*	*	*	*

[a]O II ORL temperatures from Paper II.
[b]Values from a fixed-slit spectrum of the nebula;
[c]Values for the whole nebula from a scanned spectrum.

levels of O II and showed that the intensity of the [O II] $\lambda\lambda7320$, 7330 auroral lines due to recombination excitation can be fitted in the range $0.5 \leqslant t \leqslant 1.0$ by

$$\frac{I_R(\lambda7320 + \lambda7330)}{I(H\beta)} = 9.36t^{0.44}\frac{O^{2+}}{H^+}. \qquad (2)$$

For NGC 3242, which has $T_e(\text{O III}) = 11\,700$ K, the observed $\lambda1750$ multiplet flux yields $N^{2+}/H^+ = 1.90 \times 10^{-5}$, for $T_e = 11\,700$ K and $N_e = 1200$ cm^{-3} (Tables 6 and 7). Inserting this value into equation (1), we have $I_R(\lambda5754)/I(H\beta) = 0.0064$, or 10 per cent of the observed intensity of the $\lambda5754$ line relative to Hβ, $I(\lambda5754)/I(H\beta) = 0.0635$. After subtracting $I_R(\lambda5754)$ from the observed intensity, the [N II] nebular to auroral line ratio yields $T_e = 10\,850$ K, i.e. 2550 K lower than the value derived before the correction. If one uses $N^{2+}/H^+ = 1.28 \times 10^{-4}$ instead, as derived from N II recombination lines (cf. Paper II for N^{2+}/H^+ and O^{2+}/H^+ abundances from N II and O II ORLs), one gets $I_R(\lambda5754)/I(H\beta) = 0.0408$, which is about 64 per cent of the observed value. After correcting for this $I_R(\lambda5754)$, the temperature deduced from the revised [N II] line ratio is only 7950 K.

Regarding the [O II] auroral lines, for $O^{2+}/H^+ = 2.80 \times 10^{-4}$ as derived from the $\lambda\lambda4959$, 5007 lines (Table 9), equation (2) predicts a recombination intensity relative to Hβ of 0.262 on a scale where H$\beta = 100$ for the [O II] $\lambda\lambda7320$, 7330 lines, or 29 per cent of their observed intensity. According to Liu et al., the recombination contribution to the $\lambda\lambda3726$, 3729 nebular lines is 7.7 times that of $I_R(\lambda7320 + \lambda7330)$, at $T_e = 10\,000$ K. Thus we have, $I_R(\lambda3726 + \lambda3729) = 2.02$ on a scale where H$\beta = 100$, or 21 per cent of the observed overall intensity. Again, if we use instead the ORL abundance ratio of $O^{2+}/H^+ = 6.28 \times 10^{-4}$ derived for this PN, we get a recombination contribution of 0.588 to the [O II] auroral lines (65 per cent of the observed value), while a contribution of 4.53 relative to Hβ (46 per cent of the observed intensity), is found for the nebular lines.

Therefore, using O^{2+}/H^+ as given by the CEL lines, the revised [O II] nebular to auroral line ratio yields $T_e = 15\,800$ K, i.e. 3750 K lower than the value derived before the correction. If we instead

Table 8. [N II] and [O II] electron temperatures after correcting for the effects of recombination excitation.

PN	$T_e(\text{O III})$	$T_e(\text{BJ})$	$T^{cor}_e(\text{N II})$	$T^{cor}_e(\text{O II})$
			(K)	
NGC 3242	11700	10300	10850|7950[a]	15800|12050[a]
NGC 5882	9400	9700	9900|9550	14500|13750
My Cn 18	7325	*	10225|9450	12150|12100

[a]Values before the vertical dashes are where recombination excitation contributions were calculated adopting CEL abundances; those after are where the ORL abundances from Paper II were adopted.

use the O^{2+}/H^+ abundance ratio given by the ORLs, the corrected $T_e(\text{O II})$ is 7500 K lower, at 12 050 K, and only 300 K higher than the $T_e(\text{O III})$.

Applying the same procedure to NGC 5882, which has $T_e(\text{O III}) = 9400$ K, we obtain from $N^{2+}/H^+ = 1.10 \times 10^{-4}$, as given by the CELs, a corrected nebular to auroral line ratio which yields a $T_e(\text{N II})$ of 9900 K; if we assume $N^{2+}/H^+ = 1.63 \times 10^{-4}$, as given by the ORLs, the corrected temperature is $T_e(\text{N II}) = 9550$ K. Similarly, the corrected [O II] nebular to auroral line ratio results in a $T_e(\text{O II})$ of 14 500 K, using $O^{2+}/H^+ = 4.48 \times 10^{-4}$ as given by CELs; in the case of $O^{2+}/H^+ = 9.70 \times 10^{-4}$, as given by ORLs, the corrected temperature is $T_e(\text{O II}) = 13\,750$ K.

For My Cn 18, which has $T_e(\text{O III}) = 7325$ K, the [N II] line ratio does not change appreciably for $N^{2+}/H^+ = 2.20 \times 10^{-4}$ as given by CELs, so there is a negligible change in $T_e(\text{N II})$; however if $N^{2+}/H^+ = 20.4 \times 10^{-4}$, as given by the ORLs, the corrected temperature becomes $T_e(\text{N II}) = 9450$ K. Finally, the corrected [O II] ratio results in a $T_e(\text{O II})$ of 12 150 K, using $O^{2+}/H^+ = 3.54 \times 10^{-4}$ as given by CELs; and for $O^{2+}/H^+ = 6.43 \times 10^{-4}$, as given by ORLs for this object, the corrected temperature is $T_e(\text{O II}) = 12\,100$ K.

In the above discussion we have neglected the contribution of recombination excitation to the observed [N II] $\lambda\lambda6548$, 6584 nebular intensities; this is estimated to be small and amounts to only 7, 8 and 8 per cent for NGC 3242, NGC 5882 and My Cn 18, respectively, even when adopting ORL N^{2+}/H^+ abundances. We

Table 9. Helium abundances derived from optical recombination lines and CEL O, N, C, Ne, Ar, S and Cl abundances relative to hydrogen in Galactic PNe[a].

λ_0 (Å)		NGC 2022	NGC 2440	NGC 3132	NGC 3242	NGC 3918	NGC 5315
4471	He^+/H^+	0.0135	0.0575	0.1229	0.0811	0.0721	0.1243
5876	He^+/H^+	0.0129	*	0.1151	0.0789	0.0655	0.1205
6678	He^+/H^+	*	*	0.1103	0.0762	0.0631	0.1174
Avg.	He^+/H^+	0.0130	0.0575	0.1157	0.0789	0.0663	0.1206
4686	He^{2+}/H^+	0.0970	0.0627	0.0031	0.0208	0.0350	0.0000
	He/H	0.110	0.120	0.119	0.100	0.101	0.121
2326	C^+/H^+	*	*	*	*	3.73(−5)	1.54(−5)
1908	C^{2+}/H^+	8.69(−5)	1.13(−4)	1.50(−4)	1.18(−4)	2.40(−4)	1.92(−4)
1550	C^{3+}/H^+	6.55(−5)	3.44(−5)	1.67(−5)	*	1.33(−4)	*
	icf(C)	1.02	1.28	1.89	1.18	1.06	1.02
	C/H	2.12(−4)	2.37(−4)	3.15(−4)	1.39(−4)	4.35(−4)	2.12(−4)
6548+6584	N^+/H^+	1.66(−7)	*	1.29(−4)	3.20(−7)	1.27(−5)	3.15(−5)
1750	N^{2+}/H^+	1.29(−5)	7.10(−5)	9.95(−5)	2.20(−5)	6.25(−5)	1.93(−4)
57 μm	[b]	*	*	8.68(−5):	1.90(−5):	2.92(−5):	4.26(−5):
	[c]	*	*	1.33(−4):	4.13(−5):	8.70(−5):	2.76(−4):
1486	N^{3+}/H^+	1.33(−5)	2.71(−5)	*	*	6.77(−6)	1.09(−4)
1240	N^{4+}/H^+	*	1.22(−5)	*	*	2.35(−5)	*
	icf(N)	1.09	1.31	1.03	1.53	1.00	1.00
	N/H	2.87(−5)	1.44(−4)	2.36(−4)	3.41(−5)	1.05(−4)	3.34(−4)
2470	O^+/H^+	*	*	*	*	*	4.24(−5):
3727	...	1.60(−6)	*	3.03(−4)	2.54(−6)	2.23(−5)	4.19(−5)
7320+7330	...	1.02(−6):	*	3.00(−4):	4.12(−6):	4.37(−5):	4.24(−5):
1663	O^{2+}/H^+	5.72(−5)	5.86(−5):	2.35(−4):	1.11(−4):	2.34(−4):	6.02(−4):
4931	...	1.04(−4):	2.34(−4):	2.71(−4):	2.73(−4):	2.57(−4):	3.48(−4):
4959+5007	...	8.07(−5)	9.71(−5)	3.39(−4)	2.80(−4)	2.90(−4)	4.26(−4)
52+88 μm	[b]	*	*	2.94(−4):	2.20(−4):	1.64(−4):	8.81(−5):
	[c]	*	*	3.48(−4):	3.16(−4):	3.91(−4):	4.95(−4):
1401	O^{3+}/H^+	2.86(−4)	8.68(−5)	*	*	3.51(−4)	1.55(−4)
	icf(O)	1.24	1.34	1.02	1.17	1.10	1.00
	O/H	4.55(−4)	2.46(−4)	6.55(−4)	3.31(−4)	7.28(−4)	6.23(−4)
3868+3967	Ne^{2+}/H^+	1.59(−5)	3.36(−5)	1.58(−4)	6.61(−5)	2.03(−5)	1.26(−4)
15.5 μm	[c]	*	3.75(−5):	2.41(−5):	3.71(−5):	5.75(−5):	9.61(−5):
1601	Ne^{3+}/H^+	5.35(−5)	*	*	*	5.10(−5)	7.35(−5)
2423	...	*	2.03(−5)	*	*	*	1.04(−5):
4725	...	4.47(−5)	*	*	9.18(−6):	5.95(−5)	*
1574	Ne^{4+}/H^+	3.85(−6)	9.38(−5):	*	*	*	1.60(−3):
3426	...	*	5.59(−5)	*	*	1.80(−5)	*
	icf(Ne)	1.00	1.00	1.96	1.18	1.00	1.00
	Ne/H	6.89(−5)	1.10(−4)	3.10(−4)	7.80(−5)	9.36(−5)	2.00(−4)
4069+4076	S^+/H^+	*	*	2.43(−6):	3.37(−9):	2.89(−7):	1.30(−6):
6716+6730	...	1.50(−8)	*	3.21(−6)	1.45(−8)	2.83(−7)	1.24(−6)
6312	S^{2+}/H^+	7.92(−7)	*	6.80(−6)	6.62(−7)	1.93(−6)	1.05(−5)
	icf(S)	4.57	*	1.06	3.52	2.24	1.74
	S/H	3.69(−6)	*	1.06(−5)	2.38(−6)	4.96(−6)	2.04(−5)
5517+5537	Cl^{2+}/H^+	1.76(−8)	*	1.48(−7)	2.44(−8)	5.02(−8)	1.31(−7)
	icf(Cl)	4.66	*	1.56	3.59	2.57	1.95
	Cl/H	8.20(−8)	*	2.31(−7)	8.77(−8)	1.29(−7)	2.55(−7)
7135	Ar^{2+}/H^+	3.39(−7)	*	2.37(−6)	4.13(−7)	8.87(−7)	3.00(−6)
4711+4740	Ar^{3+}/H^+	7.82(−7)	5.12(−7)	6.12(−8)	5.48(−7)	5.88(−7)	1.49(−7)
7005	Ar^{4+}/H^+	2.13(−7)	*	*	7.16e−9	1.15(−7)	*
	icf(Ar)	1.00	*	2.21	1.01	1.08	1.16
	Ar/H	1.33(−6)	*	5.37(−6)	9.79(−7)	1.72(−6)	3.65(−6)

base this on the fact that for pure recombination excitation the [N II] nebular to auroral line ratio has a value of 5.9 at $T_e = 10\,000$ K (Liu et al. 2000). On the other hand, the observed ratios for these three PNe are, respectively, 10, 12 and 13 times larger than that. We summarize our findings for these three objects in Table 8.

To conclude, for low-density uniform nebular media, as assumed above, appreciable fractions of the [O II] nebular and auroral and [N II] auroral lines can be accounted for by recombination processes. However, even after recombination excitation has been taken into account, the agreement between the various CEL temperature diagnostics remains quite poor, especially for NGC 5882 and My Cn 18 (see Table 8). In addition, the current treatment has not taken into account collisional de-excitation of the metastable levels that are populated by recombination. It is obvious that an exact analysis of this problem requires detailed knowledge of the actual electron

Table 9 – *continued*

λ_0 (Å)		NGC 5882	NGC 6302	NGC 6818	IC 4191	IC 4406	My Cn 18
4471	He^+/H^+	0.1102	0.0850	0.0488	0.0971	0.1163	0.1057
5876	He^+/H^+	0.1064	0.0775	0.0482	0.1126	0.1180	0.0984
6678	He^+/H^+	0.1036	0.0118	0.0445	0.1100	0.1187	0.0862
Avg.	He^+/H^+	0.1066	0.0658	0.0476	0.1090	0.1178	0.0974
4686	He^{2+}/H^+	0.0022	0.0696	0.0510	0.0110	0.0067	0.0004
	He/H	0.109	0.135	0.099	0.120	0.124	0.098
2326	C^+/H^+	*	*	2.63(−5)	*	1.34(−4)	*
1908	C^{2+}/H^+	1.29(−4)	3.08(−5)	2.04(−4)	*	2.11(−4)	*
1550	C^{3+}/H^+	*	1.43(−5)	2.21(−5)	*	1.81(−5)	*
	icf(C)	1.17	1.72	1.03	*	1.00	*
	C/H	1.51(−4)	7.74(−5)	2.60(−4)	*	3.63(−4)	*
6548+6584	N^+/H^+	3.06(−6)	4.48(−5)	8.29(−6)	9.64(−6)	5.90(−5)	8.11(−5)
1750	N^{2+}/H^+	1.10(−4)	1.03(−4)	3.44(−5)	*	1.10(−4)	*
57 μm	*b*	5.08(−5):	5.20(−5):	*	2.45(−5)	9.05(−5):	*
	c	1.03(−4):	3.13(−4):	*	1.34(−4):	2.63(−4):	*
1486	N^{3+}/H^+	*	7.80(−5)	6.06(−6)	*	*	*
1240	N^{4+}/H^+	*	9.45(−5)	6.24(−6)	*	*	*
	icf(N)	1.35	1.00	1.00	1.14	1.25	2.71
	N/H	1.52(−4)	3.34(−4)	5.50(−5)	3.89(−5)	2.11(−4)	2.20(−4)
2470	O^+/H^+		1.67(−5):	2.37(−5):	*	2.03(−4):	*
3727	...	1.31(−5)	8.42(−6)	2.28(−5)	2.26(−5)	1.79(−4)	2.08(−4)
7320+7730	...	2.17(−5):	2.03(−5):	2.37(−5):	2.81(−5):	1.70(−4):	4.78(−4):
1663	O^{2+}/H^+	4.35(−4):	9.35(−5):	1.51(−4):	*	3.86(−4):	*
4931	...	4.38(−4):	2.66(−4):	1.68(−4):	4.05(−4):	3.67(−4):	3.76(−4):
4959+5007	...	4.72(−4)	9.18(−5)	2.52(−4)	5.46(−4)	3.80(−4)	3.54(−4)
52+88 μm	*b*	2.70(−4):	4.20(−4):	*	1.90(−4):	3.90(−4):	*
	c	4.70(−4):	9.90(−5):	*	8.36(−4):	7.78(−4):	*
1401	O^{3+}/H^+	*	8.22(−5)	1.84(−4)	*	*	*
	icf(O)	1.01	1.37	1.11	1.07	1.04	1.00
	O/H	4.90(−4)	2.50(−4)	5.08(−4)	6.08(−4)	5.81(−4)	5.64(−4)
3868+3967	Ne^{2+}/H^+	1.31(−4)	2.65(−5)	5.57(−5)	1.47(−4)	1.39(−4)	7.74(−5)
15.5 μm	*c*	1.47(−4):	1.81(−5):	5.18(−5):	*	*	*
1601	Ne^{3+}/H^+	*	3.53(−5)	5.00(−5)	*	*	*
2423	...	*	7.59(−5):	1.45(−5):	*	1.01(−5):	*
4724	...	*	2.37(−5)	5.55(−5)	7.21(−5):	*	*
1574	Ne^{4+}/H^+	*	*	2.05(−4)	*	*	*
3426	...	*	2.00(−5)	9.57(−6)	*	*	*
	icf(Ne)	1.04	1.00	1.00	1.11	1.53	1.59
	Ne/H	1.36(−4)	7.60(−5)	1.18(−4)	1.64(−4)	2.13(−4)	1.23(−4)
4069+4076	S^+/H^+	8.91(−8):	8.20(−7):	1.17(−7):	3.45(−7):	4.20(−7):	1.43(−6):
6716+6730	...	1.44(−7)	1.04(−6)	2.73(−7)	5.59(−7)	4.77(−7)	8.64(−7)
6312	S^{2+}/H^+	3.50(−6)	1.57(−6)	1.54(−6)	5.49(−6)	1.38(−6)	1.35(−5)
	icf(S)	2.30	2.14	2.01	2.10	1.14	1.20
	S/H	8.38(−6)	5.59(−6)	3.64(−6)	1.27(−5)	2.12(−6)	4.43
5517+5537	Cl^{2+}/H^+	7.59(−8)	2.76(−8)	5.24(−8)	1.02(−7)	9.37(−8)	2.09(−7)
	icf(Cl)	2.40	3.56	2.37	2.31	1.54	1.17
	Cl/H	1.82(−7)	9.83(−8)	1.24(−7)	2.36(−7)	1.44(−7)	2.45(−7)
7135	Ar^{2+}/H^+	1.37(−6)	6.51(−7)	8.41(−8)	1.66(−6)	1.64(−6)	1.88(−6)
4711+4740	Ar^{3+}/H^+	6.31(−7)	7.75(−7)	6.08(−7)	5.99(−7)	1.80(−7)	*
7005	Ar^{4+}/H^+	*	4.67(−7)	9.57(−8)	7.37(−8)	*	*
	icf(Ar)	1.02	1.16	1.11	1.33	1.39	*
	Ar/H	2.04(−6)	2.19(−6)	8.73(−7)	3.10(−6)	2.53(−6)	*

[a]Values followed by ‘:’ have not been used in order to derive total abundances;
[b]Derived using the N_e from the [O III] 52 μm/88 μm line ratio;
[c]Derived using the mean of the N_e values obtained from the optical [Cl III] and [Ar IV] line ratios.

temperature and N^{2+}/H^+ and O^{2+}/H^+ abundances. To complicate matters more, if the nebulae are not homogeneous, but also contain a higher-density component, then the observed [O II] and [N II] emission pattern can be more difficult to evaluate. In nebulae that contain condensations whose electron density is *higher* than the critical densities of the low-lying atomic levels – from which the $\lambda\lambda$6548, 6584 and 3727 nebular lines originate – but *lower* than that of the auroral

lines, the former lines will be preferentially emitted from the lower density medium. This could lead to apparently high temperatures as deduced from the [N II] and [O II] nebular to auroral ratios, because their component transitions would be disproportionately affected in regions of high density; there, the nebular lines will be suppressed by collisional de-excitation, but the auroral lines will not be (Viegas & Clegg 1994).

Table 10. Ionic and total elemental abundances relative to hydrogen for helium derived from ORLs and for heavy elements derived from CELs in Magellanic Cloud PNe[a].

λ_0 (Å)		SMC N87	LMC N66	LMC N141
4471	He$^+$/H$^+$	0.0965	0.0572	0.1058
5876	He$^+$/H$^+$	*	0.0375	*
6678	He$^+$/H$^+$	0.0981	0.0435	0.1119
Avg.	He$^+$/H$^+$	0.0972	0.0440	0.1085
4686	He^{2+}/H$^+$	0.0000	0.0607	0.0003
	He/H	0.097	0.105	0.109
2326	C$^+$/H$^+$	3.59(−5)	*	3.02(−5)
1908	C^{2+}/H$^+$	3.22(−4)	5.92(−6)	1.49(−4)
1550	C^{3+}/H$^+$	1.92(−5)	7.77(−6)	2.04(−5)
	icf(C)	1.00	2.40	1.00
	C/H	3.77(−4)	3.29(−5)	2.00(−4)
6548+6584	N$^+$/H$^+$	6.10(−7)	7.44(−6)	2.03(−6)
1750	N^{2+}/H$^+$	*	1.84(−5)	*
1486	N^{3+}/H$^+$	*	4.46(−5)	*
1240	N^{4+}/H$^+$	*	2.70(−5)	2.81(−5):
	icf(N)	58.7	1.00	44.0
	N/H	3.58(−5)	9.74(−5)	8.93(−5)
3727	O$^+$/H$^+$	1.84(−6)	5.95(−6)	4.48(−6)
7320+7330	...	1.38(−5):	2.15(−5):	3.25(−5):
1663	O^{2+}/H$^+$	*	4.58(−5):	*
4931	...	7.94(−5):	*	1.04(−4):
4959	...	1.06(−4)	7.81(−5)	1.93(−4)
1401	O^{3+}/H$^+$	*	*	*
	icf(O)	1.00	3.77	1.00
	O/H	1.08(−4)	3.17(−4)	1.97(−4)
3868+3967	Ne^{2+}/H$^+$	1.04(−5)	1.74(−5)	2.35(−5)
1601	Ne^{3+}/H$^+$	*	*	*
2423	...	*	1.39(−5)	*
4724	...	*	1.90(−5)	*
1574	Ne^{4+}/H$^+$	*	*	*
3426	...	*	8.24(−6)	*
	icf(Ne)	1.02	1.00	1.02
	Ne/H	1.06(−5)	4.21(−5)	2.40(−5)
4069	S$^+$/H$^+$	4.10(−8):	*	1.21(−7):
6716+6730	...	2.85(−8)	2.43(−7)	1.48(−7)
6312	S^{2+}/H$^+$	*	7.69(−7)	1.50(−6)
	icf(S)	*	2.11	2.47
	S/H	*	4.30(−6)	4.06(−6)
7135	Ar^{2+}/H$^+$	1.76(−7)	4.28(−7)	6.39(−7)
4711+4740	Ar^{3+}/H$^+$	3.13(−8)	5.43(−7)	1.03(−7)
7005	Ar^{4+}/H$^+$	*	1.57(−7)	*
	icf(Ar)	1.02	1.13	1.02
	Ar/H	2.11(−7)	1.27(−6)	7.59(−7)

[a]Values followed by ':' have not been used in order to derive total abundances.

As our schematic treatment has pointed out, the [N II] and [O II] nebular to auroral temperature diagnostic ratios provide values which are probably poor indicators of T_e in the low-ionization regions of these three objects. Therefore, in the abundance analysis that follows in Section 7, we have adopted T_e(O III) when calculating forbidden-line N$^+$/H$^+$ and O$^+$/H$^+$ abundances for NGC 3242, NGC 5882 and My Cn 18.

4.2.2 Balmer discontinuity electron temperatures

Apart from temperatures derived from the CEL ratios, Table 7 also lists the mean nebular Balmer jump temperatures, T_e(BJ), derived from the ratio of the nebular continuum discontinuity at 3646 Å to H 11 λ3770 [Δ(BJ)/H 11]. Values of the Balmer jump intensity were

determined from the lower resolution 4.5-Å FWHM scanned spectra, apart from the cases of NGC 5882, 6302 and 6818 for which their higher resolution (1.5-Å FWHM) $\lambda\lambda$3040–4040 fixed-slit spectra were used. The observed nebular continuum on either side of the Balmer discontinuity was modelled with low-order polynomials. Redwards of 3646 Å the crowding of high-order nebular Balmer lines frustrates the determination of the local continuum level on the lower resolution spectra, which was then estimated by linear extrapolation using continuum data points with wavelengths longer than 3800 Å. In the higher resolution spectra the high-order Balmer lines are clearly resolved and the local continuum is better estimated with no significant extrapolation from longer wavelengths. In practice, the Balmer jump temperatures were derived by comparing the observed and predicted values of the Balmer discontinuity to H 11 ratio, defined as Δ(BJ)/H$\beta \equiv [I_c\,(\lambda3643) - I_c\,(\lambda3681)]/I$(H 11). By thus defining the Balmer discontinuity we include in our computation two weak discontinuities of the He I and He II continua which are present at 3678 and 3646 Å, respectively and are inseparable from the H I Balmer jump at the resolution of our observations. By definition then, the temperature thus deduced has a weak dependence on the He$^+$/H$^+$ and He^{2+}/H$^+$ abundance ratios (Table 9). Equation (3) of Liu et al. (2001b) takes into account the Balmer jump dependence on these abundance ratios and we have used it to derive the Balmer jump temperatures listed in Table 7.

Inspection of Table 7 shows that, apart from NGC 3132, all of the Balmer jump temperatures in column 6 of Table 7 are lower than the corresponding optical [O III] temperatures listed in column 5 (10 per cent lower on average). This behaviour has been found from previous observations too (e.g. Peimbert 1971; Liu & Danziger 1993) and has often been attributed to nebular temperature fluctuations, since the optical [O III] lines, whose strengths have an exponential dependence on electron temperature, will be more biased towards regions with higher than average T_e than will the hydrogen Balmer series lines and discontinuity, which have only an inverse power-law dependence of T_e. However, the strengths of the far-IR fine-structure (FS) lines of [O III] have an even weaker dependence on T_e, because of their low excitation energies. Thus, if significant temperature fluctuations are present, electron temperatures derived from the ratio of [O III] IR FS lines to optical nebular lines might be expected to show less bias to higher temperatures than those derived from the more temperature-sensitive auroral to nebular line ratio. In the next section, we will investigate whether this expectation is confirmed by the observations.

4.2.3 Electron temperatures using the far-IR [O III] 52- and 88-μm lines

We have also derived [O III] electron temperatures using the far-IR fine structure lines and optical nebular lines of this species, in a similar manner to Dinerstein, Lester & Werner (1985). These T_e values are designated as T_e(O III)^{IR} in Table 7 and were obtained from the dereddened flux ratio $I(\lambda4959 + \lambda5007)/I$(52 μm + 88 μm) using our scanned-slit optical line fluxes and the IR line fluxes of Liu et al. (2001a), for the eight Galactic PNe in our sample that were observed by the ISO LWS. Two alternative values of T_e(O III)^{IR} are listed for each of the eight nebulae. The first value, listed in column 7 of Table 7, was obtained using the [O III] 52 μm/88 μm electron density listed in column 6 of Table 6, whereas the second value, designated T_e(O III)$^{IR}_{CIII}$ and listed in column 8 of Table 7, was derived using the (higher) optical [Cl III] electron densities listed in column 4 of Table 6.

Inspection of Table 7 shows that, apart from IC 4406, the $T_e(\text{O\,III})^{\text{IR}}$ values derive using [O III] 52 μm/88 μm electron densities are always higher (often much higher) than the purely optical $T_e(\text{O\,III})$ values listed in column 5 of Table 7. On average, $T_e(\text{O\,III})^{\text{IR}}$ based on the 52 μm/88 μm electron density is 40 per cent higher than the purely optical $T_e(\text{O\,III})$. In contrast to this, $T_e(\text{O\,III})^{\text{IR}}$ based on the optical [Cl III] electron density shows much closer agreement with the optical $T_e(\text{O\,III})$. For one nebula (NGC 3242), this $T_e(\text{O\,III})^{\text{IR}}$ is higher than the optical $T_e(\text{O\,III})$ by 6 per cent, whereas for NGC 5882 the two values agree exactly. For the other six nebulae, the $T_e(\text{O\,III})^{\text{IR}}$ values based on [Cl III] electron densities are lower than the purely optical $T_e(\text{O\,III})$ values by only 14 per cent on average. We note that the trend from our ISO-based results disagrees with that found by Dinerstein et al. (1985), who used 52- and 88-μm fluxes and electron densities from KAO spectra of six PNe to derive $T_e(\text{O\,III})^{\text{IR}}$ values that were systematically *lower* than T_e values derived from auroral to nebular [O III] line ratios.

Our results indicate that the observed $I(\lambda4959 + \lambda5007)/I(52 \text{ μm} + 88 \text{ μm})$ ratios are much more weighted to the higher electron densities diagnosed by the optical [Cl III] $\lambda5517/\lambda5537$ ratio than to the lower electron densities diagnosed by the 52 μm/88 μm ratio. In most cases, an electron density just below that from the [Cl III] ratio would yield agreement between the optical and IR $T_e(\text{O\,III})$ values. We note that if significant nebular temperature fluctuations were the cause of the Balmer jump electron temperatures being lower than the optical [O III] temperatures (Section 4.2.2), we would expect [O III] temperatures that made use of the more temperature insensitive 52- and 88-μm lines to be significantly lower than [O III] temperatures based on the much more temperature sensitive auroral λ4363 line. This is not the case – the [O III]$^{\text{IR}}$ temperatures based on 52 μm/88 μm electron densities are significantly *higher*, while [O III]$^{\text{IR}}$ temperatures based on [Cl III] electron densities are close to, or only slightly smaller, than the optical $T_e(\text{O\,III})$ values. We therefore conclude that nebular temperature fluctuations are not a significant contributor to the trends shown by the various T_e diagnostics.

5 IONIC AND TOTAL ELEMENTAL ABUNDANCES

5.1 Helium abundances

Helium abundances derived from He I and He II recombination lines are given in Tables 9 and 10. For the He I lines, Case A recombination was assumed for the triplet lines λ4471, λ5876 and Case B for the singlet λ6678 line. The adopted effective recombination coefficients were from Brocklehurst (1972). Contributions to the observed fluxes by collisional excitation from the He^0 2s ^{3}S metastable level by electron impacts were corrected for using the formulae derived by Kingdon & Ferland (1995). The He^+/H^+ abundance ratios thus derived were then averaged, weighted according to the intensities of the three He I lines. The tabulated He^{2+}/H^+ ratios were obtained from the He II λ4686 line only, using the effective recombination coefficients of Storey & Hummer (1995). The tabulated total He/H number ratio for each nebula was given by He/H = He^+/H^+ + He^{2+}/H^+.

5.2 Abundances from collisionally excited lines

In this section we present our results for the heavy element ionic abundances of the 12 Galactic and three Magellanic Cloud PNe that were observed, derived from collisionally excited UV, optical and IR lines. These are presented in Tables 9 and 10 for the Galactic and

Cloud nebulae, respectively. The emission lines detected by the *IUE* satellite gave us access to important ionic stages such as: C^+– C II] λ2326, C^{2+}– C III] λ1908, and C^{3+}– C IV λ1550 (resonantly excited doublet line); N^{2+}– N III] λ1750, N^{3+}– N IV] λ1486, and N^{4+}– N V λ1240 (resonant doublet); O^+– [O II] λ2470, O^{2+}– O III] λ1663, and O^{3+}– O IV λ1401; Ne^{3+}– [Ne IV] λλ1601, 2423, and Ne^{4+}– Ne V λ1574.

Especially with regard to carbon, the consideration of UV lines facilitated the calculation of forbidden line abundances for this element, which has no emission lines in the optical domain other than recombination lines (of C^{2+}, C^{3+} and C^{4+}). The nitrogen abundance estimate also benefits greatly from the inclusion of UV lines in the analysis, since in the optical region – in terms of CELs – this important element is represented only by the [N II] λλ5754, 6548, 6584 lines, which are typically indicative of just a small fraction of the total N abundance.

A complementary analysis of the more frequently employed optical CELs allowed us to obtain total CEL elemental abundances for C, N, O, Ne, S, Cl, and Ar.

In order to derive ionic abundances we used the EQUIB code, which solves the statistical balance equation for each ion and yields level populations and line emissivities for a specified (T_e, N_e), appropriate to the zones in a nebula where the ions are expected to exist. The following expression was then used in order to convert the observed line intensities to ionic abundance fractions;

$$\frac{N(\text{X}^{\text{m}+})}{N(\text{H}^+)} = \frac{N_e h\nu_{42}\alpha_{\text{eff}}(\text{H}\beta)}{A_{ij}n_i E_{ij}} \frac{I(\lambda)}{I(\text{H}\beta)}$$

where $I(\lambda)$ are dereddened line fluxes, A_{ij} are the radiative transition probabilities for $i \rightarrow j$, n_i is the fractional population of level i, E_{ij} is the excitation energy of level i above j, $\alpha_{\text{eff}}(\text{H}\beta)$ is the effective recombination coefficient of Hβ and $h\nu_{42}$ is the energy of an Hβ photon.

Generally, when deriving CEL abundances, $T_e(\text{N\,II})$ is assumed to represent the electron temperature appropriate for singly ionized species, while $T_e(\text{O\,III})$ is used for higher excitation ions. However, as discussed in Section 4.2.1, in some cases the [N II] and [O II] nebular-to-auroral line ratios can be affected in ways that result in them being unreliable diagnostics of the temperature pertinent to the lower excitation zones of PNe. Therefore, for our CEL abundance analysis we have adopted the following scheme: abundances of singly ionized species were derived using $T_e(\text{N\,II})$ and $N_e(\text{O\,II})$, apart from the cases of NGC 3242, NGC 5882 and My Cn 18, where $T_e(\text{O\,III})$ was used instead; whenever $N_e(\text{O\,II})$ was not available, $N_e(\text{S\,II})$ was employed. For all doubly ionized species (C^{2+}, N^{2+}, O^{2+}, Ne^{2+}, S^{2+}, Cl^{2+} and Ar^{2+}), $T_e(\text{O\,III})$ and $N_e(\text{Cl\,III})$ were used. For triply ionized species (O^{3+}, N^{3+}, Ne^{3+}, Ar^{3+}), $T_e(\text{O\,III})$ + 1000 K with $N_e(\text{Ar\,IV})$ were used, except for C^{3+}, where $T_e(\text{O\,III})$ + 650 K was used instead. Finally, $T_e(\text{O\,III})$ + 2270 K was used for all four-times ionized species (N^{4+}, Ne^{4+}, Ar^{4+}) – from ionization potential considerations as discussed by Kingsburgh & Barlow (1994, hereafter KB94).

Abundances of neutral species were not derived; it is assumed that heavy element neutral fractions are the same as hydrogen neutral fractions and therefore that total elemental abundances relative to hydrogen can be obtained using ionic fractions only. In Tables 9 and 10 the abundances for all observed ionic species of C, N, O, Ne, S, Cl and Ar are presented, together with the adopted ionization correction factors (ICFs) and total elemental abundances, as derived using CELs only. The adopted ICF scheme is that of KB94; details on the derivation of the total abundances for C, N and O are discussed in the Appendix.

The adopted O^+/H^+ fractions used to calculate the total oxygen abundances were obtained from the $\lambda3727$ doublet only. The abundances derived from the [O II] $\lambda\lambda7320$, 7330 lines are generally higher, as is evident from Tables 9 and 10; the reason could be that a larger fraction of these line fluxes with respect to that of $\lambda3727$ can be due to recombination excitation and/or the fact that the emission of $\lambda\lambda7320$, 7330 is biased towards higher density regions (cf. Section 4.2.1). However, the ionic fractions deduced from $\lambda3727$ may represent upper limits only due to contributions from recombination.

In the case of O^{2+} we adopted ionic fractions obtained from the nebular [O III] $\lambda\lambda4959$, 5007 lines only, in order to derive total oxygen abundances. For comparison, in Tables 9 and 10 we also present O^{2+}/H^+ abundances derived from the O III] $\lambda1663$ and [O III] $\lambda4931$ lines. We further present O^{2+}/H^+ abundances derived from the far-IR [O III] 52- and 88-μm fine-structure lines for eight nebulae, using the *ISO* LWS line fluxes published in Liu et al. (2001a); two values per nebula are listed – for the first we used the (lower) electron densities obtained from the 88 μm/52 μm line ratio and for the second we used the (higher) N_e values obtained from the optical [Ar IV] and [Cl III] density diagnostics (Table 6).

Similarly, we present N^{2+}/H^+ ionic fractions from both the N III] $\lambda1750$ line and from the far-IR [N III] 57-μm line (using the *ISO* LWS 57-μm line fluxes of Liu et al. 2001a); abundance ratios from the latter line are tabulated for both the low and high nebular electron density cases, just as for the [O III] far-IR lines.

Both the [O III] and [N III] far-IR lines originate from atomic levels that have quite low critical densities, $N_{cr} \sim (2–4) \times 10^3$ cm^{-3}, lower than the average electron density of most PNe in our sample. The ionic abundances derived from these lines are therefore acutely sensitive to our assumption of the actual density of the emitting medium. For example, adopting a density significantly higher than the N_{cr} of the collisional line will result in a proportional increase of

the deduced abundance, because for the same flux to be emitted the presence of more ions is required, otherwise the emission line would be quenched. On the other hand, the nebular [O III] $\lambda\lambda4959$, 5007 lines have much higher critical densities, $N_{cr} \sim 6.9 \times 10^5$ cm^{-3}, so that the abundances deduced from them are much less sensitive to the adopted nebular density; the same is true for the N III] $\lambda1750$ line which has $N_{cr} \sim 11 \times 10^9$ cm^{-3}.

Thus O^{2+}/H^+ and N^{2+}/H^+ ionic abundances derived from far-IR lines are expected to be underestimated in the presence of density variations in nebulae (Rubin 1989; Liu et al. 2001a). The likelihood of systematic bias in abundance determinations from CELs becomes less when lines with fairly high critical densities are used, as long as N_e values in the nebula are well below those values. These expectations are confirmed by our observations. Table 6 compares the electron densities derived from the 88 μm/52 μm line ratio with those derived from the higher critical density [Cl III], and [Ar IV] ratios, for the eight PNe in common between our sample and Liu et al.'s (2001a) *ISO* LWS sample, and shows that on average the latter diagnostics yield N_e values about a factor of 6 higher than the far-IR ratio, confirming the existence of density inhomogeneities in these nebulae, in agreement with Liu et al.'s conclusions. In accord with the predictions of Rubin, the bias in the ionic N^{2+} and O^{2+} abundances derived from the far-IR lines becomes *less* when the higher electron densities from the [Cl III] and [Ar IV] are adopted – the values returned are then in good agreement, in most cases, with those derived from the N III] $\lambda1750$ and [O III] $\lambda\lambda4959$, 5007 lines (cf. Table 9). For instance, in the case of NGC 5882 the 'high' density IR O^{2+} abundance is within 1 per cent of the optical CEL value, while the 'high' density IR N^{2+} abundance is within 7 per cent of the UV CEL value; in the case of NGC 3918, the UV N^{2+} and optical O^{2+} abundances agree to within 8 and 5 per cent with the corresponding values that are *half-way* between the listed IR abundances. A notable exception is IC 4406, for which the O^{2+}/H^+
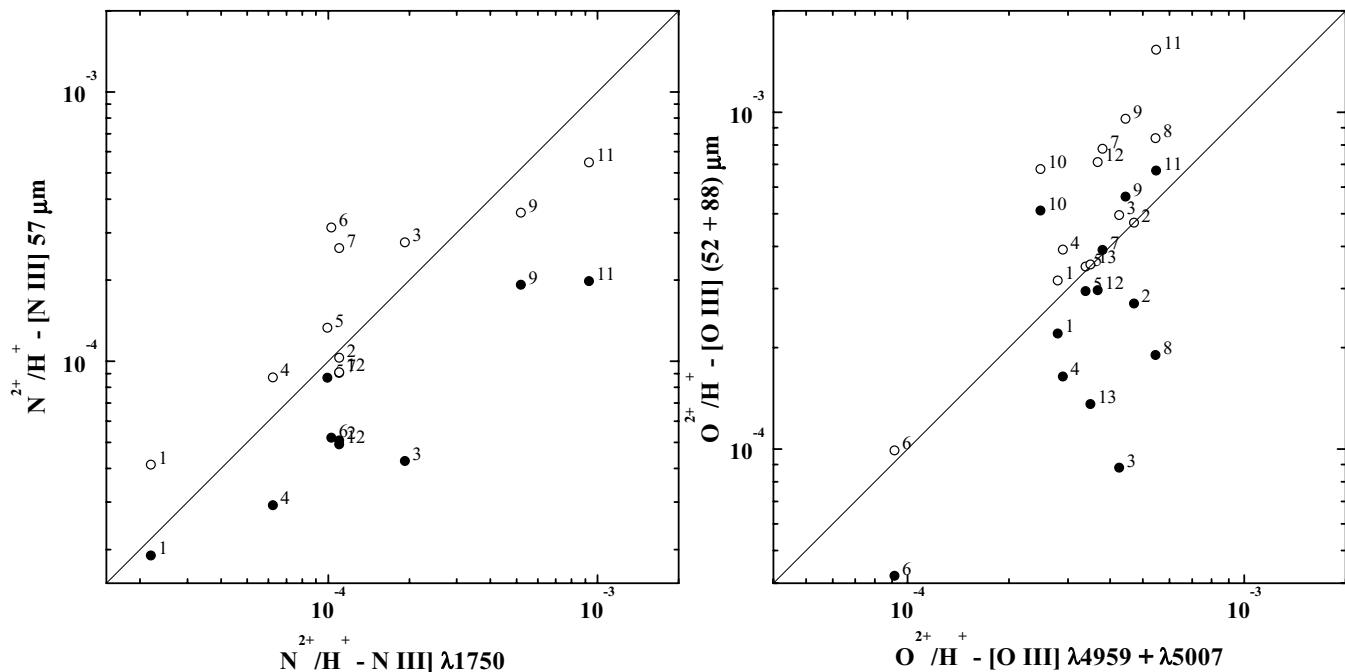

Figure 3. Comparison of N^{2+}/H^+ abundance ratios derived from the N III] $\lambda1750$ and [N III] 57 μm lines, and O^{2+}/H^+ ratios derived from the [O III] $\lambda\lambda4959$, 5007 and 52, 88 μm lines; solid and open circles denote abundances derived from adopting 'low' far-IR [O III] 88 μm/52 μm electron densities and 'high' [Cl III], [Ar IV] electron densities, respectively; the data labelling refers to the designated PN numbers of Table 11, column 2.

abundance derived from the far-IR lines in the low density case agrees with the corresponding value derived from the optical lines. In Fig. 3 we plot abundance ratios of N^{2+}/H^+ and O^{2+}/H^+ derived from UV and optical lines respectively and compare them with those derived from far-IR transitions. Regarding the abundances from the IR lines, we plot using different symbols both those resulting from adopting the low 88 μm/52 μm ratio N_e values as well as those derived from adopting the higher [Cl III], [Ar IV] N_e values. We see that for the majority of nebulae very satisfactory agreement is found amongst the UV, and optical abundances on the one hand and the far-IR abundances on the other, after accounting for the modest density variations within the nebular volumes, exposed from the disparity between the IR and optical density diagnostic line ratios. In general, the adoption of electron densities just a little below those diagnosed by the [Cl III] and [Ar IV] ratios would lead to agreement between the abundances deduced from the IR FS lines of [O III] and [N III] and those derived from the optical or UV lines of the same ions. These results are of importance in the context of the discussion about the existence of temperature fluctuations in nebulae and their potential impact on abundances derived from CELs (cf. Section 4.2.3).

We derived Ne^{2+}/H^+ abundances from the optical [Ne III] $\lambda\lambda 3868, 3967$ lines for all 15 PNe. For nine of them we also determined this abundance ratio using the *IRAS* [Ne III] 15.5-μm line fluxes of Pottasch et al. (1984). For the 15.5-μm line, $N_{cr} = 2 \times 10^5$ cm^{-3}, and the resulting ionic abundances do not depend on the adopted N_e, for the range of nebular densities presented in Table 6. Inspection of Table 9 shows quite good agreement between the optical and IR Ne^{2+}/H^+ abundances. As with other ions, the abundances from the optical CELs are those adopted.

In all these cases where IR collisionally excited lines were analyzed, we adopted the T_e(O III) values for abundance determinations. IR CELs have small excitation energies, $E_{ex} < 1000$ K, much smaller than those of UV and optical forbidden lines. Thus their emissivities have only a weak dependence on the adopted nebular electron temperature, very similar to those of H I Balmer lines. Their intensities relative to $H\beta$ are therefore virtually insensitive to the assumed temperature, unless the emitting medium has $T_e \ll 1000$ K; the electron temperatures of all nebulae in our sample, derived from CEL intensity ratios, are consistently much higher than that. On the other hand, at the temperatures implied by the O II ORLs (cf. Table 7 and Paper II) the far-IR CELs would be expected to be suppressed to various degrees depending on the exact temperature and density of the emitting material.

Ne^{3+}/H^+ ionic fractions were derived from the [Ne IV] $\lambda\lambda 4724, 4726$ and $\lambda 1601$ lines, which usually showed good agreement with each other. For the Ne^{4+}/H^+ ratio, whenever available the values obtained from [Ne V] $\lambda 3426$ were preferred over those from the Ne V $\lambda 1574$ line.

We adopted the S^+/H^+ abundance derived from the [S II] $\lambda\lambda 6716, 6731$ doublet, rather than from the transauroral $\lambda\lambda 4068, 4076$ lines, as the latter are potentially affected by recombination processes and density effects (the ^2D and ^2P atomic levels of S^+, from which the $\lambda\lambda 6716, 6731$ and $\lambda\lambda 4068, 4076$ lines respectively arise, are directly analogous to the levels of O^+ from which the [O II] nebular and auroral lines originate; especially in terms of critical densities).

5.3 Abundances – summary

Table 11 presents a comparison between CEL abundances derived here and values previously published in the literature for the same objects. The ionization correction factor (ICF) scheme of KB94 was adopted for the abundances derived in this paper, as well as for

Table 11. Comparison of elemental abundances from different sources, in units where log $N(H) = 12.0$.

PN	He	C	N	O	Ne	Ref.[a]
NGC 2022	11.041	8.33	7.46	8.66	7.84	This paper
	11.029	8.53	7.88	8.29	8.04	AC83
	11.079		<8.76	8.81	8.05	TPP77
NGC 2440	11.086	8.37	8.26	8.39	8.04	This paper
	11.111	8.30	8.94	8.72	8.04	KB94
	11.185		9.09	8.82	8.14	TPP77
NGC 3132	11.076	8.50	8.37	8.82	8.49	This paper
	11.072		8.68	8.98	8.56	TPP77
NGC 3242	11.000	8.14	7.53	8.52	7.89	This paper
	10.959	8.41	7.96	8.64	8.04	B85
	10.949	8.43	7.91	8.66	7.85	AC83
	11.033		7.71	8.72	8.03	TPP77
NGC 3918	11.004	8.64	8.02	8.86	7.97	This paper
	11.049		8.28	8.90	8.16	TPP77
NGC 5315	11.082	8.33	8.52	8.79	8.30	This paper
	11.093	8.64	8.66	8.72	8.20	Pott02
	10.959		8.79	8.80	8.27	KB94
	11.025		8.44	8.88	8.03	DfP91
	11.086		8.83	8.85	8.27	TPP77
NGC 5882	11.037	8.18	8.18	8.67	8.13	This paper
	11.009	8.87	8.04	8.74	8.19	KB94
	11.053		8.10:	8.92:	8.34:	TPP77
NGC 6302	11.130	7.89	8.52	8.40	7.88	This paper
	11.230		8.76	8.41		dFP91
IC 4406	11.093	8.56	8.32	8.76	8.33	This paper
	11.124:		8.52:	8.98:	8.51:	TPP77
SMC N87	10.986	8.58	7.55	8.03	7.03	This paper
	10.959		7.04	8.04	7.00	MBC88
LMC N66	11.021	7.52	7.99	8.50	7.62	This paper
	11.064		7.95	8.24	7.70	Pena95
	11.136		7.65	8.26	7.61	DM91
	10.973		8.36	8.51	7.76	MBC88
LMC N141	11.037	8.30	7.95	8.29	7.38	This paper
	11.097		7.20	8.28	7.41	DM91
	10.924		7.85	8.46	7.43	MBC88

[a]References: TPP77 = Torres-Peimbert & Peimbert (1977); AC83 = Aller & Czyzak (1983); B85 = Barker (1985); MBC88 = Monk et al. (1988); DM91 = Dopita & Meatheringham (1991); dFP91 = de Freitas Pacheco et al. (1991); KB94 = Kingsburgh & Barlow (1994); Pena95 = Peña et al. (1995); Pott02 = Pottasch et al. (2002).

those derived by KB94 and by Peña et al. (1995). The other sources adopted different ICF schemes, which may account for some of the spread in the N, O and Ne abundances. The papers by Monk, Barlow & Clegg (1988), KB94, and Peña et al. (1995) explicitly allowed for collisional excitation in deriving He^+/H^+ abundances, as did the current paper. The lack of such corrections in some of the other sources of abundances listed in Table 11 accounts for a significant part of the observed dispersion in helium abundances for the same objects.

Table 12 presents total elemental abundances by number, expressed in units of log $(X/H) + 12.0$, for X = He, C, N, O, Ne, S, Cl and Ar, for the 15 PNe analyzed in this work, plus the Galactic nebulae NGC 7009 (LSBC), NGC 6153 (Liu et al. 2000), and M 1-42 and M 2-36 (Liu et al. 2001b) which were previously observed in the context of our ongoing programme. Peimbert & Torres-Peimbert (1983) defined type I PNe, believed to represent the high-mass end of the PN distribution, as those having He/H $\geqslant$ 0.125 and N/O $\geqslant$ 0.5 by number. KB94 refined the type I classification to refer to those

Table 12. Elemental abundances relative to H derived from CELs, except for the helium abundances which are from ORLs, in units where log N(H) = 12.0.[a]

PN	No.	He	C	N	O	Ne	S	Cl	Ar
NGC 2022		11.04	8.33	7.46	8.66	7.84	6.57	4.91	6.12
NGC 2440 (I)		11.08	8.37	8.26	8.39	8.04	*	*	*
NGC 3132	(5)	11.08	8.50	8.37	8.82	8.49	7.03	5.36	6.73
NGC 3242	(1)	11.00	8.14	7.53	8.52	7.89	6.38	4.94	5.99
NGC 3918	(4)	11.00	8.64	8.02	8.86	7.97	6.70	5.11	6.24
NGC 5315	(3)	11.08	8.33	8.52	8.79	8.30	7.31	5.41	6.56
NGC 5882	(2)	11.04	8.18	8.18	8.67	8.13	6.92	5.26	6.31
NGC 6153[b]	(9)	11.14	8.44	8.36	8.70	8.23	7.21	5.62	6.43
NGC 6302 (I)	(6)	11.13	7.89	8.52	8.40	7.88	6.75	4.99	6.34
NGC 6818		11.00	8.41	7.74	8.71	8.07	6.56	5.09	5.94
NGC 7009[c] (I)	(12)	11.04	8.66	8.50	8.61	8.24	6.98	*	6.27
IC 4191	(8)	11.08	*	7.59	8.78	8.21	7.10	5.37	6.49
IC 4406	(7)	11.09	8.56	8.32	8.76	8.33	6.33	5.16	6.40
My Cn 18		10.99	*	8.34	8.75	8.09	7.24	5.39	*
M 1-42[d] (I)	(10)	11.17	7.80	8.68	8.63	8.12	7.08	5.26	6.56
M 2-36[d]	(11)	11.13	8.73	8.42	8.85	8.57	7.47	5.42	6.66
Mean non-type I		11.06	8.46	8.30	8.75	8.23	7.04	5.30	6.37
Mean type I		11.11	8.32	8.51	8.52	8.09	6.96	5.15	6.41
KB94 non type-I[e]		11.05	8.81	8.14	8.69	8.10	6.91	*	6.38
KB94 type-I[e]		11.11	8.48	8.72	8.65	8.09	6.91	*	6.42
Solar[f]		10.99	8.39	7.97	8.69	8.09	7.21	5.50	6.56
M 42[g]		10.99	8.53	7.78	8.52	7.89	7.17	5.33	6.80
SMC N87		10.99	8.58	7.55	8.03	7.03	*	*	5.32
LMC N66		11.02	7.52	7.99	8.50	7.62	6.63	*	6.10
LMC N141		11.04	8.30	7.95	8.29	7.38	6.61	*	5.88

[a]Values are for the whole nebulae, except NGC 6302, 6644, 6572, 6818, 7009, My Cn 18, IC 4406, LMC N66 and M 42, where values are from fixed-slit spectra. A "(I)" after a PN's name indicates that it is a type I nebula (see text).

[b]From Liu et al. (2000).

[c]From LSBC for He & O; Henry, Kwitter & Bates (2000) for C & N; Luo, Liu & Barlow (2001) for Ne; KB94 for S & Ar.

[d]From Liu et al. (2001b).

[e]From KB94 mean abundances.

[f]Solar photospheric abundances from Grevesse, Noels & Sauval (1996), except C and O which are from Allende Prieto & Lambert (2001, 2002).

[g]CEL abundances for M 42 from Esteban et al. (1998), except O, which is from our unpublished ESO 1.52-m and AAT 3.9-m data, and C, which is from Rubin et al. (1991).

PNe which have N/O ratios larger than the original (C + N)/O ratios of the parent galaxy ISMs out of which they formed, implying that any nitrogen in excess of this value must be primary in origin, e.g. via hot bottom burning of carbon brought up by the third dredge-up. For the Milky Way, the KB94 type I criterion translates into N/O ⩾ 0.74. Using this, we classify NGC 2440, NGC 6302, NGC 7009 and M 1-42 as type I. Table 12 also presents mean elemental abundances for the 12 non-type I and four type I Galactic PNe listed there and compares them with the mean non-type I and type I PN abundances of KB94 (who used the same ICF scheme as here), as well as with solar and M 42 (Orion Nebula) abundances. The mean N, O, Ne and S abundances for the 12 non-type I Galactic PNe are slightly larger than the means found by KB94 for their larger sample of Galactic PNe. However, this may be because M 2-36, which has unusually large abundances for all elements, skews the mean values for our sample.

In Paper II we will use the much weaker heavy element optical recombination lines (ORLs) measured in the spectra reported here to derive ionic abundances and electron temperatures that can be compared with those derived in this paper from the CELs, in order to investigate whether our data replicate, and can throw light on, the significant discrepancies that have previously been found between CEL and ORL ionic abundances measured for a number of other planetary nebulae.

ACKNOWLEDGMENTS

REFERENCES

Allen C. W., 1973, Astrophysical Quantities. The Athlone Press, London
Allende Prieto C., Lambert D. L., 2001, ApJ, 556, L63
Allende Prieto C., Lambert D. L., 2002, ApJ, 573, L137
Aller L. H., Czyzak S. J., 1983, ApJS, 51, 211
Barker T., 1985, ApJ, 294, 193
Barlow M. J., 1987, MNRAS, 227, 161
Brocklehurst M., 1972, MNRAS, 157, 211
Burstein D., Heiles C., 1982, AJ, 87, 1165
Cahn J. H., Kaler J. B., Stanghellini L., 1992, A&AS, 94, 399 (CKS92)
Clegg R. E. S., Harrington J. P., Barlow M. J., Walsh J. R., 1987, ApJ, 314, 551
de Freitas Pacheco J. A., Maciel W. J., Costa R. D. D., Barbuy B., 1991, A&A, 250, 159
Dinerstein H. L., Lester D. F., Werner M. F., 1985, ApJ, 291, 561

Dopita M. A., Meatheringham S. J., 1991, ApJ, 367, 115

Esteban C., Peimbert M., Torres-Peimbert S., Escalante V., 1998, MNRAS, 295, 401

Feibelman W. A., 1998, ApJ, 506, 773

Feibelman W. A., 2001, ApJ, 550, 785

Grevesse N., Noels A., Sauval A. J., 1996, in Holt. S. S., Sonneborn G., eds, ASP Conf. Ser. Vol. 99, Cosmic Abundances. Astron. Soc. Pac., San Francisco, p. 117

Hamuy M., Suntzeff N. B., Heathcote S. R., Walker A. R., Gigoux P., Phillips M. M., 1994, PASP, 106, 566

Henry R. B. C., Kwitter K. B., Bates J. A., 2000, ApJ, 531, 928

Howarth I. D., 1983, MNRAS, 203, 201

Hyung S., Aller L. H., Feibelman W. A., 1999, ApJ, 514, 878

Kingdon J. B., Ferland G. J., 1995, ApJ, 442, 714

Kingsburgh R. L., Barlow M. J., 1994, MNRAS, 271, 257 (KB94)

Kohoutek L., Laustsen S., 1977, A&A, 61, 761

Kuhn H. G., 1969, Atomic Spectra, 2nd edn. Longman

Kwok S., 1994, PASP, 106, 344

Liu X.-W., Danziger I. J., 1993, MNRAS, 263, 256

Liu X.-W., Storey P. J., Barlow M. J., Clegg R. E. S., 1995, MNRAS, 272, 369 (LSBC)

Liu X.-W., Storey P. J., Barlow M. J., Danziger I. J., Cohen M., Bryce M., 2000, MNRAS, 312, 585

Liu X.-W. et al., 2001a, MNRAS, 323, 343

Liu X.-W., Luo S.-G., Barlow M. J., Danziger I. J., Storey P. J., 2001b, MNRAS, 327, 141

Luo S.-G., Liu X.-W., Barlow M. J., 2001, MNRAS, 326, 1049

Milne D. K., Aller L. H., 1975, A&A, 38, 183

Monk D. J., Barlow M. J., Clegg R. E. S., 1988, MNRAS, 234, 583

Nussbaumer H., Storey P. J., 1984, A&AS, 56, 293

Peimbert M., 1971, Bol. Obs. Tonantzintla y Tacubaya, 6, 29

Peimbert M., Torres-Peimbert S., 1983, in Flower D. R., ed., Proc. IAU Symp. 103, Planetary Nebulae. Reidel. Dordrecht, p. 233

Peña M., Ruiz M. T., 1988, Rev. Mex. Astron. Astrofis., 16, 55

Peña M., Peimbert M., Torres-Peimbert S., Ruiz M. T., Maza J., 1995, ApJ, 441, 343

Péquignot D., Petitjean P., Boisson C., 1991, A&A, 251, 680

Pottasch S. R. et al., 1984, A&A, 138, 10

Pottasch S. R., Beintema D. A., Bernard Salas J., Koornneef J., Feibelman W. A., 2002, A&A, 393, 285

Prévot M. L., Lequeux J., Maurice E., Prévot L., Rocca-Volmerange B., 1984, A&A, 132, 389

Rubin R. H., 1986, ApJ, 309, 334

Rubin R. H., 1989, ApJS, 69, 897

Rubin R. H., Simpson J. P., Haas M. R., Erickson E. F., 1991, ApJ, 374, 564

Sahu K. C., Desai J. N., 1986, A&A, 161, 357

Schachter J., 1991, PASP, 103, 457

Storey P. J., Hummer D. G., 1995, MNRAS, 272, 41

Torres-Peimbert S., Peimbert M., 1977, Rev. Mex. Astron. Astrofis., 2, 181

Tsamis Y. G., 2002, PhD thesis, Univ. London

Tsamis Y. G., Barlow M. J., Liu X.-W., Danziger I. J., Storey P. J., 2003a, MNRAS, 338, 687

Tsamis Y. G., Barlow M. J., Liu X.-W., Storey P. J., Danziger I. J., 2003b, MNRAS, submitted

Viegas S., Clegg R. E. S., 1994, MNRAS, 271, 993

Walsh J. R., 1993, ST-ECF Newsletter, 19, 6

Zeippen C. J., 1982, MNRAS, 198, 111

APPENDIX A: ICF METHOD FOR THE DERIVATION OF C, N, AND O

Generally, in order to calculate total elemental abundances we made use of the *icf* scheme of KB94, with some modifications in those cases *only* where our observations of heavy-element optical recombination lines (and the resultant ORL abundances; Paper II) enabled us to account in a satisfactory manner for missing ionic stages. Below we describe how we derived the *icf*s for C, N, and O from this method.

NGC 2022. In the case of carbon we use the standard KB94 correction factor $1 + O^+/O^{2+}$ to account for missing C^+, while from the ratio C^{4+}/C^{3+} as derived from ORLs and the CEL C^{3+} abundance we estimate $C^{4+}/H^+ = 5.53 \times 10^{-5}$ [thus $icf(C) = 1.02$]. For N, we use the ratio N^{4+}/N^{3+} as derived from ORLs and the CEL N^{3+} abundance to estimate $N^{4+}/H^+ = 2.35 \times 10^{-6}$ [thus icf(N) = 1.09]. Similarly for O, we estimate $O^{4+}/H^+ = 8.69 \times 10^{-5}$ from the O^{4+}/O^{3+} ratio derived from ORLs and the CEL O^{3+} abundance [thus icf(O) = 1.24].

NGC 2440. We treat C exactly as in the case of NGC 2022, using the standard correction for C^+ and estimating $C^{4+}/H^+ = 3.77 \times 10^{-5}$ with the help of the ORL C^{4+}/C^{3+} ratio and the CEL C^{3+} abundance [thus icf(C) = 1.89]. Our C abundance is only 2 per cent higher than the one found if we follow the standard *icf* scheme based on nitrogen. For nitrogen, we make use of the CEL N^+/N^{2+} ratio given by KB94 and our own N^{2+} abundance to estimate $N^+/H^+ = 3.37 \times 10^{-5}$ [thus icf(N) = 1.31]. For oxygen, since our spectral coverage of the nebula did not allow the derivation of an O^+ abundance, we made use of the CEL ratio O^+/O^{2+} from Liu & Danziger (1993, from their 270 deg. slit), along with our O^{2+} abundance to estimate $O^+/H^+ = 2.76 \times 10^{-5}$. We also estimate $O^{4+}/H^+ = 3.43 \times 10^{-5}$ using our ORL ratio O^{4+}/O^{3+} and the CEL O^{3+}/H^+ abundance ratio [thus icf(O) = 1.34].

NGC 3132. The standard schemes were used in the case of C and O, while for nitrogen we use our ORL N^{3+}/N^{2+} ratio and the CEL N^{2+} abundance to estimate $N^{3+}/H^+ = 7.22 \times 10^{-6}$ [thus icf(N) = 1.03].

NGC 3242. For C and O we used the standard scheme, while for nitrogen using our ORL N^{3+}/N^{2+} ratio and the CEL N^{2+} abundance we find $N^{3+}/H^+ = 1.18 \times 10^{-5}$ [thus icf(N) = 1.53].

NGC 3918. For N and O we follow the standard scheme, while for carbon we use the ratio C^{4+}/C^{3+} as derived from ORLs and the CEL C^{3+} abundance to estimate $C^{4+}/H^+ = 2.62 \times 10^{-5}$ [thus icf(C) = 1.06].

NGC 5315. For N and O we follow the standard scheme, while for carbon we use our ORL C^{3+}/C^{2+} ratio and the CEL C^{2+} abundance to estimate $C^{3+}/H^+ = 4.61 \times 10^{-6}$ [thus icf(C) = 1.02].

NGC 5882. For O we used the standard scheme; for carbon we estimate $C^{3+}/H^+ = 1.81 \times 10^{-5}$ from the ORL C^{3+}/C^{2+} ratio and the CEL C^{2+} abundance [thus icf(C) = 1.17]. For nitrogen we use our ORL N^{3+}/N^{2+} ratio and the CEL N^{2+} abundance to estimate $N^{3+}/H^+ = 3.88 \times 10^{-6}$ [thus icf(N) = 1.35].

NGC 6818. For carbon we used the ratio C^{4+}/C^{3+} as derived from ORLs and the CEL C^{3+} abundance to estimate $C^{4+}/H^+ = 7.20 \times 10^{-6}$ [thus icf(C) = 1.03]. For N we used the standard scheme, while for oxygen we use our ORL ratio O^{4+}/O^{3+} and the CEL O^{3+} abundance to estimate $O^{4+}/H^+ = 4.97 \times 10^{-5}$ [thus icf(O) = 1.11].

IC 4191. We used the standard scheme for C and O, whereas for nitrogen we used our ORL N^{3+}/N^{2+} ratio and the CEL N^{2+} abundance to estimate $N^{3+}/H^+ = 4.80 \times 10^{-6}$ [thus icf(N) = 1.14].

IC 4406. We used the standard scheme for C and O, whereas for nitrogen we used our ORL N^{3+}/N^{2+} ratio and the CEL N^{2+} abundance to estimate $N^{3+}/H^+ = 4.23 \times 10^{-5}$ [thus icf(N) = 1.25].

Finally, for NGC 6302, My Cn 18, SMC N87, LMC N66 and LMC N141 we used the standard scheme throughout.

This paper has been typeset from a TeX/LaTeX file prepared by the author.